Evaluating the Performance of a Constructed Stormwater Wetland

as a Green Infrastructure Solution

By

Ashley A. Neptune

Thesis

Submitted to the Department of Civil and Environmental Engineering

College of Engineering

Villanova University

In partial fulfillment of the requirements

for the degree of

Master of Science

In

Water Resources and Environmental Engineering

April, 2015

Villanova, Pennsylvania

Evaluating the Performance of a Constructed Stormwater Wetland

as a Green Infrastructure Solution

By: Ashley Neptune

_____ Date: _____

Bridget M. Wadzuk, Ph.D.
Faculty Advisor

_____ Date: _____

John Komlos Ph.D.
Faculty Reader

_____ Date: _____

David Dinehart, Ph.D.
Chairman of the Department of Civil and Environmental Engineering

A copy of this thesis is available for research purposes at Falvey Memorial Library

STATEMENT BY AUTHOR

This thesis has been submitted in partial fulfillment of requirements for an advanced degree at the Villanova University and is deposited in the University Library to be made available to borrowers under rules of the Library.

Brief quotations from this thesis are allowable without special permission, provided that accurate acknowledgment of source is made. Requests for permission for extended quotation from or reproduction of this manuscript in whole or in part may be granted by the head of the major department or the Associate Dean for Graduate Studies and Research of the College of Engineering when in his or her judgment the proposed use of the material is in the interests of scholarship. In all other instances, however, permission must be obtained from the author.

ACKNOWLEDGEMENTS

TABLE OF CONTENTS

LIST OF FIGURES

LIST OF TABLES

ABSTRACT

Stormwater runoff is a persisting problem due to its capability to pick up debris, chemicals, and other pollutants and carry them to nearby water bodies. These pollutants have many severe effects including but not limited to sediments, excess nutrients, pathogens, thermal pollution, and debris. In order to protect our environment, the best option is to minimize the adverse effects on the hydrologic cycle by managing stormwater runoff. Treatment of stormwater runoff is not limited to only one measure of controlling pollutants; there are many treatment systems that can effectively restore the natural hydrology of an area. In particular, a constructed stormwater wetland (CSW) is an excellent example of green infrastructure that provides multiple functions and sustainable solutions.

The stormwater control measure (SCM) was constructed in 2000 when the first CSW (CSW 1.0) was retrofit from a detention basin up until July 2010 when it was redesigned (CSW 2.0). The CSW lays on approximately one acre of land and receives runoff from 42.6 acres through the campus. The drainage area consists of more than 50% being impervious surfaces. Through hydraulic data collection at the inlets and outlet, the CSW has demonstrated success in its ability to control and minimize flooding by reducing peak flow rates.

Additional storm event monitoring expanded beyond flow rates and looked at water temperature. The influence of heated pavement runoff on the CSW inlet reveals spikes in water temperature. Though water temperature is not considered a vital parameter when designing SCMs, its importance does lie in aquatic organisms and fisheries. Another temperature concern is regarding thermal stratification in the summer. Though more commonly seen in lakes and ponds, the slow flow plunge pools at the CSW depict similar conditions, which could result in extremely warm surface temperatures and 10 to 15°C cooler temperatures at the bottom.

Water quality parameters were also analyzed during both storm and baseflow conditions. Most stormwater control measures are designed to reduce nitrogen and phosphorus resulting from stormwater runoff. Through the long shallow meanders and deep stagnant pools, the CSW was intended on removing these constituents. In addition, seasonal factors were investigated for nitrogen, phosphorus, total suspended solids, total dissolved solids, and chlorides from inlet to outlet. The analysis concluded that nitrogen removal is the strongest parameter affected by temperatures.

CHAPTER 1 INTRODUCTION

1.1: Introduction

As the human population continues to increase, so does the need to develop landscapes for civilization. When a natural ecosystem is developed, the after effects impose complications on the hydrology and hydraulics of that land. Hydrology is defined by how the water cycle interacts with the environment. Simply put, hydrology includes issues pertaining to precipitation, runoff, infiltration, evaporation, and transpiration. On the other end is hydraulics, which relates to the issues of stormwater controls and flooding. Figure 1-1, portrays a before and after scenario on how the hydrologic cycle is affected when natural ground is developed with impervious cover.
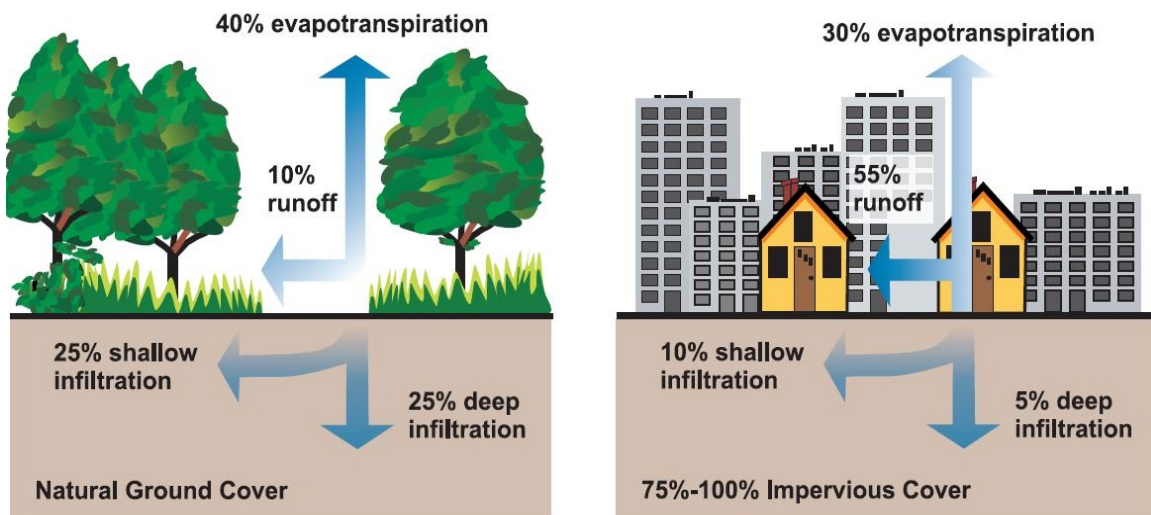
Figure 1-1: Surface runoff relationship between natural ground cover and impervious cover (USEPA 2003).

The most obvious effect is the estimated increase of runoff from 10% to 55% (US EPA 2003). The reason being for such a dramatic increase is impervious surfaces take over the porous terrain of the natural landscapes, thus not allowing rain and snowmelt to infiltrate the ground.

The disturbance on the hydrologic cycle, primarily resulting in increased runoff and decreases in infiltration and evapotranspiration, contributes to significant problems regarding nonpoint source (NPS) pollution. Nonpoint source pollution occurs when rainfall or snowmelt caries pollutants to nearby streams, which is a major contributor to increased pollutant loads. Contributors of NPS pollution consist of agriculture, mining, construction, and urban activities (US EPA 2005).

Stormwater runoff is a persisting problem because of its capability to pick up debris, chemicals and other pollutants and carry them to nearby water bodies. Unlike wastewater treatment plants, stormwater is usually not treated before it is discharged into local streams or lakes. These receiving water bodies that may be used for swimming, fishing, or drinking water are thus affected by high levels of pollutants. Stormwater runoff pollutants have many severe effects including but not limited to sediments, excess nutrients, pathogens, thermal pollution, and debris. These pollutant effects can kill aquatic life, cause recreational areas to be unsafe, and even contaminant drinking water.

In order to protect our environment, we do not have to put a stop on economic growth. The best option to minimize adverse effects on the hydrologic cycle is to manage stormwater runoff. How to manage stormwater runoff varies from simply sweeping impervious surfaces instead of using a hose to constructing a rain garden.

Treatment of stormwater runoff is not limited to only one measure of controlling pollutants, there are many treatment systems that can effectively restore the natural hydrology of an area. From rain gardens and wetlands to permeable pavement, the options for treating stormwater runoff is enormous. However, the most effective treatment choice will strongly

depend on the objectives regarding stormwater management. These objectives consist of peak rate control, volume control, and water quality control.

The Villanova University Stormwater Research and Demonstration Park manages several stormwater control measures (SCM) to monitor the treatment systems for water quality and peak flow reduction. The various treatment sites include bioretention gardens, a green roof, infiltration trench, porous pavement, and a constructed wetland. These SCMs are studied in order to evaluate their effectiveness and later compare them with other SCMs. The Constructed Stormwater Wetland (CSW) at Villanova University is an excellent example that demonstrates the importance and success of their stormwater control sites. Beginning in 2000 when the first CSW (CSW 1.0) was constructed and up until July 2010 when it was retrofitted (CSW 2.0), this SCM has provided valuable information on the efforts to create an effective stormwater management site.

1.2: Plan of Study

The research within this thesis focuses around the theme of retention. The first section emphasizes on the retention time in the CSW. Mean retention time is calculated by performing dye tracer tests during storm and baseflow events. These tracer tests provide crucial information in understanding the hydraulic performance of the CSW and lay the groundwork for future research on water quality treatment going through a constructed stormwater wetland.

The retention of temperature from inlet to the outlet of the CSW is the second part to this research. For this study, water temperature is analyzed in the context of a pollutant. Like some other water quality parameters, temperature fluctuates greatly based on climate conditions. The goal of the temperature study is to analyze how the CSW handles temperature fluctuations throughout the seasons, with emphasis during the warmer months.

Besides temperature, other water quality parameters and their retention are also analyzed on the basis of seasonal performance at the CSW. As temperatures become colder and rain turns to snow, the performance of the CSW is suspected to be less effective. This hypothesis is investigated in greater detail with the water quality parameters tested at the Villanova University Water Resources Laboratory. In addition, the transition from grab samples to autosamplers for storm events is also studied and evaluated on the importance and influence of during versus after storm results.

Lastly, storm events are also analyzed on the basis of peak flow reduction. One of the main goals in controlling floods is to reduce the peak flow rates from impervious runoff. Like water quality treatment, peak flow reduction is suspected to be influenced by climate parameters as well.

CHAPTER 2 LITERATURE REVIEW

2.1: Introduction

Discussions relevant to the research presented in this study will be given in this chapter. Issues pertaining to nonpoint source pollution and the stormwater control measures to treat them will be addressed in greater detail. In regards to stormwater control measures, wetlands and in particular constructed wetlands are discussed to provide a deeper understanding on this research study. Finally, water quality parameters sensitive to temperature changes will be touched on.

2.2: Nonpoint Source Pollution

Since the 1970s, nonpoint source water pollution has been an increasing concern in the United States. The United States Environmental Protection Agency (US EPA) monitored and gathered information on the health of numerous streams and rivers across the nation. Figure 2-1 reveals this scientific data published from the 2008-2009 National Rivers and Stream Assessment.
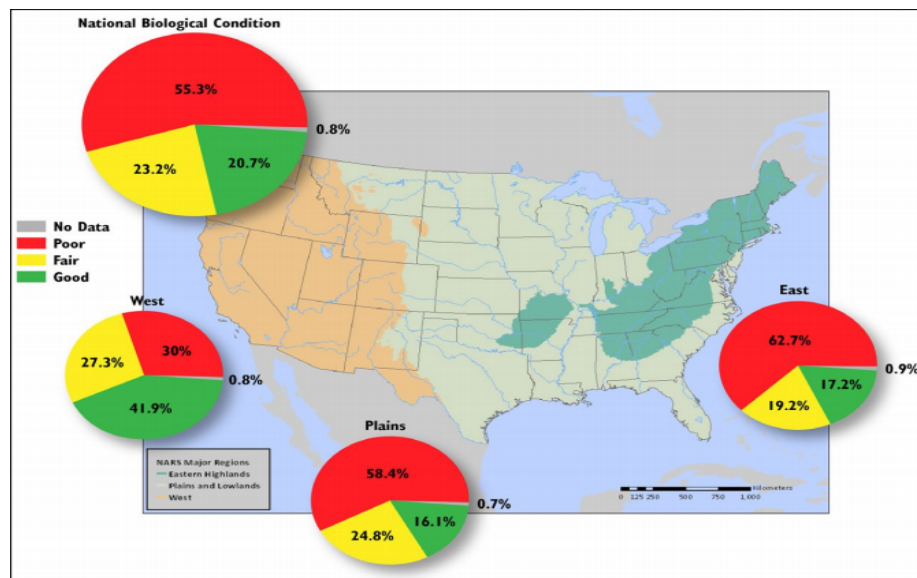
Figure 2-1: Survey of stream and river miles classified as good, fair or poor condition (US EPA 2013)

These poor and fair conditions are attributed to various pollution types, however, nonpoint source (NPS) pollution is the leading source of water quality impairment (US EPA 2013). Nonpoint source pollution is when there is rainfall, snowmelt, or flooding, the water runs over the land picking up pollutants and depositing them into nearby rivers and lakes. Agriculture, urban runoff, construction, and mining are identified as common sources of NPS pollution.

One of the most harmful source of NPS pollution is urban runoff, more specifically stormwater runoff. Stormwater consists of many harmful contaminants that are runoff from roofs, roads, and other impervious surfaces. These pollutants include waste from residential, commercial, agricultural, and construction environments. Table 2-1 provides a summary of major stormwater runoff pollutants and the negative environmental effects they impose (US EPA 2003).

Table 2-1: Stormwater pollutants and their imposing environmental effects

Stormwater Contaminants	Environmental Effects
Sediment	Increasing turbidity that will inhibit or prevent aquatic plant growth.
Oil, grease, and toxic chemicals from vehicles	Poison aquatic life that can eventually harm humans and wildlife.
Pesticides and excess nutrients	Algal blooms
Bacteria and pathogens	Human health danger in recreational areas and drinking water
Road Salts	Increase in chlorides
Thermal pollution from streets and rooftops	Dissolved oxygen decreasing, toxic to aquatic life.

An extreme environmental effect from excess nutrients into water bodies is the process of eutrophication, which leads to growth of algae and cyanobacteria by means of ever-enrichment of phosphorus and nitrogen (Shaw et al. 2003). Figure 2-2 illustrates the process of eutrophication from an agricultural perspective.
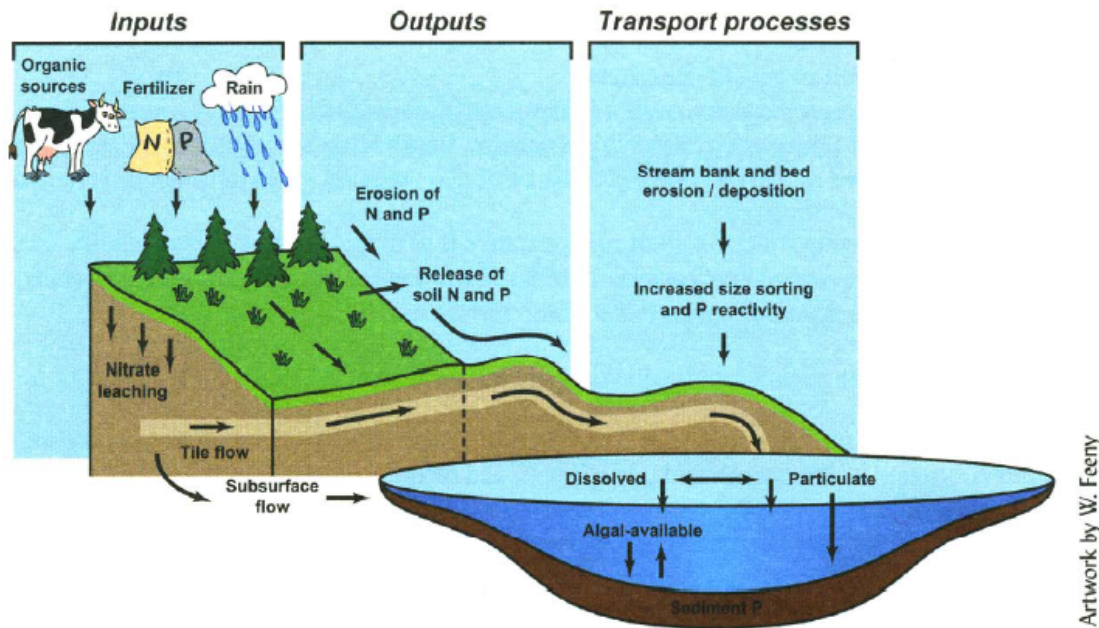
Figure 2-2: Process of eutrophication in agricultural runoff (Carpenter et a.l 1998)

Besides the visual effects of turning a clear water body into turbid green, eutrophication also results in oxygen shortages by means of bacterial decomposers (Carpenter et al. 1998). These zones of little or no oxygen are referred to as "dead zones." In the Chesapeake Bay, about 30% of the bottom waters are dead zones (mawaterquality.org).

Though the Chesapeake Bay Watershed demonstrates the most significant nutrient problem, the Delaware River Watershed, which Philadelphia lies within, presents its own pollutant issues. The Delaware River spans 330 miles from New York down through Pennsylvania and New Jersey and then deposits into the Delaware Bay (Delawareriverkeeper.org). The watershed provides many benefits to us in the forms of drinking water, recreation, variety of wildlife, as well as economic value. However, these benefits did not exist from the 1760s until the 1970s when the Delaware River was known as "one of the most grossly polluted areas in the United States" (Water Resources Agency 2013).

The Delaware River became so polluted that the American shad were unable to migrate through Philadelphia because of the zero oxygen barrier. All of this was turned around as a result

of the establishment of the United States Environmental Protection Agency (US EPA) in 1970.
Implementing these water quality standards led to exceeding the minimum dissolved oxygen
levels for the fish by 2005 (Water Resources Agency 2013). Though the Delaware River has
demonstrated the success of improving water quality, controlling the pollution is another issue in
itself. The tributaries to the river present numerous nonpoint source pollution that require a
variety of control methods to sustain contributing pollution to the Delaware River. One such
tributary is the Schuylkill River, in which its primary cause of impairment is from stormwater
runoff.

The Schuylkill River Watershed is approximately 1900 square miles, making it the
largest tributary to the Delaware River and a major contributor to the Delaware Estuary
(Philadelphia Water Department 2013). Figure 2-3 illustrates the entire Schuylkill River
watershed.
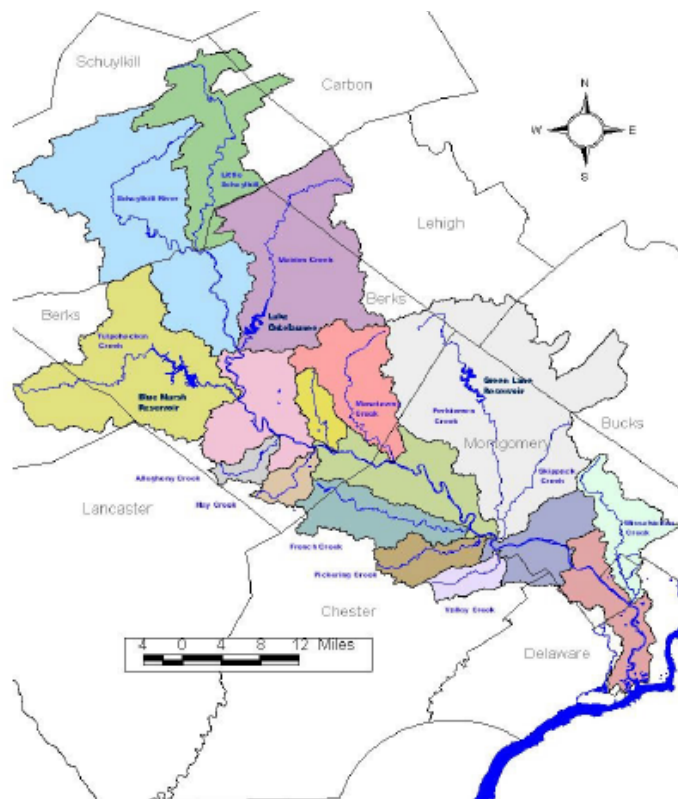
Figure 2-3: Schuylkill River Drainage Basin (Philadelphia Water Department 2002).

About 40% of the Schuylkill River is used for drinking water for about 1.75 million people (Philadelphia Water Department 2002). Having a watershed that is an important drinking water source only exemplifies the importance of keeping this river clean and unpolluted. The more polluted a drinking water source, the more expensive and difficult it becomes to treat the water to be within the drinking water quality standards.

In the 19th and 20th centuries when industrialization and mining was at its peak, the Schuylkill River felt the after effects of these pollutant contributing industries by becoming the most polluted rivers in the nation. As mining declined, a new source of pollution entered the Schuylkill River in the late 1800s, known as sewage. Sewage is a point source pollution and though it took almost 50 years from the 1905 Purity of Waters Act, a plan was finally implemented to prevent polluted sewage from entering the river (Philadelphia Water Department 2013). Controlling these point source pollutions became successful, nonetheless, nonpoint source pollutants are beginning to become a peak concern in the Schuylkill River. These nonpoint sources of interest are agricultural runoff, acid mine drainage, and of most alarm stormwater runoff.

The Schuylkill River watershed lies within some heavily populated counties such as Montgomery and Philadelphia, which contributes to altering the hydrologic cycle. As discussed before, impermeable rooftops and surfaces increase the total amount of storm runoff while minimizing infiltration and evapotranspiration. Within the Schuylkill River watershed, stormwater runoff is the primary cause of impairment for 273 mile of polluted streams (Philadelphia Water Department 2004).

2.3: Stormwater Control Measures

Though we cannot stop it from raining or prevent economic development, there have been ways developed to manage stormwater runoff. These preventative measures are referred to as best management practices or stormwater control measures. Stormwater control measures can be dated back to the Mesopotamian Empire during the second millennium BC with evidence of flood control practices as well as storing rain water for household and irrigation uses (NRC 2009). Nowadays, there are numerous types of SCMs that can control peak flow rates and also pollutants. To be more discrete, there are two subcategories of stormwater management practices, nonstructural and structural. Nonstructural measures are preventative practices that help in stopping the accumulation and pollution contamination of runoff, while structural measures attempt to control the volume and pollutants of storm runoff (Carson et al. 2009).

Whether the practice is structural or nonstructural, there are plenty of options for controlling stormwater runoff. These options vary based on the landscape, budget, and stormwater runoff goals. With smaller budgets and lot sizes, nonstructural practices are the best option and can consist of installing silt fences, proper lawn and auto care, as well as rain barrels or rain gardens. Most government agencies, educational institutions, and larger businesses enlist structural control measures for their stormwater management plans. These control measures included detention/retention practices (stormwater wetlands, detention ponds, etc.), vegetated swales, and infiltration methods (porous pavement, infiltration trenches, infiltration islands, etc.).

Beginning in the late 1990s, a completely new stormwater management approach was introduced to the United States as low-impact development (LID). LID represents "the ability to protect surface and ground water quality, maintain the integrity of aquatic living resources and ecosystems, and preserve the physical integrity of receiving streams" (Department of Environmental Resources 1999). The LID concept presents excellent values when disturbing or

altering a landscape is necessary, however, some may argue its effectiveness in treating stormwater runoff and interfering with land development. LID designs are introduced at the beginning of a site design with concept ideas of reducing impervious surfaces, increasing drainage flow paths, and minimizing directly connected impervious areas (Department of Environmental Resources 1999). An example of using LIDs in site design can be viewed in Figure 2-4, where the city of Puyallup, WA integrated rain gardens by reducing pavement into a local subdivision.

Figure 2-4: LID Example at city of Puyallup, WA (City of Puyallup 2013)

Though there are many options to consider in regards to stormwater management, there is only one best option to choose per landscape. These choices are highly dependent on the surrounding land, amount of land available, budget, and of course stormwater runoff goals. The most common stormwater management feature is rain gardens, a type of bioretenion device. Rains gardens manage stormwater by capturing runoff from surrounding impervious surfaces in which the plants and soils will absorb and filter pollutants before discharging the runoff to nearby streams (Carson et al. 2009). This type of stormwater treatment approach is only effective for short term treatment with low incoming flow. If an area is needed to treat incoming flow from several stormwater pipes, then a rain garden may not be the best SCM to select.

Nonetheless, rain gardens still provide an attractive and effective stormwater BMP for most residential or commercial site.

2.4: Natural and Constructed Wetlands

Before the 1970s, wetlands were recognized as providing little economic value and thus were constructed to other beneficial uses. As a result, about half of the natural wetlands that were established since the mid-1800s are now drained and filled within the United States (Mitsch and Gosselink 1993). Not until recently were these declining numbers halted because of research demonstrating a wetlands' ecological necessity in maintaining the hydraulics and hydrology of an area as well as providing wildlife habitat. The U.S. established several federal laws and regulations that prohibit any construction on or nearby a natural wetland. As of 2009, there is an estimated 110.1 million acres of wetlands in the United States, which may seem like a significant amount, but is only 5.2% of the surface area (US EPA 2013).

The value of wetlands lies within their natural ability to improve water quality. For example, a 1990 study on the Congaree Bottomland Hardwood Swamp in South Carolina showed that without this wetland, the area would need to construct a $5 million wastewater treatment plant (US EPA 2003). Wetlands are capable of removing pollutants through a combination of biological, physical, and chemical mechanisms. These processes include filtration and sedimentation (physical), sorption, precipitation, and evaporation (chemical), and microbial transformations and vegetative uptake (biological) (US EPA 2013). The way in which a wetland effectively uses these processes for each pollutant depends upon the wetland's hydrology and water chemistry. Both of these factors are dependent on landscape position, climate, soils, vegetation, and geology of the area (US EPA 2003).

Besides being able to treat water for contaminants, wetlands are also capable of peak flow reduction or as commonly referred to as flood control. In fact, the Mississippi river was capable of storing at least 60 days of flood water, but now only stores up to 15 days due to destruction of surrounding natural wetlands (US EPA 2013). Wetlands receive their water from nearby streams, rivers, or other discharge sources. When the flow of that particular water source is low, the volume of the wetland is significantly lowered. Wetlands can be referred to as nature's sponge because it traps and slowly releases the surface water, ground water, and precipitation (US EPA 2003). This holding capacity helps control floods and prevent future expenses of dredging a river.

Natural wetlands, being of diminished capacity, became protected by federal law and thus the constructed wetland was introduced. Beginning in the late 1970s, constructed wetlands were being researched and developed for the sole purpose of treating water. These studies indicated that constructed wetlands can be organized into three specific flow profiles; free water surface (FWS), horizontal subsurface flow (HSSF), and vertical flow (VF) (Kadlec and Wallace 2009). Though these types of wetlands differ on layout, plants, media, and flow patterns, their ability to treat water effectively is relatively the same. Although, the type of wetland should be chosen appropriately based upon treatment goals, landscape conditions, and climate.

Constructed wetlands serve a variety of treatment options ranging from acid mine drainage, wastewater, stormwater, and even agriculture. Most early applications of constructed wetlands were designed for domestic and municipal wastewater. It was not until the 1980s that constructed wetlands were built to treat acid mine drainage in the United States (Kadlec and Wallace 2009). The primary concern with mine water treatment is raising pH and removing metals, which wetland processes are capable of by having organic-rich substrates that exchange

dissolved metals (Smith 1997). The context of this study will pertain exclusively to using constructed wetlands to treat stormwater runoff.

2.5: Constructed Stormwater Wetlands

Though treating wastewater using constructed wetlands was implemented first, stormwater treatment was applied shortly after beginning in 1985 (Kadlec and Wallace, 2009). Like other applications of constructed wetlands, the design of the treatment system is crucially dependent on numerous factors as discussed previously. Various types of pollutants can enter a constructed stormwater wetland, and thus each must be factored into the design for proper treatment. Aside from pollutants, CSWs also are effective at controlling peak flow and reducing volume during storm events. In order to achieve optimal wetland design to treat for water quality and quantity, the hydraulic performance needs to be optimized. As a result of this hydraulic treatment, the hydrology and hydraulic conditions of a CSW became critical factors in determining the vegetation, pollutant treatment capacity, and overall performance.

The hydraulic performance in a stormwater wetland is dependent upon numerous factors, however, the most influential is hydraulic residence time (Fisher et al. 2009). The concept of hydraulic residence time (HRT) will be discussed in detail only pertaining to this research. For more introductory information in regards to hydraulic efficiency and hydraulic residence time of wetlands, please refer to Rinker 2013.

Hydraulic residence time is the time of travel of flow from inlet to outlet. Residence time is normally calculated by dividing the wetland volume by the flow rate through the wetland:

$$\tau_n = \frac{V_n}{Q}$$

14

Where τ_n = the hydraulic residence time, $V_{nominal}$ is the nominal wetland volume, and Q is the flow rate. Hydraulic residence time is a favorable variable to manipulate in order to increase treatment efficiency due to chemical and biological processes being heavily time dependent. Maximizing HRT will result in better treatment for a constructed wetland. Hydraulic residence time can be influenced by altering the shape and depth of the wetland, the length to width ratio, and adding more vegetation for flow resistance (Persson et al. 1999).

An expansion on HRT is residence time distribution (RTD) plots. Residence time distribution is a probability density function of the amount of time a particle remains in a wetland (Kadlec and Wallace 2009). These distribution curves provide indication of a wetlands preferred flow path, as well as stagnation and mixing effect (Kadlec and Wallace 2009). Knowing the RTD profile will assist in better constructing or retrofitting CSWs. For example, Villanova University's CSW 1.0 was retrofitted (CSW 2.0) with three meanders and a larger, deeper inlet pond in order to increase HRT.

In order to accurately determine hydraulic residence time and analyze a residence time distribution, a tracer study must be conducted. Introducing an inert tracer at an inlet with concentrations being measured at the desired outlet as a function of time is the basis of a field tracer study. The inert tracer should be chosen based on detection level and expense, with the idea that the tracer has low toxicity and high solubility (Kadlec and Wallace 2009). Three tracer type options, isotopes, ions and dyes, are the most popular to choose from (Chang et al. 2011). Isotopic tracers, like ^{15}N as ammonium, provides high accuracy in determining "the fate and transport of isotopic nitrogen in nutrient treatment" (Chang et al. 2011). Ionic tracers, such as Bromide, are not subject to degradation and are widely used in groundwater tracer tests (Kadlec and Wallace 2009). The most common inert tracer are dyes due to their low cost and low

detection limits, in particular the Rhodamine WT dye (Chang et al. 2011). Choosing Rhodamine WT does present downsides as it is susceptible to degradation and adsorption; this is why the dye is recommended for short term tests (retention time less than three days) and fields of study that are not abundant in organics (Kadlec and Wallace 2009). The conditions at CSW 2.0 allow for Rhodamine WT to be the most appropriate tracer selection, as well as it being inexpensive.

Besides providing HRT, tracer tests are also subjective to hydraulic indices. Short-circuiting indices are related to the distribution position along the x-axis of a concentration versus time plot (Wahl 2010). Faster flow paths as a result of topographic variations is considered short-circuiting. Another hydraulic index of concern in a CSW is mixing, which refers to the spread of residence time distribution (Wahl 2010). Wetlands contain numerous sections of water that are not cleared by the main flowing path, for example algae clusters or large patches of vegetation. These stagnant areas are commonly referred to as dead zones. The mixing index is primarily a result of dead zones. Figure 2-5 clarifies these two hydraulic indices on a concentration versus time plot.
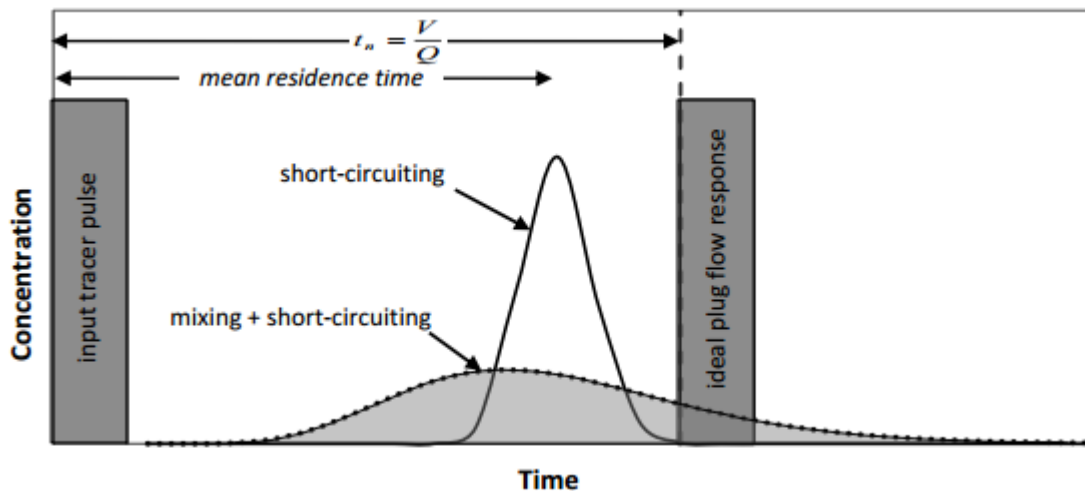
Figure 2-5: Residence time distribution curve for a tracer pulse injection demonstrating short-circuiting and mixing effects (Persson et al. 1999).

16

These hydraulic indices provide information pertaining to various wetland parameters that influence the RTD. Vegetation, the wetland shape and size, topography, and climate are the typical factors. Rinker (2013) provides mathematical reasoning into how residence time is affected by wetland vegetation. The tracer tests performed in this study will demonstrate how much these hydraulic indices affect CSW 2.0.

2.6: Thermal Enrichment

One of the many goals of constructed wetlands is to reduce peak flows by holding water in sediment forebays or sending it through various meanders. By keeping the water in the wetland as long as possible without becoming stagnant, the question of whether the temperature is affected negatively comes into play. There are numerous inputs and outputs that go into the energy budget of a wetland, all of which influence the water temperature (Figure 2-6).
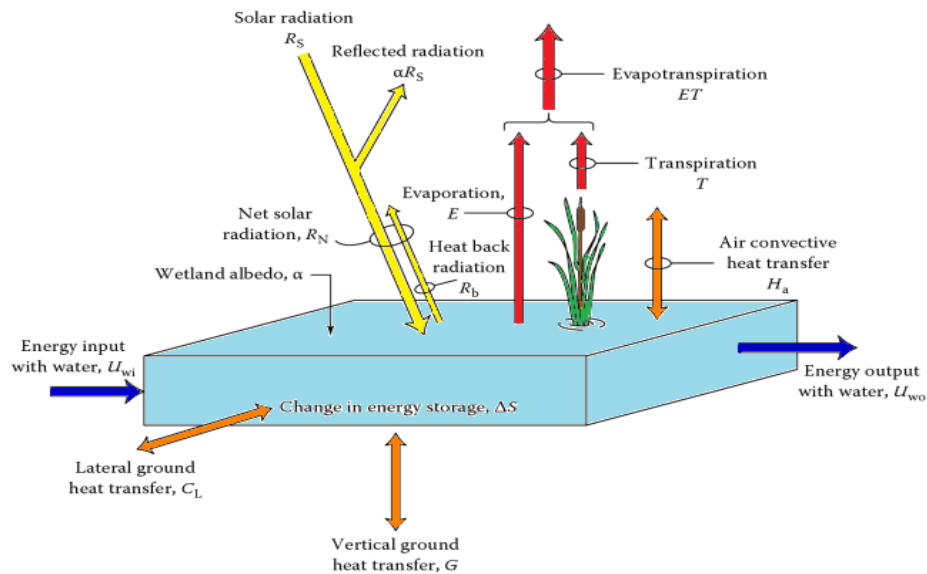
Figure 2-6: Components of a wetland energy balance (Adapted from Kadlec and Knight 1996)

Though a simple parameter to measure, temperature can provide insight into more complex water quality measures such as microbial life, dissolved oxygen, and nutrients. Nitrification and

denitrification are known to be highly temperature dependent in a wetland, thus affecting the overall treatment efficiency.

During the hot summer months, thermal impacts from urban stormwater runoff can result in poor treatment efficiency. Impervious surfaces, in particular asphalt, capture solar radiation and transfer this stored energy to stormwater runoff that results in elevated runoff temperatures. Asphalt can lead to surface temperatures beyond 60°C because of its low thermal conductivity and reflectivity (Asaeda et al. 1996). Especially in the detention ponds, there is no shade so these temperatures increase from runoff will result in negative effects on the treatment processes.

Evapotranspiration (ET) also plays a significant part in a CSWs treatment efficiency in regards to temperature fluctuations. The parameter is highly involved in an ecosystems' hydrologic cycle since it accounts for the sum of evaporation and plant transpiration from the surface to the atmosphere (Bois et al. 2005). Evaporation and transpiration are both influenced by the air temperature, solar radiation and humidity. According to the Penman-Monteith equation, when the air temperature increases so does the ET rate, however, there is some speculation that solar radiation can overcome temperature effects (Bois et al. 2005). Evapotranspiration is an important cooling mechanism in a treatment wetland. The ET rate serves the wetland as an energy loss process by means of the latent heat of vaporization of water (Kadlec and Wallace 2009). Without this energy loss system, the wetland temperatures would increase as a result of solar radiation not being dissipated (Kadlec and Wallace 2009). Due to the complexity of evapotranspiration in a wetland, this study will not be focusing on this cause of thermal pollution.

Turbidity, a measure of water clarity, also has a relationship with increasing water temperatures. In a stormwater wetland, turbidity can be the result of soil erosion, urban runoff,

eroding stream banks, and excessive algae growth (US EPA 2013). These factors can increase the turbidity, thus increasing the water temperature due to suspended particles absorbing more heat. Turbidity also causes many other treatment problems besides raising the water temperature, however, this research will only focus on turbidity as a factor of algae growth and urban runoff.

Figure 2-7: Turbidity effect on wetlands in respect to algae growth and urban runoff.

Temperature is an important controlling parameter for numerous water quality pollutants. One of such role of water temperature involves the rate influence of plant growth, more specifically with algae. Algae thrive off of excess nutrients by means of photosynthesis. Warmer water increases the rate of photosynthesis, so with the right amount of nitrogen and phosphorus algae can bloom throughout a body of water (Queensland Department of Natural Resources and Mines 2012). Excess algal blooms are very prone to becoming eutrophic. Eutrophic water bodies are extremely harmful and toxic; fish and other aquatic organisms are killed because of depleting oxygen levels (Shaw et al. 2003).

Though algal blooms are only a concern with rising water temperatures, dissolved oxygen levels are affected at warm and cold temperatures. The amount of oxygen that water can hold is very dependent upon the water temperature (Queensland Department of Natural Resources and Mines 2012). Dissolved oxygen (DO) concentrations are inhibited during warm weather and enriched in the cooler winter months (Kadlec and Reddy 2001). Figure 2-8

emphasizes the linear relationship between dissolved oxygen and water temperature. Fish are put under significant stress that can result in death when DO levels are below 5 mg/L (Chambers and Mill 1996). If DO levels rise above 9.0 mg/L then gaseous bubble disease can establish, which is fatal to aquatic life (Chambers and Mill 1996).
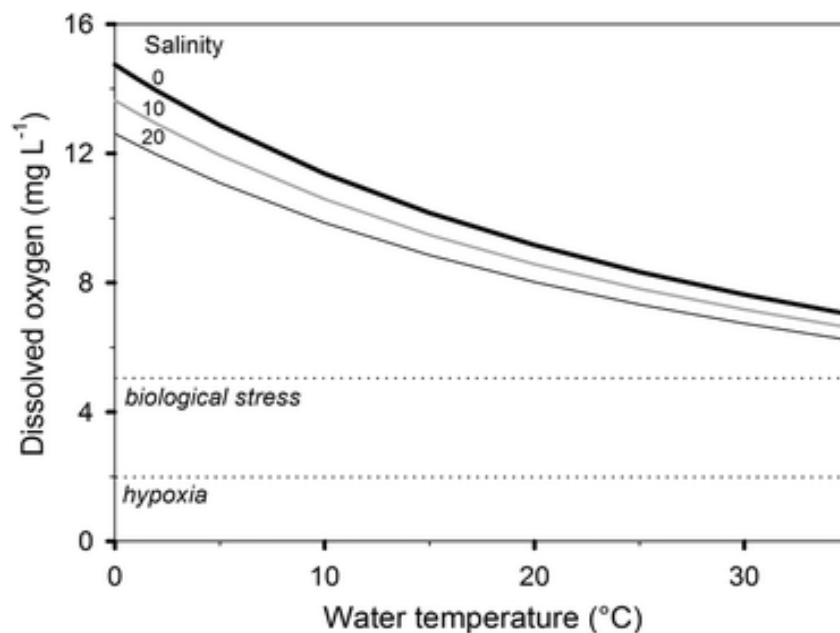
Figure 2-8: Dissolved oxygen versus water temperature with respect to salinity (Kadlec and Reddy 2001).

Not only are certain DO levels harmful to fish and other aquatic life, but so are water temperatures. In Pennsylvania Code 25, Chapter 93, there is a water temperature threshold for different types of fisheries. The fisheries are as follows; warm water fishery (WWF), trout stock fishery (TSF), and cold water fishery (CWF). Table 2-2 illustrates these maximum water temperature thresholds on a monthly and bimonthly level.

Table 2-2: PA Code water temperature thresholds for cold water, trough stock, and warm water fisheries

TIME PERIOD	CWF (°C)	WWF (°C)	TSF (°C)
January 1-31	3.3	4.4	4.4
February 1-29	3.3	4.4	4.4
March 1-30	5.6	7.8	7.8
April 1-15	8.9	11.1	11.1
April 16-30	11.1	14.4	14.4

May 1-15	12.2	17.8	17.8
May 16-31	14.4	22.2	20.0
June 1-15	15.6	26.7	21.1
June 16-30	17.8	28.9	22.2
July 1-31	18.9	30.6	23.3
August 1-15	18.9	30.6	26.7
August 16-31	18.9	30.6	30.6
September 1-15	17.8	28.9	28.9
September 16-30	15.6	25.6	25.6
October 1-15	12.2	22.2	22.2
October 16-31	10.0	18.9	18.9
November 1-15	7.8	14.4	14.4
November 16-30	5.6	10.0	10.0
December 1-31	4.4	5.6	5.6

The criterion for these specific temperatures is based on seasonal ambient temperature and biological thermal effects. These biological principles are based on gonad maturation, spawning, egg development, growth, and survival (PA DEP 2009). An additional stipulation to the fish temperatures is for the water temperature rate changes not to exceed 3.6°C per hour in order to eliminate thermal shock to the fish (PA DEP 2009). Though no duration for these maximum temperatures is specified, it can be presumed the compliance occurs over a 24 hour time frame, which accounts for the diurnal temperature fluctuation. For the practicality of this study, only WWF and TSF temperatures will be compared in regards to the outlet temperatures at the CSW.

Thermal stratification is the layering of water temperature and dissolved oxygen. Though this phenomena is typically only in lakes and ponds, stratification is still possible in the detention ponds of a wetland. Figure 2-9 illustrates the layering effect of water temperature and dissolved oxygen in the winter, spring, summer and fall.
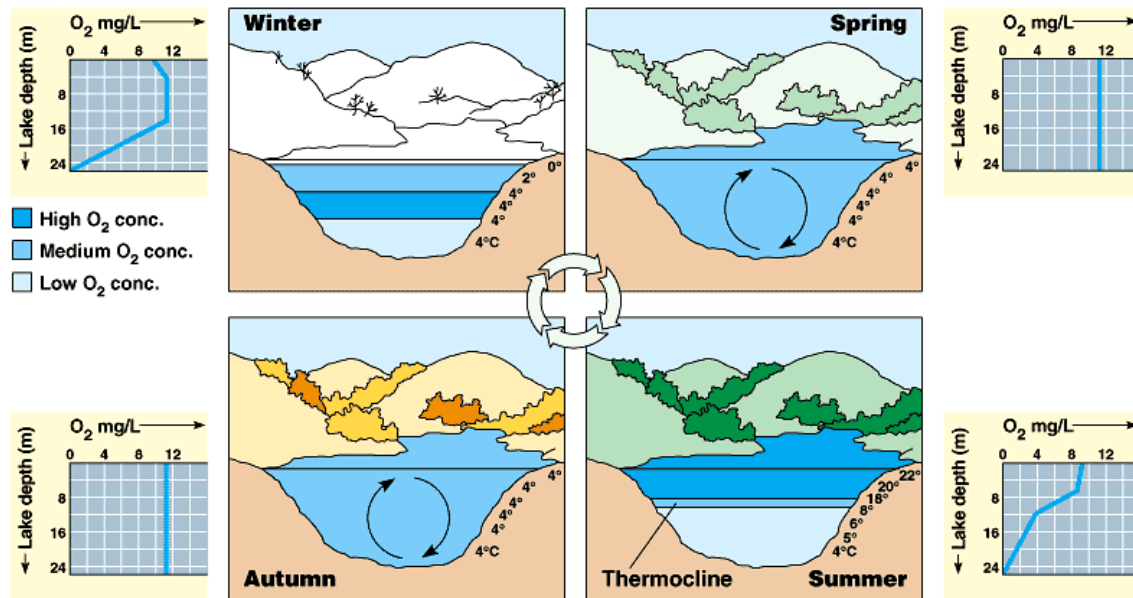
Figure 2-9: Lake stratification demonstrating seasonal temperature and dissolved oxygen variability (Johnson 2013).

During the spring and fall, the changing temperatures and higher wind speeds cause the water at the bottom to mix with the surface, resulting in no stratification. Summer presents the issue of thermal stratification by resulting in three water temperature layers; epilimnion, metalimnion, and hypolimnion. The warmest water is at the upper layer, or the epilimnion, where it is the least dense (Johnson 2013). The thermocline is where a rapid drop in temperature occurs before gradually cooling to the hypolimnion layer. The metalimnion prevents wind from mixing the entire volume of water, thus causing stratification between the epilimnion and hypolimnion.

Unseen to the naked eye, microorganisms play an essential role in maintaining a healthy ecosystem. Specifically in CSWs, microbes are key biological indicators of successful treatment due in part to their involvement in decomposition and the nitrogen cycle. Though there are few studies that relate thermal effects on microbial communities in wetlands, broader research topics on dissolved oxygen influence on microbes has been heavily studied. One such temperature study from Webster and Benfield (1986) indicated that at higher water temperatures, microbes

22

demonstrate faster decomposition of organic matter and induce high microbial production. However, faster organic breakdown can attribute to depletion of dissolved oxygen levels. If the water column is under anoxic conditions, then some bacteria will use sulfate instead of oxygen to decompose organic matter, resulting in accumulating sulfide by-product (Diaz and Rosenberg 1995). Toxic to many organisms, sulfide at large concentrates can also inhibit nitrogen treatment (Diaz and Rosenberg 1995).

A habitat constraint in aquatic environments, water temperature also directly impacts nitrogen removal processes. Figure 2-10 illustrates the complexity of the nitrogen cycle in a wetland. Microorganisms can remove nitrogen from water by way of two important biological processes; nitrification and denitrification. Both of which are dependent upon water temperature. From Figure 2-10, nitrification occurs when a bacteria known as *Nitrosomonas* converts ammonium and ammonia into nitrite then another bacteria called *Nitrobacter* turns nitrite into nitrate (UNHSC 2010). Nitrification occurs at aerobic conditions, meaning dissolved oxygen levels need to be above 1.0 mg/L. Besides being influenced by DO, nitrification rates are also affected by water temperatures. Temperatures between 25 and 35°C is the optimal range for successful nitrification rates. Above 40°C nitrification rates will drop near zero, while temperatures below 20°C will result in slower rates (The Water Planet Company 2009). However, if nitrifying bacteria are not present, nitrification will not occur until water temperatures rise to above 10°C (The Water Planet Company 2009).
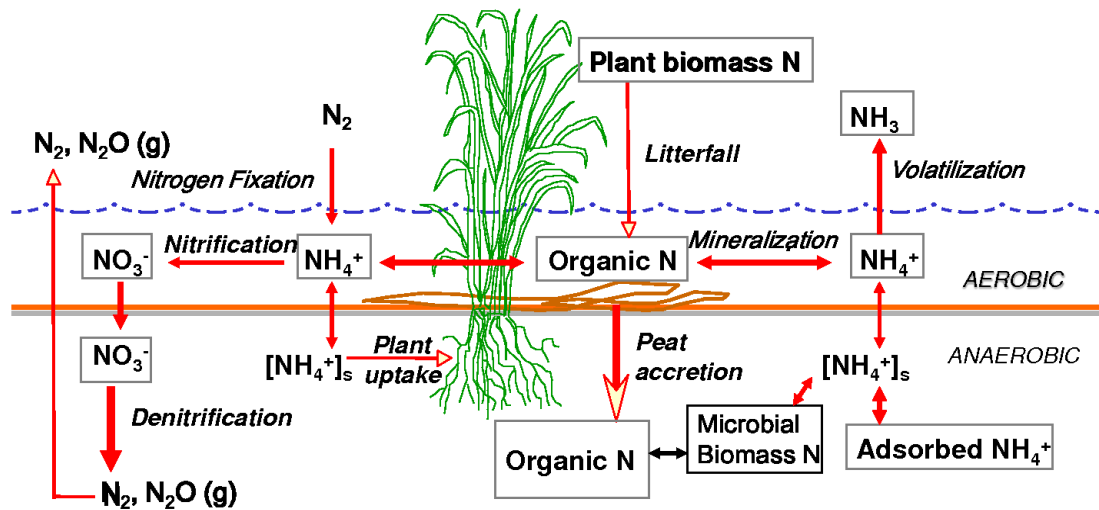
Figure 2-10: Nitrogen cycle in a natural wetland (Reddy and DeLaune 2008).

Denitrification requires opposite dissolved oxygen and water temperature conditions from the process of nitrification. Facultative heterotrophic bacteria reduce nitrate to nitrogen gas in the denitrification process (Reddy and DaLaune 2008). The bacterial organisms require a carbon source in an anoxic environment where dissolved oxygen levels are below 0.5 mg/L. Unlike nitrification, denitrification has broader temperature range for growth rate. Between 5 and 30°C, denitrification is occurring with growth rates increasing simultaneously with temperatures (The Water Planet Company 2009). In accordance to Figure 2-11, the denitrification growth rate increases as the water temperature becomes warmer.
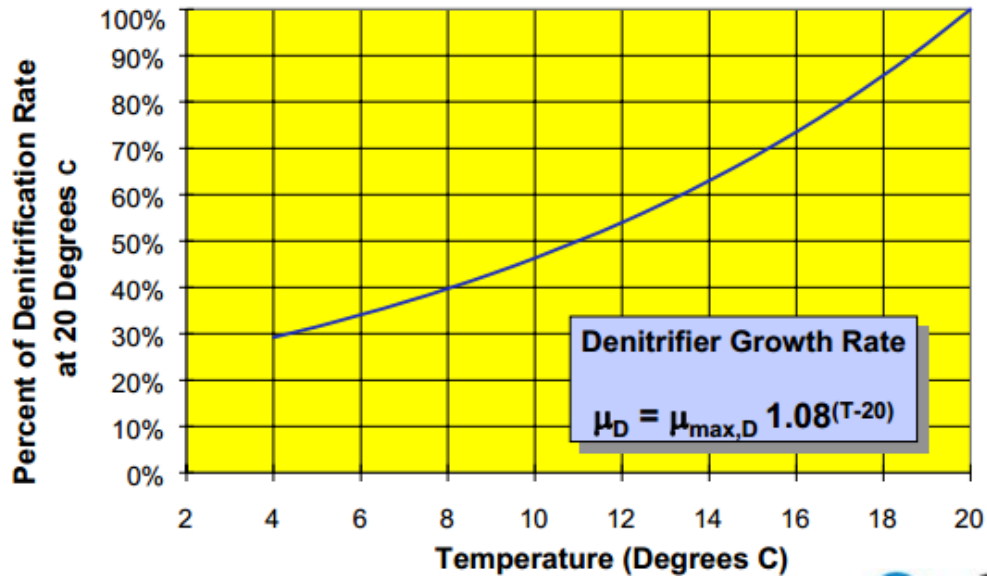
Figure 2-11: Denitrification rate versus water temperature in accordance to Arhennius expression (NY Department of Environmental Conservation 1996).

The denitrifier growth rate equation as seen in Figure 2-11, is a part of the Arhennius expression. According to Messer and Bresonik (1984), the Arhennius expression is the most commonly used for temperature-dependent biological processes:

$$k_{d,T2} = k_{d,T1}\theta^{T2-T1}$$

Where:

$k_{d,T}$ = *specific rate constant at temperature T (Celsius) with units inverse of time*

θ = *dimensionless empirical constant*

CHAPTER 3 METHODOLOGY

3.1: Introduction

The methodology section will entail the instrumentation and procedures used to analyze data that pertains to monitoring and assessing the CSW and its performance. The data collected in this research is divided into two sections; continuously monitored equipment and water quality laboratory testing.

3.2: Continuously Monitoring Instrumentation

In order to constantly monitor equipment at the CSW, Campbell Scientific CR1000 data logger (yellow font) were installed at five separate locations throughout the CSW – IT Inlet Main, SWW_FLOW, SWW_ET, M1, SWW_OUT (Figure 3-1).
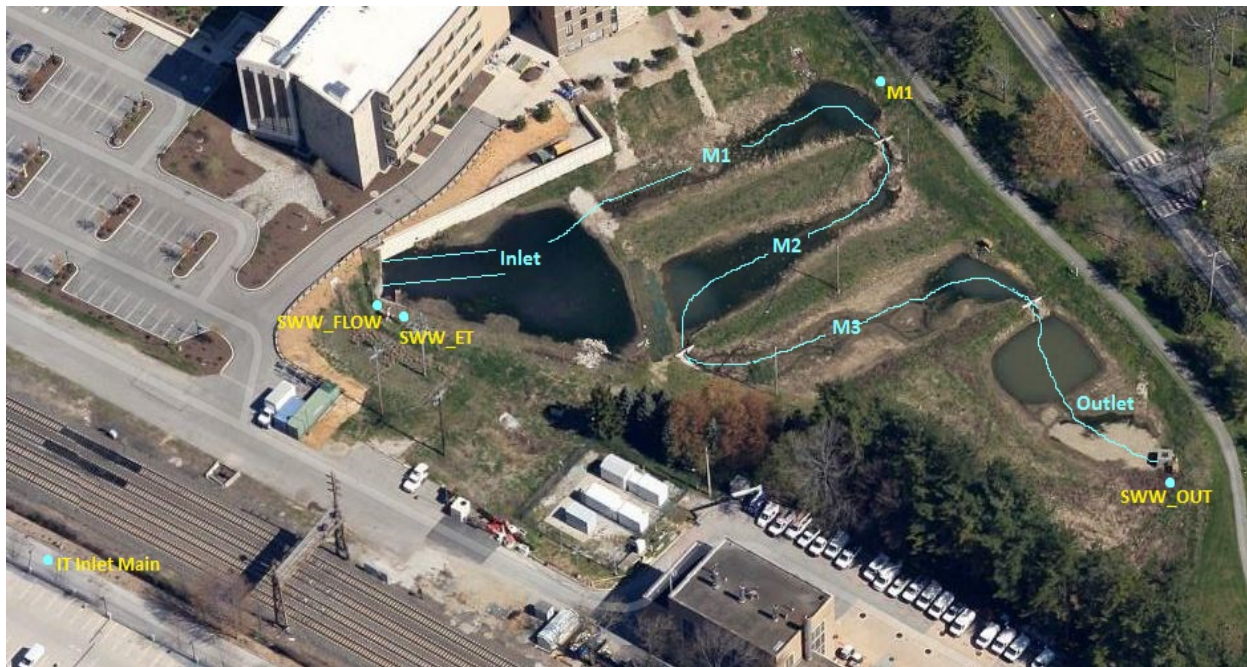
Figure 3-1: Location of CR1000 stations in the CSW

The CR1000 data loggers are programmable logic controllers that allow for certain instruments (e.g. flow or level meter) to be powered and communicate for data collection through a wireless server, i.e. Loggernet. For each instrument there is a computer code, CRBasic, written in order to

connect with the server. Each code is different for each instrument, nonetheless, the data collection procedure is the same for each. Data is scanned every twenty seconds and then output into a five minute average. Even though the location of the CR1000 data loggers has not changed, the instruments which are powered through them have. As a result, the monitoring equipment will be discussed based on the data they provided, and not by their location.

To provide hydrologic analysis of the CSW, there are flow meters located at the Inlet Main (IM), Inlet West (IW), and outlet. The flow meters at the CSW underwent recent upgrades due to inaccuracy and equipment failure. Since March 2012 and February 2013, the IM and outlet flow rates, respectively, are recorded using Greyline Instruments Inc., Area Velocity Flow Meters (AVFM 5.0). These flow meters have a ±2% accuracy on velocity and a ±0.25% on level. The velocity measurement range is from -5 to 20 ft/s; with the negative indicating reverse flow. Up until June 2014, the IW flow was measured using a Greyline Instruments Inc, AVFM II. Due to equipment failure, the flow meter was replaced with a Unidata Starflow 6526H Flow Meter in December 2014. The Starflow uses similar technology to the Greyline AVFM 5.0 flow meters with a velocity range between 0.07 to 14.8 ft/s bidirectional and a 2% accuracy of the measured velocity and 0.25% on depth. Besides measuring velocity and area (via measured depth and pipe shape) needed to calculate flow rate and volume, the Starflow also records the temperature. As a result of the broken IW flow meter, from June to November 2014 EPA's Stormwater Management Model (SWMM) was utilized to replace the missing flow data. More detail of the SWMM model development and usage is described in James Pittman (2011) and Mike Rinker (2013) theses.

The CSW also has two pressure transducers (PTs) that measure water depth and temperature. There is a pressure transducer at the exit of the IM pipe, which up until June 2014

was an Instrumentation North West (INW) PS9800. This PT was replaced with an INW PS9805 in July. The outlet also utilizes a pressure transducer, INW PS9805, which records the water depth going over a 90° V-notch weir at the outlet structure. The PS9805 PTs read between 0 and 5 psig with a ±0.1% Full Scale Output (FSO) typical accuracy. The operating temperature range is -5°C to 70°C. The thermistor of the PT has an operating temperature range between -24°C and 48°C with an accuracy of ±0.75°C (max) and ±0.3°C (typically).

At the inlet of the CSW there is also a weather station, which records solar radiation, wind speed, relative humidity, and ambient air temperature. The equipment is maintained for evapotranspiration research by Amanda Hess (2014). Also included in the weather data is a tipping bucket rain gage that records precipitation at 0.01 inch readings. Up until September 2014, an American Sigma 2149 rain gage was utilized, but then was replaced with a Met-One 375 Heated Rain Gage. Both rain gages have a resolution of 0.01 inch rainfall per bucket tip, as well as accuracy of 0.5% at 0.5 in/hour. The heater for the Met-One rain gage has a funnel and base heater that is set at 40°F. Having a heated rain gage allows for more accurate hydrologic analysis on snowfall events. The new heated rain gage was also factory calibrated before installation.

Aside from hydrologic and weather data, the CSW is also equipped with Dissolved Oxygen (DO) probes. Four In-Situ RDO Pro Dissolved Oxygen probes were purchased in early 2012. The DO probes provide readings between 0 and 20 mg/L with an accuracy of ±0.1 mg/L from 0 to 8 mg/L and ±0.2 mg/L from 8 to 20 mg/L. The operating temperature of the probes is 0°C to 50°C with a resolution of 0.01°C. The DO probes are calibrated approximately once every 6 months by a one point calibration method, which is at 100% saturation.

The locations of the DO probes has been changed frequently between the years of 2012 and 2014. In the 2012, a float that can hold three of the probes with different depth profiles at the deep zone of Meander 1 (M1) was constructed by Mike Rinker (2013). The depth profiles are 3 inches, 6 to 8 inches, and 10 to 18 inches below the water surface. The purpose of the DO instruments is to understand the diurnal fluctuation of DO levels and the effects DO has on the nitrogen cycle. There was also a fourth DO probe located approximately 10 feet upstream from the M1 float. In June 2013, the DO probe in M1 at 6-8 in depth was moved to the inlet at the concrete pier, while in April 2014 the DO probe upstream of M1 was placed at the outlet. Having a DO probe at the inlet, two at the M1 float, and the other at the outlet allocates for greater knowledge into the dissolved oxygen profile throughout the CSW.

Since the DO probes are equipped with temperature data, a thermal enrichment study of the CSW was able to be conducted. To supplement the temperature data from the DO probes and the PTs, four Campbell Scientific 107 temperature probes were installed throughout the CSW. These temperature sensors have an operating range of -35°C to 50°C with an accuracy of ±0.10°C over 0 to 50°C and ±0.4°C at -30°C. The 107 temperature probes do not require any sort of calibration. For more information on the temperature probes refer to Section 3.2.1.

3.2.1 Temperature Study

As stated previously, Campbell Scientific 107 temperature probes, In-Situ RDO Pro probes, and INW PS9805 PT are used to analyze temperature data in the CSW. The temperature accuracy and precision of the instrument is discussed in the previous section. Figure 3-2 illustrates the locations of the temperature reading instruments. Temp2IN and Temp3 were both located about 6 to 12 inches below the water surface, respectively, while the other temperature

probes (TempIMOut, Temp1, TempM1, TempM3, TempForebay, PT_OutTemp, and

Temp4Out) were effectively at the surface (i.e. only under 2 to 5 inches of water).
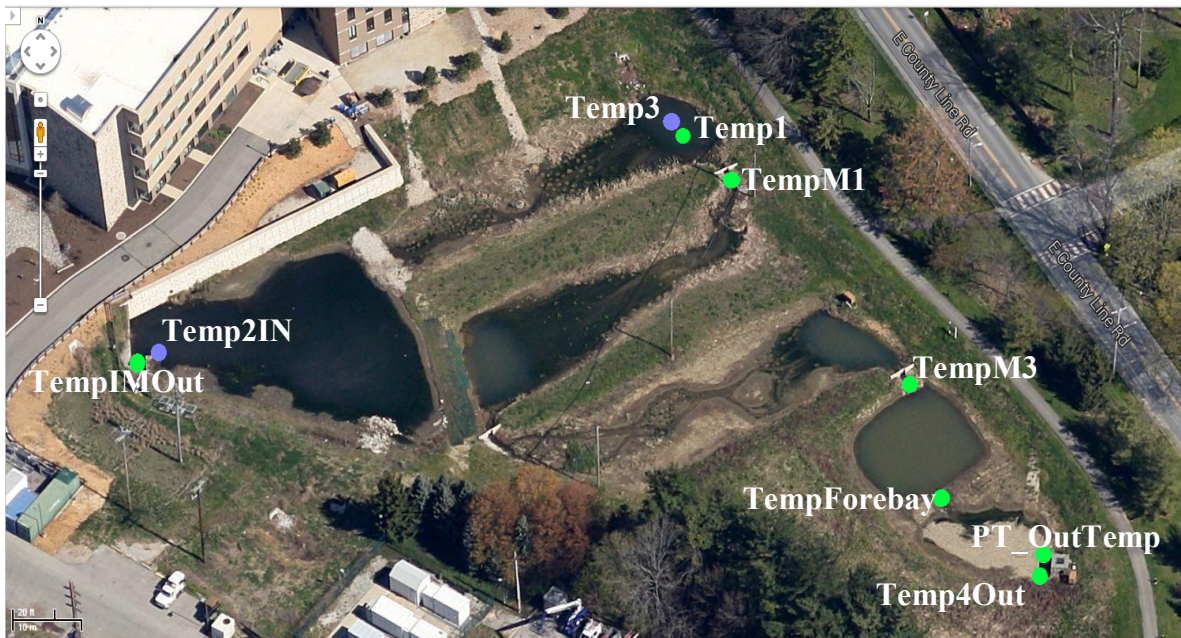
Figure 3-2: Temperature reading instrumentation locations (Green is close to water surface, purple is temperature reading about 6 to 12 inches below water)

At the outlet, PT_OutTemp records the water temperature through a one inch PVC pipe. Refer to

Figure 3-3 for illustrations of the outlet temperature instrumentations.
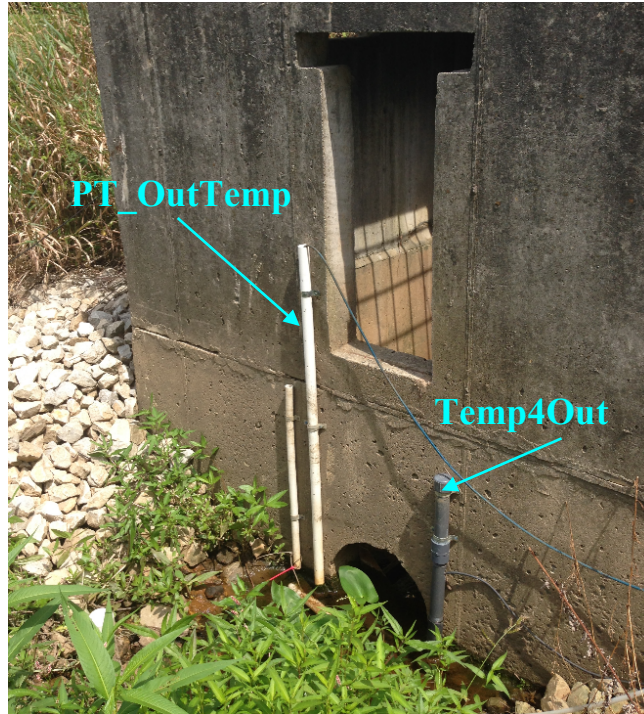
Figure 3-3: Outlet temperature reading instruments

Lastly, it should be noted that the installation dates of the instruments varies in 2013 and 2014 (Table 3-1). The dissolved oxygen probes (Temp2IN, Temp1, Temp3, and Temp4Out) cannot withstand temperatures below 0°C, and are taken out of the CSW in the winter.

Table 3-1: Temperature reading instruments and their deployment dates into the CSW

Instrument	Deployment Date(s)
Temp2IN	*June 21 to September 18, 2013* *March 18 to December 12,2014*
TempIMOut	*June 9, 2014 to Present*
Temp1	*April 18 to October 30, 2013* *April 5 to November 10, 2014*
Temp3	*April 18 to October 30, 2013* *April 5 to November 10, 2014*
TempM1	*August 1, 2014 to Present*
TempM3	*August 1, 2014 to Present*
TempForebay	*July 18, 2014 to Present*
Temp4Out	*April 5 to November 18, 2014*

| PT_OutTemp | *July 27, 2012 to Present* |

To study temperature as a water quality parameter at the CSW, numerous graphs and statistics were analyzed. On the basis of storm events for this study, only cumulative rainfall greater than 0.10 inches within 24 hours were accounted for. Storms are differentiated on the basis of six hours of dry time separation after rainfall has ended. A storm event is considered finished when the outlet flow rate drops below 0.10 cfs within 72 hours after the rainfall has ended. A MATLAB program was created to generate storm events based on the rainfall data presented in five minute intervals. Storm events were analyzed beginning in April 2014 until the end of February 2015.

Besides storm events, temperature data was also analyzed on a daily and monthly level. Organizing the data on a daily basis allowed for investigation on weather parameter (e.g. air temperature, solar radiation and wind) influence on the CSW's water temperature. To limit the amount of daily temperature data, only the 2014 months of June through November were analyzed for daily temperatures. For the monthly analysis, 2013 and 2014 available temperature data was used. Using monthly data allowed for statistical analysis on how the inlet water temperatures varied from the outlet, in addition to the rainfall amount and air temperature influence on the CSW water temperature.

Thermal stratification was analyzed at two separate locations within the CSW. At the M1 float, as seen in Figure 3-4, there are two DO probes in which one is located near the water surface and the other about 12 inches below.

Figure 3-4: M1 Dissolved oxygen monitoring station

The second location was at the inlet where a temperature probe was near the water surface, while a DO probe was under 6 to 12 inches of water, which varied during baseflow and storm events and evaporation. Figure 3-5 illustrates the location of the two inlet temperature instruments.

Figure 3-5: Locations of inlet temperature instruments

The inlet and M1 temperatures were statistically analyzed on a daily and monthly basis. For the inlet, only the 2014 months of June through December were available. The thermal stratification analysis at M1 utilizes data from 2014.

The observed water temperatures at the CSW were compared to aquatic life temperature thresholds. The Pennsylvania Code 25 Chapter 93 contains the maximum water temperature threshold for three types of fisheries; warm water fishery (WWF), trout stock fishery (TSF), and cold water fishery (CWF). For the practicality of this study, only WWF and TSF temperatures will be compared in regards to the outlet temperatures at the CSW.

3.2.2: Rhodamine Tracer Study

For the tracer dye tests performed at the CSW, two Precision Measurement Engineering Inc. Cyclops-7 Loggers were utilized. These field-deployed instruments measure Rhodamine WT concentration using a fluorescent light sensor. The data is recorded at five minute intervals and stored into a 2GB SD card. Because of the SD card, the loggers are not integrated with the CR1000 data loggers. Nonetheless, the loggers are still continuously monitored at 5 minute intervals when deployed at the CSW. The sensor within the instrument is a Turner Designs Cyclops 7 submersible sensor. The sensor operates using a visible light emitting diode to sense Rhodamine concentration in a solution with a range of 0 to 1,000 µg/L (ppb). The minimum detection limit of the sensor is 0.01 ppb.

Since the instruments utilize fluorescent light to measure Rhodamine concentration, it is suspected to have inaccurate readings at times. These inaccurate measurements occur when the instrument is buried in sediment or algae. For a couple of tracer tests this exact situation occurred. To correct for this problem, linear interpolation was used to fill in the missing concentration data. Sediments, algae, and dissolved solids also result in background concentrations of compounds contained in the rhodamine tracer throughout the CSW. Most background concentrations at the CSW were below 1 ppm, thus no corrections were made for

this concentration. In addition, the requirements of the study was to determine the residence time in the system, which allows for less strict precision requirements.

For this particular study, Keystone Rhodamine WT dye was used as the tracer. The tracer dye is a concentrated solution of 200,000 mg/L in a one gallon container stored at room temperature. A calibration standard of 100 ppb using the stock solution was made in the water resources laboratory. The two sondes were calibrated using a two point procedure, one solution of 0 ppb and the other being 100 ppb. The instruments were calibrated a day or two before being deployed into the field. Additional quality assurance was made by creating a calibration curve for each sonde at different Rhodamine concentrated solutions. This type of calibration was only done once every couple months in order to ensure the instruments are operating effectively. These calibration curves can be found in Figure A-1 and A-2 in the appendix. Figure 3-6 displays the various concentration levels of Rhodamine dye.
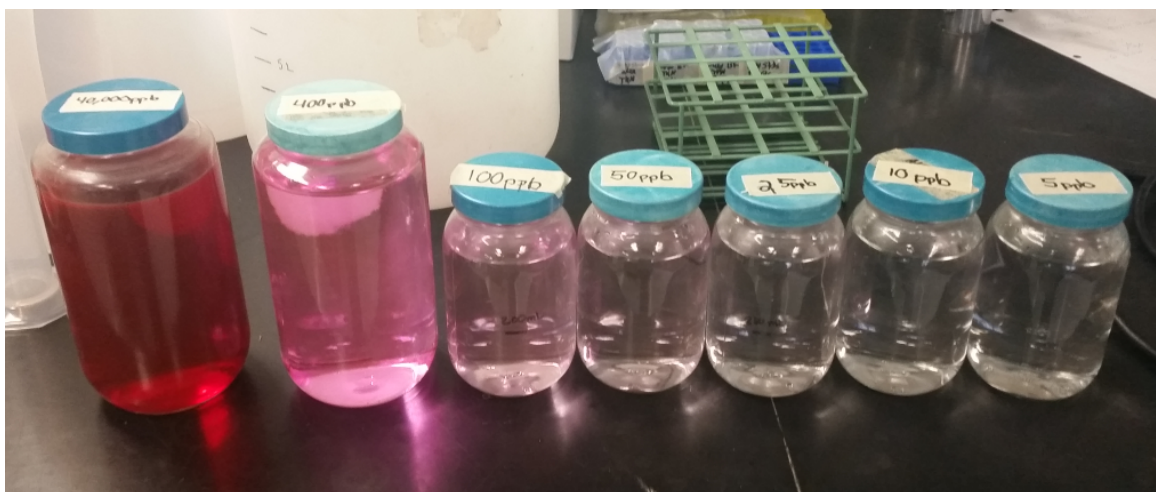
Figure 3-6: Rhodamine concentration standards (From left to right; 400,000, 400, 100, 50, 25, 10, 5 ppb)

The amount of dye released into the CSW was measured using 10mL pipettes and 250 mL graduate cylinders. To ensure all of the dye was completely rinsed from the measurement tools,

deionized water was used to wash off the glassware. The mass of tracer input into the system was calculated from the measured volume of dye released and the concentration of the stock solution.

Since there were two Rhodamine sondes, when a dye study was performed both instruments were deployed. The locations of these instruments varied for each tracer test event. For research purposes, only a couple tests were performed with a sonde located at the end of meander 2 and another at the start of meander 1. The majority of the tracer tests had a Cyclops 7 sonde at the end of meander 1 and the other at the outlet structure. Reference to these locations are illustrated in Figure 3-7.

Figure 3-7: Locations of rhodamine dye discharge and Cyclops-7 sondes (Blue and pink indicate where the dye was released and its corresponding sonde locations for the matching color)

The tracer tests performed and analyzed are depicted in Table 3-2. Unless noted, the dye for the tracer tests was released at the beginning of the inlet pond.

Table 3-2: Tracer tests performed between 2013 and 2014 (Blue indicating storm events; Green represents baseflows)

Tracer Test Date	Location 1	Location 2	Pathway 3	Dye Duration Study (hrs)	Dye Released (mL)
11.7.2013*	End of M2	Outlet	End of M2 to Outlet	120.8	60
12.6.2013*	End of M2	Outlet	End of M2 to Outlet	51.7	60
3.28.2014*	End of M2[1]	Outlet[2]	End of M2 to Outlet	122.2[1] and 53.3[2]	25
4.7.2014	Start of M1	End of M1	Start of M1 to End of M1	70.9	28
4.25.2014	End of M1	Outlet	End of M1 to Outlet	66.3	25
5.18.2014	Start of M1	End of M1	Start of M1 to End of M1	72.0	25
6.19.2014	End of M1	Outlet	End of M1 to Outlet	140.9	40
7.14.2014	End of M1	Outlet	End of M1 to Outlet	137.8	52
8.1.2014	Start of M1	End of M1	Start of M1 to End of M1	139.7	39
8.8.2014	End of M1	Outlet	End of M1 to Outlet	172.2	65
8.28.2014	End of M1	Outlet	End of M1 to Outlet	191.8	52
9.13.2014	End of M1	Outlet	End of M1 to Outlet	213.2	100
10.22.2014	End of M1	Outlet	End of M1 to Outlet	213.2	105
11.11.2014	End of M1	Outlet	End of M1 to Outlet	186.8	100
12.6.2014	End of M1	Outlet	End of M1 to Outlet	189.6	100
3.18.2015	Start of M1	Outlet	Start of M1 to Outlet	196	102

Dye was released at End of M1

Due to the unpredictability of storms, each storm event tracer test varied based on rainfall accumulation up until the dye was released. The ideal protocol was to discharge a measured amount of Rhodamine dye at the inlet after 0.20 to 0.25 inches has fallen, which is large enough to be considered a storm event.

Baseflow tracer events were performed in addition to storm events. A baseflow is when there has been no more than 0.10 inches of rainfall within the past 72 hours. For each tracer test, the Cyclops 7 probes are left in the CSW between 5 and 8 days to ensure complete dye recovery. As a result of the slim chance of their being 7 days without any rain, the duration of a baseflow tracer test would occasionally have a storm or two. These spontaneous storm events are noted with each dye tracer test performed.

Once the data was downloaded and organized from the Cyclops-7 sondes, a MATLAB program analyzed the recorded concentration according to several parameters, including peak concentration and corresponding time, mean retention time, variance, and standard deviation. The mean retention time represents the first moment of the residence time distribution (RTD) curve, while the variance is the second moment. Equations 3-1 to 3-2 display the formulas used to calculate mean retention time ($\bar{t}$) and variance (σ_t^2)

$$Eq\ 3.1 \quad \bar{t} = \frac{\int_0^\infty t\, C(t)dt}{\int_0^\infty C(t)dt}$$

$$Eq\ 3.2 \quad \sigma_t^2 = \frac{\int_0^\infty C(t)(t - \bar{t})^2 dt}{\int_0^\infty C(t)dt}$$

where C(t) is the concentration of Rhodamine dye with time (t). Besides time based analysis on the RTD, dye mass recovery was also determined for certain tracer tests. Due to mass recovery (M_r) requiring flow rate (Q) for the calculation (Equation 3-3), only events in which a sonde was placed at the outlet were analyzed.

$$Eq \ 3.3 \ M_r = \sum (C\Delta t) \, Q$$

3.2.3 Peak Flow Analysis

Data collected from the Greyline and Starflow flow meters is processed according to storm events and baseflows. Pertaining to this research, only storms will be analyzed and discussed as opposed to baseflow events. To prevent bias data due to inaccurate flow meters, flow rates will only be analyzed from March 2013 to February 2015.

A Matlab program was created to analyze the flow data for storm events. Storm events (more than 0.10 inches in 24 hours, with at least 6 hours of dry time between events and an outlet flow rate below 0.10 cfs within 72 hours after rainfall has ended). After 72 hours of dry time (cumulative rainfall not exceeding 0.10 inches), the CSW is at baseflow conditions.

The IM and IW locations are not the only pipes that discharge into the CSW. There are also two other locations which can produce a significant amount of flow during storm events. Figure 3-8 illustrates all of the inlet pipes, including the non-monitored locations.
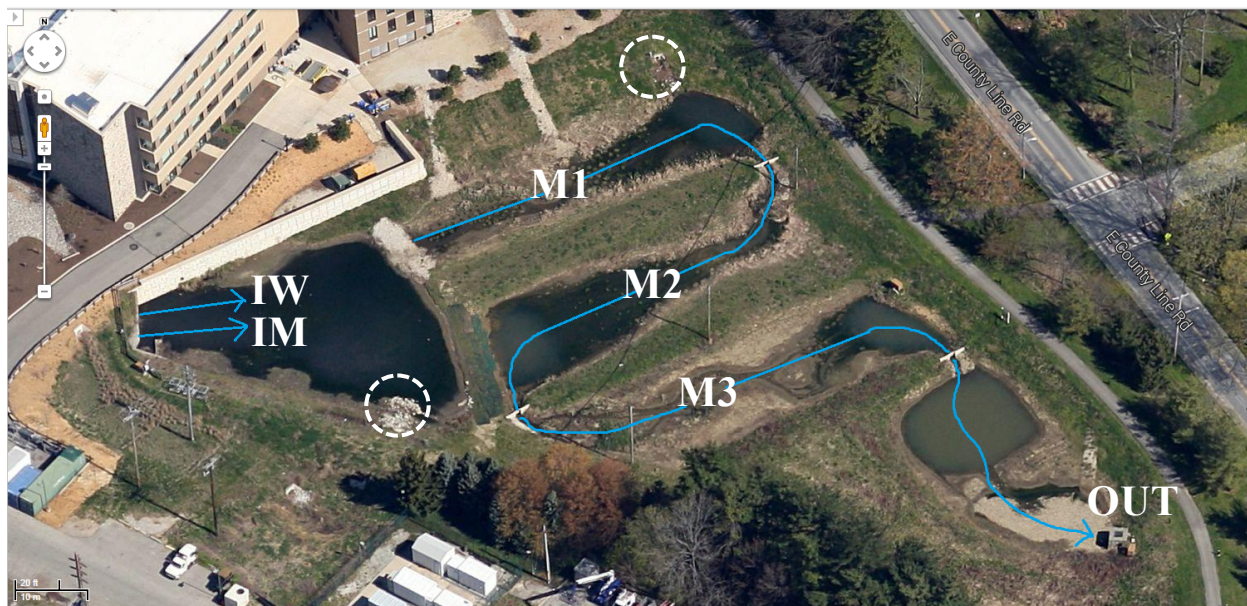
Figure 3-8: Aerial view of CSW with reference to the two unmonitored inflow pipes (dashed circles)

Rinker (2013) performed a SWMM analysis on these pipes and concluded that during times of precipitation 17% of additional flow on average is added to the inlet flows. Accounting for the additional flow is referred to as adjusted inlet, as opposed to just inlet which only includes the flows of the two monitored pipes.

The hydraulic performance of the CSW during storm events will be studied on the basis of peak flow and volume reduction. Peak flow reduction is calculated by taking the highest adjusted or unadjusted inlet flow rate and subtracting it from the highest outlet flow rate during a storm event. Peak lag time is also taken into account by determining the time difference between the highest inlet and outlet flow rates. The storm inlet and outlet volume is the sum of the flow rates for the entire event and multiplied by the time interval of 300 seconds. The time interval is a result of the flow rates being a five minute average.

3.3: Sample Collection Protocol

Sample collection for water quality analysis is written in the Quality Assurance Project Plan (QAPP) and approved by the US EPA Region III. The CSW is sampled at least once a month for storm and baseflow events. Storm events are specified as cumulative rainfall greater than 0.25 inches within a 24 hour time period. A baseflow event is less than 0.10 inches of rain within the past 48 to 72 hours. The sampling technique, locations, and bottles for the CSW underwent new protocols in early 2014. From 2011 to February 2014, 350mL glass bottles were used to sample the CSW. Beginning in March 2014, new HACH 575mL polyethylene bottles were then used to accommodate for more sample volume to be filtered in the total dissolved solids (TDS) and total suspended solids (TSS) testing. The new sampling bottles were also utilized in the autosamplers for storm events. To ensure quality control, these sampling bottles

were washed in a dishwasher with laboratory approved detergent and then acid washed in Hydrochloric Acid (HCl) solution.

Before the use of autosamplers, storm events were sampled as duplicate grab samples at the inlet, meander 1, 2 and 3, and at the outlet. These grab samples were usually collected within 24 hours after a storm has ended. In the case that the autosamplers did not work during a storm event then the grab sampling technique was enacted instead at the inlet, meander 1, and the outlet.

The reason for switching to 575mL sampling bottles is due to the use of American Sigma 900MAX autosamplers for capturing storm events. There are three autosamplers at the CSW; one at the inlet, meander 1 and at the outlet. Using autosamplers allows for a more representative water sample during a storm event, as opposed to grab sampling a day after a storm. The use of these autosamplers did not begin until April 30, 2014. Sampling at M2 and M3 for storm events was eliminated because of no access to power the autosamplers. The autosamplers are programmed according to rainfall accumulation in a 24 hour time frame. For more detailed information on the autosampler programs refer to Appendix A. There are three samples taken per bottle; these samples are triggered by a pulse sent from the CR1000 via a HACH auxiliary cord and correlate to rainfall depths. Figure 3-9 displays the four sampling bottles in each autosampler and the amount of rainfall needed for the sample to be taken.
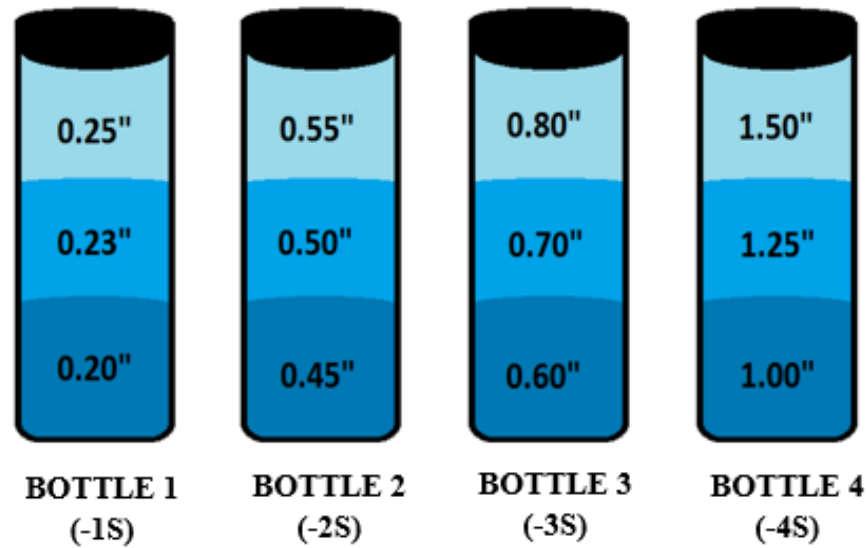
Figure 3-9: Autosampler bottles for sampling of CSW during a storm event.

Each sample is approximately 190 mL, give or take a few milliliters due to air pockets in the intake line and the small opening space of the sample bottle. To eliminate some of the missing sample volume for each bottle, polyethylene funnels were used to capture most of the water. Figure 3-10 illustrates the setup of the sampler bottles in an autosampler.
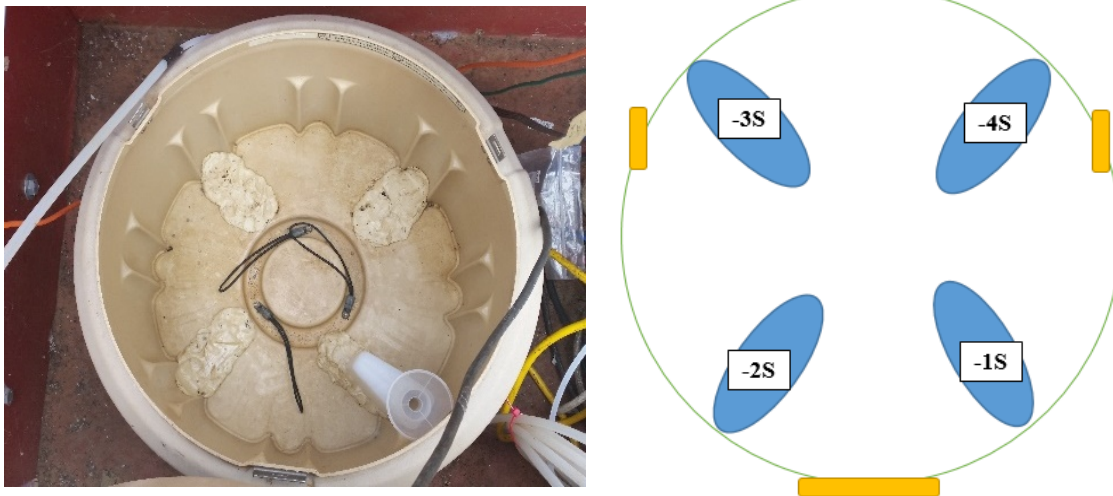
Figure 3-10: Photograph of CSW autosampler bottle setup (left) and Schematic and sample labeling of autosampler bottle locations (right)

In regards to the air bubble issue, the intake line at the inlet is placed under six inches of water right beside the inlet DO probe. However, the meander 1 and outlet has a much shallower water

depth, so HACH high velocity/shallow depth intake line strainers were added as an attempt to eliminate some of the air pockets. The two strainers are 3.9 inches long with a 0.406 inch outer diameter.

Baseflow sampling utilized the same grab sampling technique up until June 2014. From July 2014 to February 2015, the grab sample location at meander 2 was temporarily removed due to sampling access limitations of overgrown vegetation. Figure 3-11 depicts the various sampling locations for the most recent baseflow and storm events.

Figure 3-11: Baseflow and autosampler storm event water quality sampling locations (Green is baseflow and Blue is storm events)

The sampling names for both autosampler storm events and grab samples are documented in Table 3-3. The grab samples are for storm and baseflow events.

Table 3-3: CSW water quality sampling location names

Location	Grab Sample Names	Autosampler Names	
Inlet	IN1	IN-1S	IN-3S
	IN2	IN-2S	IN-4S
Meander 1	M1-1	M1-1S	M1-3S
	M1-2	M1-2S	M1-4S

Meander 2	M2-1 M2-2		
Meander 3	M3-1 M3-2		
Outlet	OUT1 OUT2	OUT-1S OUT-2S	OUT-3S OUT-4S

3.4 Water Quality Testing and Instrumentation

After sample collection, the water samples are taken to the Water Resources Laboratory at Villanova University. All laboratory glassware, containers, and other measuring devices are acid washed in the appropriate solution and stored in cabinets or bins to prevent contamination. The two acid wash solutions are 1:10 HCl and Nitric Acid.

Once the samples are brought to the laboratory, pH, conductivity, TSS and TDS are tested the same day as collection. Samples are preserved by adding 0.1 mL of Nitric Acid for every 50 mL of sample. The preserved samples serve for additional water quality tests with required holding times longer than 24 hours. Once the samples are poured into the raw sample bottles, they are then used to test for pH and conductivity. These two water quality parameters are tested by using a HACH HQ40d multiprobe. The pH probe of the multiprobe is calibrated before use in solutions containing a pH of 4.00, 7.00 and 10.00. Conductivity is calibrated in a 1,000 µS/cm solution.

For TSS and TDS testing before March 1, 2014 (when 300 mL bottles were used) 150mL of sample, if available, was poured into a vacuum apparatus and filtered through a Whatman 47 mm microfiber filter. After March 1, 2014 (when the 575 mL sample bottles were used), 300mL of the sample, if available, was filtered. If there was not enough sample volume, the reduced amount is accounted for in the TSS and TDS analysis calculations. After filtering, the TSS filters were placed in an oven at 100°C between 4 and 6 hours and the TDS beakers were put in an oven

at 400°C for at least 24 hours. After the beakers and filters were dried, they were weighed (with

an accuracy of 1/10,000 g) and recorded into an Excel spreadsheet that calculated the TSS and

TDS in mg/L.

For further water quality testing on the raw samples, the Laboratory Director utilized a

Systea Scientific LLC, EasyChem Plus spectrophotometer. There are seven tests performed on

the CSW samples using the EasyChem (Table 3-4).

Table 3-4: Water quality parameters tested on the EasyChem

Parameter	Raw or Preserved	Holding Time
Nitrite	Raw	24 hours
Phosphate	Raw	48 hours
Ammonia	Raw	48 hours
Nitric oxides	Raw or Preserved	48 hours for Raw 28 days for Preserved
Total Kjedhal Nitrogen	Preserved	28 days for Preserved 48 hours after digestion
Total Phosphorus	Preserved	28 days for Preserved 48 to 72 hours after digestion
Chloride	Raw	28 days

Both Total Kjeldahl Nitrogen (TKN) and Total Phosphorus (TP) require digestion before

being analyzed on the EasyChem. The TKN digestion involves 25 mL of preserved sample along

with standard into digestion tubes. Then 5 mL of copper sulfate digestion matric is added to each

glass tube, which are then placed in a digester for two different heating cycles. The samples are

first heated for 60 minutes at 160°C and then at 380°C for 90 minutes. Once digestion is

completed, the remaining solution in each digestion tub is diluted with Milli-Q water into a 25

mL flask. After shaking the flasks to ensure complete mixing, the samples are poured into EasyChem sample cups and ready to testing on the EasyChem.

The TP digestion is significantly different from the TKN procedure as it utilizes a Tuttnaer 2540M autoclave instead. The procedure begins by pipetting 5 mL of the preserved sample and standards along with 0.1 mL of 11 N sulfuric acid and 0.04 g of ammonium persulfate crystals into a glass vial. The prepared vials are placed into the autoclave, which is set at 121°C and 15 psi for 30 minutes. After 30 minutes has elapsed, the remaining samples are poured into EasyChem cups and analyzed on the EasyChem.

For each water quality parameter, the EasyChem uses a particular wastewater method for sample analysis. There are also restrictions to the EasyChem in the context of concentration range and method detection limits (MDL) (Table 3-5).

Table 3-5: EasyChem concentration detection limits and ranges

Inorganic Test	EPA Method	Range (mg/L)	MDL (mg/L)
Ammonia	310.2	0.010 – 5.0	0.0010
Chloride	325.2	0.5 – 200	0.2
Nitrite	353.2	0.010 – 10.0	0.0015
Nitric oxides	353.2	0.010 – 10.0	0.005
Ortho-Phosphate	365.1	0.010 – 5.0	0.005
TP	365.4, 365.1	0.01 – 20.0	0.005
TKN	351.2	0.10 – 20.0	0.05

It should be noted when a sample exceeds the highest concentration range, particularly for chlorides, that sample is then diluted until it reaches the maximum quality assurance concentration. Afterwards the dilution is then accounted for in the final concentration value. When a sample is below detection limit, referred to as non-detects, the value is reported as half the detection limit (EPA Technical Guidance Manual). Additional information on the quality

assurance and quality control measures taken for water quality testing on the CSW are in the QAPP, which is available online from the VUSP website, www.villanova.edu/VUSP.

Aside from using the EasyChem for measuring water quality parameters, two additional constituents can be determined. Nitrate (NO_3^-) is calculated by subtracting nitrite from nitric oxides. Total Nitrogen (TN) is determined by adding TKN and nitric oxides together.

3.5 Water Quality Data Analysis

The water quality data analyzed herein spans from 2011 to the end of 2014. For quality assurance and quality control purposes, not every parameter was available per testing event.

Since grab samples were duplicates at each location, the average along with standard deviation between the two samples was calculated in order to analyze removal efficiency at the CSW. As a result of switching from grab samples to autosamplers for storms, the autosampler storms were separated from the overall CSW storm event performance analysis. Instead, the two types of storm event performances, grabs and autosamplers, were compared based on inlet and outlet concentrations. In addition, the trend of water quality concentrations from bottle 1 to bottle 4 were also studied to research the impact of rainfall amount and intensity.

In addition to overall storm and baseflow performance at the CSW, a seasonal analysis was conducted for these events. The seasons are organized as Summer (June 1 to August 31), Spring (March 1 to May 31), Fall (September 1 to November 30), and Winter (December 1 to February 28). By breaking down the water quality data by seasons allows for further understanding on the influences surrounding the removal processes. These removal processes consist of nitrification, denitrification, and phosphorus reduction through chemical adsorption, physical sedimentation, or vegetation and microbial uptake.

47

CHAPTER 4 TRACER TESTS RESULTS AND DISCUSSION

4.1: Introduction

Water quality and quantity treatment are highly governed by a system's hydraulic residence time (HRT). Knowing the CSW's residence time will provide insight into the removal of constituants, as well as peak flow and volume reduction and general flow dynamics. Over the course of one year, tracer tests were performed to determine the HRT of the system. Storm and baseflow events were analyzed to determine the mean time, peak concentration time, and variance for each. Since multiple tracer tests were performed, an average for each pathway in the CSW was calculated for baseflow and storm conditions. These pathway averages were used to compare baseflow against storm HRTs.

4.2: Storm Events Tracer Results

Statistics obtained from residence time distribution (RTD) curves for each storm event tracer test on the CSW are provided in Table 4-1. As previously mentioned in the methodology chapter, there were two rhodamine sensors (1 and 2) used in each test. The rhodamine dye was typically released at the inlet, unless otherwise noted. The color coding of Table 4-1 is for reference to the location of each sonde per event.[1] The yellow designates Sonde 1 was at end of M2 and Sonde 2 was at the outlet, and the rhodamine was released at the End of M1. The mean time 1, peak time 1, and variance 1 is end of M1 to end of M2. Mean time 2, peak time 2, and variance 2 are for the pathway from the end of M1 to outlet. Blue represents Sonde 1 located at the start of M1 and Sonde 2 at the end of M1. Mean time 1, peak time 1, and variance 1 indicate the inlet to start of M1 path, while mean time 2, peak time 2, and variance 2 are the inlet to end of M1 pathway. Pink signifies Sonde 1 was at the end of M1 and Sonde 2 at the outlet. Mean

time 1, peak time 1, and variance 1 is inlet to end of M1 path, whereas mean time 2, peak time 2, and variance 2 indicate the inlet to outlet pathway. Pink and blue events had the rhodamine dye released at the inlet. The summary of all sampling events for the different flow pathways through the CSW are given in Table 4-2.

Table 4-1: Statistical results for storm event tracer tests

Tracer Test Date	Mean Time 1 (hrs)	Peak Time 1 (hrs)	Variance 1 (hrs^2)	Mean Time 2 (hrs)	Peak Time 2 (hrs)	Variance 2 (hrs^2)
12.6.2013*	10.35	0.58	224.2			
3.28.2014*	9.01	2.58	74.0	17.69	14.75	65.6
4.7.2014	17.47	5.58	379.7	21.71	6.58	318.9
8.1.2014	52.57	0.67	1,710.5	N/A	1.08	N/A
4.25.2014	16.23	2.67	262.2	25.71	4.33	418.3
6.19.2014	29.49	1.58	1,352.2	54.43	60.08	1,144.3
7.14.2014	58.39	1.17	2,077.8	N/A	4.17	1,320.6
9.13.2014	49.92	0.92	2,619.8	70.28	3.58	2,812.6
10.22.2014	30.44	2.42	1,783.0	60.44	7.08	2,881.4
12.6.2014	17.68	2.42	343.2	32.07	5.08	1,208.4

*Dye released at end of M1
[1]*Yellow is pathway 1 (end of M1 to end of M2) and pathway 2 (end of M1 to outlet).*
Blue is pathway 1 (inlet to start of M1) and pathway 2 (inlet to end of M1).
Pink is pathway 1 (inlet to end of M1) and pathway 2 (inlet to outlet).

Table 4-2: Summary storm event mean time statistics.

Pathway	Mean Time (hrs)	Standard Deviation	N (# of samples)	Minimum (hrs)	Maximum (hrs)
Inlet to Start M1	35.02	24.82	2	17.47	52.57
Start M1 to End M1	4.24		1		
Inlet to End M1	31.98	16.26	7	16.23	58.39
End M1 to End M2	9.68	0.95	2	9.01	10.35
End M2 to Outlet	8.68		1		
End M1 to Outlet	19.83	8.16	5	9.48	30.0
Inlet to Outlet	48.59	18.98	5	25.71	70.28

To visually comprehend the values from Table 4-1, normalized rhodamine concentration vs. time data for the events with an inlet to end of M1 path are illustrated in Figure 4-1. The remaining RTD curves can be found in Appendix B. The general distribution of each curve is similar; there is a sharp rise to an early peak and then a gradual decreasing limb. The shape of these curves indicates a completely mixed flow condition, as opposed to plug flow. A completely mixed system at the CSW was expected. Though the shape of each curve is similar, the variances range from 319 to 2,900 hrs^2. Variance numerically expresses the distribution spread of the RTD curves. A larger variance is indicative of being more spread out. The variance range between each event will be discussed further based on seasonal and weather related influences.

The peak times were almost consistently less than three hours, while the mean times were much greater. To restate, the mean time is the average time the tracer spends in the system. If the CSW resembled a plug flow reactor, then its peak and mean time would be similar. However, since the system is completely mixed it validates the large difference between mean and peak times.
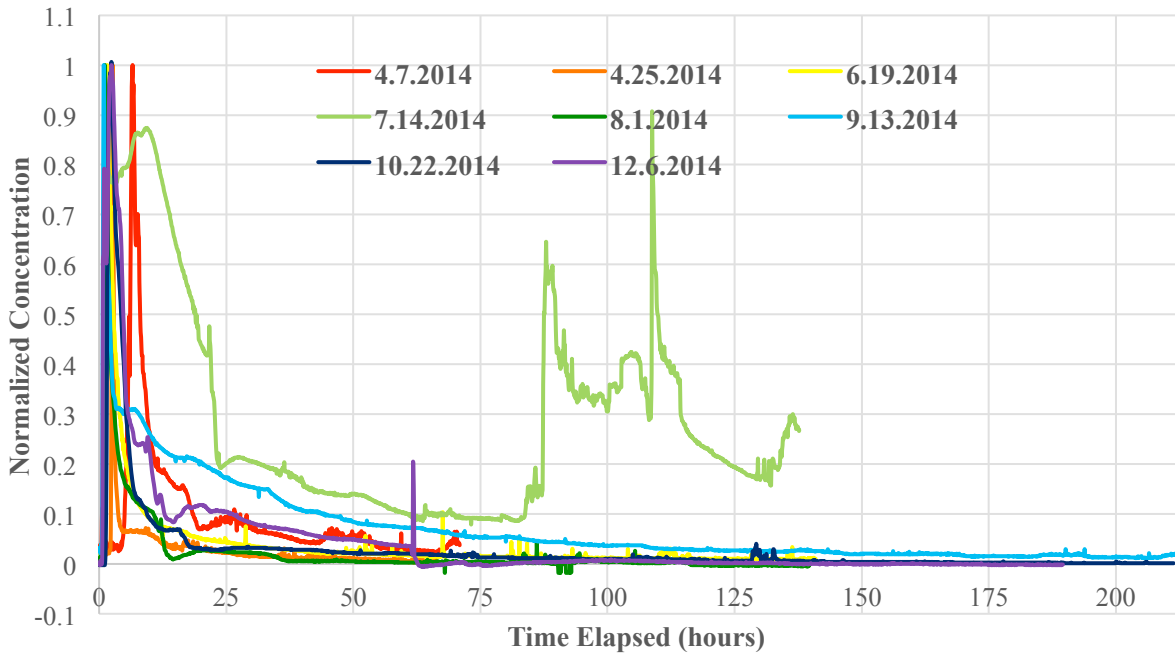
Figure 4-1: Residence time distribution curves for inlet to end of M1 tracer tests.

There are several factors that influence the HRT during storm events, including rainfall amount, rainfall intensity, vegetation density and seasonal influence (Table 4-3). The sampling events are grouped by the dominant parameter influencing the outflow rate and subsequently the HRT. Another consideration when evaluating the HRT is that due to the long duration of each tracer test, there can possibly be a second storm within the sampling event. Additionally, as mentioned in the methodology, the dye was not always released at the beginning of a storm event, therefore the total storm rainfall amount may be different than the rainfall that fell during the tracer sampling event. The tracer rain and average tracer outflow were calculated from the period when the tracer study was occurring.

Table 4-3: Weather and flow rate data for storm event tracer tests.

Tracer Test Date	Total Storm Rain (inches)	Total Avg Storm Intensity (in/hr)	Avg Total Storm Outflow (cfs)	Tracer Rain (inches)	Avg Tracer Outflow (cfs)
12.6.2013	1.30	0.15	0.86	0.97	0.62 (0.68)
3.28.2014	2.94	0.18	0.77	3.02	0.71 (0.70)

52

4.7.2014	0.37	0.13	0.50	0.37	0.54 (0.29)
8.1.2014◆	0.30	0.90	0.76	0.69	0.21 (0.41)
4.25.2014	0.60	0.21	0.42	0.43	0.43 (0.33)
6.19.2014	0.17	0.15	0.63	0.02	0.26 (0.25)
*7.14.2014**	0.97	0.90	0.53	0.27	0.16 (0.30)
9.13.2014	0.37	0.26	0.74	0.26	0.08 (0.23)
10.22.2014	0.72	0.13	0.47	0.42	0.10 (0.20)
12.6.2014✿	0.68	0.14	0.77	1.39	0.29 (0.48)

*Additional storm (0.26 in) 21 hours after dye released and storm ended.
◆Additional storm (0.48 in) 10 hours after dye released and storm ended.
✿Additional storm (0.78 in) 39 hours after tracer test storm and 54 hours after dye released.

The first two tracer tests (December 6, 2013 and March 28, 2014) vary greatly on vegetation density and storm rainfall amount, although both are larger storm sizes. The average storm outflow of 0.77 cfs for March 28 was slightly less than the December 6th event of 0.86 cfs, even though the total storm rainfall and intensity was greater for the March storm. The peak time 1 (end of M1 to end of M2) being 2 hours shorter for the December 6, 2013 depicts is more dependent on the average storm outflow than the storm precipitation or intensity. On the other hand, the mean time 1 for the March 28, 2014 event is 95 minutes faster than the December 6, 2013 storm, which can be accredited to the tracer average outflow being slightly higher for the March storm.

The April 7 and August 1, 2014 events illustrate the impact high rainfall intensity has on the peak time. The August storm had a much larger intensity and average storm outflow than the April storm, and thus both peak time 1 (inlet to start of M1) and peak time 2 (inlet to end of M1) occurred much quicker. However, the same concept cannot be said for mean time 1 since April 7th event (17.5 hours) was significantly less than August 1st (52.6 hours). The only reason can be explained through the average tracer outflow being much greater for the April storm. The vegetation density can be accounted for in the context of variance. Vegetation shapes the

variance by slowing down the tracer dye and creating pockets for it to navigate through as opposed to an open pond. The August storm had a much larger variance 1 than the April 7th event, which can be attributed to the plant density difference.

The influence of rainfall intensity on peak time, however, cannot be said for April 25 and June 19, 2014 storm events. Even though April 25 had a slightly higher intensity, its peak time 1 (inlet to end of M1) was not the fastest. On June 19th there was a previous storm (0.14 inches) 11 hours before the tracer test, which may have resulted in higher inlet flow rates. The April 25th event had about 230 hours of dry time before its storm. The amount of dry time between storm events proves influential on the peak times, as well as the CSW's storage volume. Longer dry periods allow for the CSW to recover back to baseflow conditions, allocating for the most storage volume and potentially slower flows.

The September, October, and December 2014 events are excellent examples of how the changing seasons affect the HRT. As colder temperatures approached and the plants slowly became dormant, the mean time 1 (inlet to end of M1) and mean time 2 (inlet to outlet) began to decrease. Though the September 13th storm was more intense than the October 22nd event, both mean times were smaller for October. It is suspected that because vegetation in October is decaying, the plants are losing their root and stem strength that alters flow patterns and velocities in the CSW. This decreasing mean time trend continued as well for the December 6, 2014 storm. The same concept of vegetation density can be applied to the variance 1 decreasing from the September to December storm events. The opposite can be said for peak time 1 and peak time 2 for these events. September, being the most rainfall intense event, has the quickest peak times. Peak time 1 for December and October storms are both equal at 2.42 hours. The rainfall intensities are both similar at 0.13 and 0.14 in/hr, however, the average storm outflows are

significantly different. The similarity of the rainfall intensities indicates the parameters stronger influence on peak time 1 (inlet to end of M1).

Since the outflow is continuously monitored, tracer events in which a sensor was placed at the outlet can be analyzed for dye mass recovery. Table 4-4 displays the calculated mass recovery for the pertaining tracer tests. Due to background concentrations at the CSW, there was dye recovery over 100% for the majority of the events. However, the July 14th storm only recovered 80% of the dye. The June 19th event had a similar dye study duration, but recovered 139% of the rhodamine. It could be postulated there were dead zones in the CSW for the July 14th event that resulted in under 100% recovery. The hypothesis would also explain the mean time 2 (inlet to outlet) of 51.04 hours being less than 58.4 hours for mean time 1 (inlet to end of M1) for the July 14th storm.

Table 4-4: Dye mass recovery analysis for selected storm event tracer tests

Tracer Test Date	Dye Study Duration (hrs)	Dye Released (g)	Dye Recovered (g)	Dye Recovery
4.25.2014	66.3	5.0	5.35	107%
6.19.2014	140.9	8.0	11.09	139%
7.14.2014	137.8	10.4	8.35	80%
9.13.2014	213.2	20.0	22.64	113%
10.22.2014	213.2	21.0	22.87	109%
12.6.2014	189.6	22.0	33.98	154%

4.3 Baseflow Events Tracer Results

Since the CSW is also studied during baseflow, tracer tests were performed during these low flow conditions. Table 4-5 presents the statistics calculated for the baseflow tracer tests. The color coding system from the storm event Table 4-1 applies to these events as well.[2] In addition,

the light green shading indicates the first sonde was located at start of M1 and the 2nd sonde at the outlet. The first pathway being inlet to start of M1 and the second path is inlet to outlet. By subtracting mean time 2 from mean time 1, a third mean time (mean time 3) is determined. The third pathway in this case is start of M1 to outlet.

Table 4-5: Statistical results from baseflow event tracer tests

Tracer Test Date	Mean Time 1 (hrs)	Peak Time 1 (hrs)	Variance 1 (hrs^2)	Mean Time 2 (hrs)	Peak Time 2 (hrs)	Variance 2 (hrs^2)	Mean Time 3 (hrs)
*11.7.2013**	27.94	4.92	751.4	57.53	21.33	987.2	29.6
5.18.2014	17.43	6.33	157.7	25.24	13.33	232.1	7.8
8.8.2014	57.27	34.92	720.4	96.79	114.42	907.0	39.5
8.28.2014	53.00	27.75	903.7	106.23	79.50	1,726.6	53.2
11.11.2014	79.95	52.33	1,319.3	104.31	130.33	886.7	24.4
3.18.2015	29.34	9.42	723.0	76.71	53.75	1,590.3	47.4

*Dye released at end of M1
^{2}Yellow is pathway 1 (end of M1 to end of M2), pathway 2 (end of M1 to outlet), and mean time 3 (end of M2 to outlet).
Blue is pathway 1 (inlet to start of M1), pathway 2 (inlet to end of M1), and mean time 3 (start of M1 to end of M1).
Pink is pathway 1 (inlet to end of M1), pathway 2 (inlet to outlet), and mean time 3 (end of M1 to outlet).
Green is pathway 1 (inlet to start of M1), pathway 2 (inlet to outlet), and mean time 3 (start of M1 to outlet).

Table 4-6 Summary baseflow event mean time statistics.

Pathway	Mean Time (hrs)	Standard Deviation	N (# of samples)	Minimum (hrs)	Maximum (hrs)
Inlet to Start M1	23.39	8.42	2	17.4	29.3
Start M1 to End M1	7.80		1		
Inlet to End M1	53.87	22.45	4	25.2	80.0

End M1 to End M2	27.94		1		
End M2 to Outlet	29.58		1		
End M1 to Outlet	43.66	14.98	4	24.4	57.5
Inlet to Outlet	96.01	13.50	4	76.7	106.2

Figure 4-2 visually shows the variation in the normalized to peak concentrations RTD curves for baseflow tests at the inlet to end of M1 pathway. The remaining RTD curves are presented in Figure B-4 and B-5 in the appendix. Rain occurred during several of the baseflow tracer studies due to the length of these studies (e.g. days). The rainfall for each event is correlated to the color of the concentration curve (Figure 4-2). Unlike the sharp rise to an early peak for storm events, the baseflow distribution illustrates a slower incline to peak and a much more gradual fall on the limb. However, the gradual decline for the August and November 2014 tests were not the case when storms occurred. The rainfall resulted in a sharp decrease for the rhodamine concentration due to dilution.
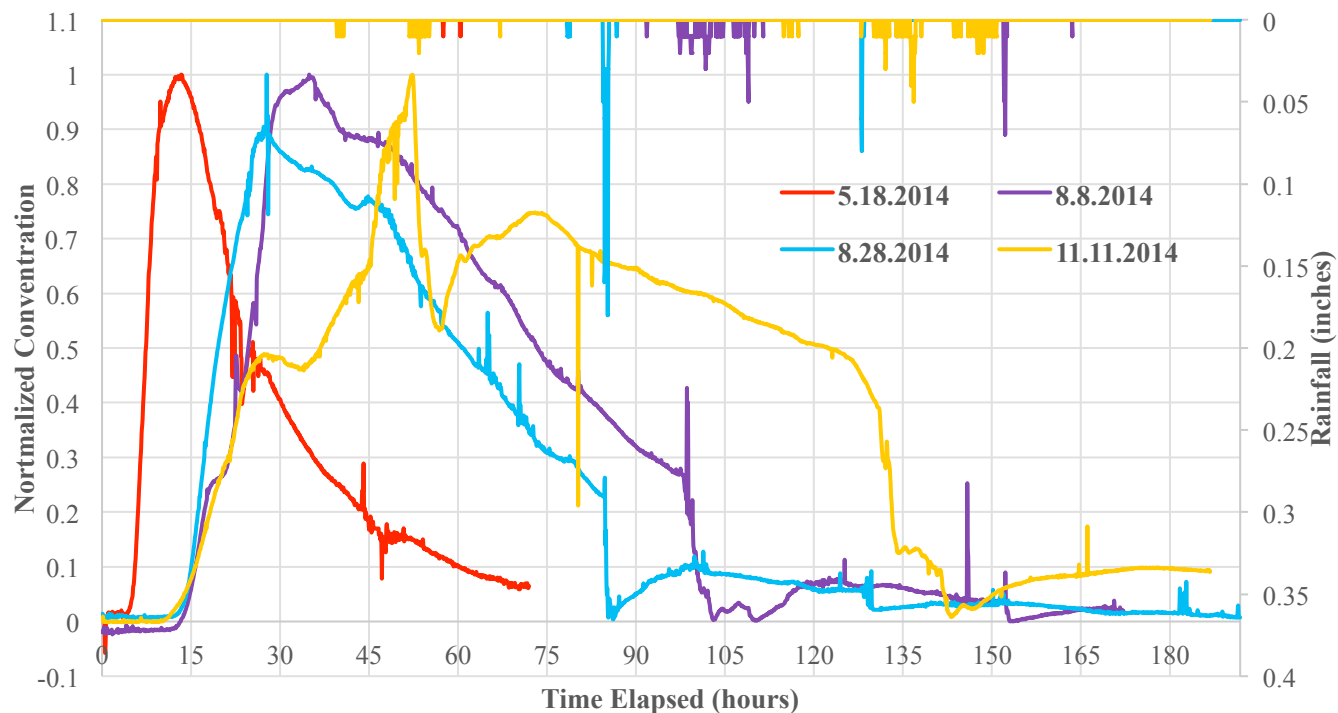
Figure 4-2: Normalized residence time distribution curves for inlet to end of M1 baseflow events.

The variation in mean times, peak times, and variances demonstrate seasonal factors influencing the hydrodynamics of the CSW. Table 4-7 depicts weather related parameters and average outflow for each tracer test. The dry time indicates the amount of time from the dye release to the start of a storm event (24 hour cumulative rainfall greater than 0.10 inches). The November 11th tracer test was under dry conditions for 51.83 hours; as the storm began the storm flow likely pushed through the slow moving dye as peak time 1 (inlet to end of M1) is 52.33 hours and accelerating the peak time as opposed to is the base flow had been maintained. The same scenario can likely be applied to the peak time 2 for the August 8th and 28th events.

Table 4-7: Weather and flow rate parameters for baseflow tracer tests.

Tracer Test Date	Total Rain (inches)	Dry Time (hrs)	Avg Air Temperature (°C)	Avg Wind Speed (mph)	Avg Outflow (cfs)

11.7.2013	0.09	120.8	7.19	0.98	0.04 (0.05)
5.18.2014	0.02	72.0	15.76	0.29	0.61 (0.04)
8.8.2014	1.22	97.17	21.81	0.95	0.22 (0.40)
8.28.2014	1.13	78.42	23.33	1.17	0.11 (0.24)
11.11.2014	1.16	51.83	3.31	1.89	0.17 (0.35)
3.18.2015	0.57	46.58	1.62	1.50	0.33

The seasonal factors of plant density and growth in the CSW provide explanations to the statistical parameters. The vegetation for the May 18th event was during the beginning of the growing season. The plants in May were not as tall and established as they were in August, thus allowing for faster velocities through the vegetated meanders. As a result, the mean time 2 (inlet to end of M1) for May 18th was half the time of the mean time 1 (inlet to end of M1) for the two August events. The influence of decomposing vegetation on retention time is observed in the November 11th baseflow tracer test. During baseflow conditions, the water is shallow and the flow is very slow, so the accumulation of plant litter creates an obstacle for the flow path, resulting in longer travel time. The decaying vegetation also affected the spread of the distribution with the largest variance for the inlet to end of M1 pathway.

The presence and density of algae can also influence the flow path of the tracer. Algal bloom impact is demonstrated for mean time 1 and peak time 1 (inlet to end of M1) for the two August 2014 events. Figure 4-3 illustrates the vast amount of algae for August 8th in comparison to the small algal bloom for August 28th. Adsorption of the rhodamine tracer onto algae affects the behavior of the dye, therefore influencing the hydraulic behavior. The algae temporarily stores the tracer and then releases it slowly resulting in longer travel times (Valero and Mara, 2009).

Figure 4-3: August 8th (left) and August 28th (right) dye release at inlet

The variations in hydraulic residence times for the inlet to outlet pathway is slightly harder to explain based primarily on vegetation and weather related parameters. The average outflow appears to influence the mean time 2 for the August 8th and 28th, November 11, and March 18 events. The March 18th tracer test had the highest average outflow (0.33 cfs), thus resulting in the smallest mean time 2. The lowest average outflow (0.11 cfs) is associated to the longest inlet to outlet HRT for the August 28th event.

A dye mass recovery analysis was also performed for the baseflow tracer tests (Table 4-8). Since the dye study duration for each event were similar, the tests can be analyzed together. The exceptionally low dye recovery for the August 28th baseflow poses as a potential failure in closing the mass balance. The implication being the possible incorrect calculation of the mean time for the inlet to outlet pathway. Ideally, the mean time 2 for the August 28th event should be longer than 106 hours since the average outflow is nearly half the flow of the August 8th test. From this, it can be hypothesized that during the late summer season there is a stronger presence of dead zones in the CSW.

Table 4-8: Dye mass recovery analysis for selected baseflow tracer tests

Tracer Test Date	Dye Study Duration (hrs)	Dye Released (g)	Dye Recovered (g)	Dye Recovery
8.8.2014	172.2	13.0	14.69	113%
8.28.2014	191.8	10.0	4.86	49%
11.11.2014	186.8	20.0	18.67	93%
3.18.2015	195.9	22.0	26.01	118%

4.4 Summary of Hydraulic Retention Times

Table 4-9 portrays the average mean times for each pathway during storm and baseflow events. As expected, the average HRT was smaller for storms than baseflow conditions. The storm mean time was nearly half that for baseflow from inlet to outlet, which is indicative of the higher inflows and outflow during storm events. One exception was from the inlet to the start of M1, as the storm travel time was about 12 hours slower than baseflow. A suspected cause is the seasonal differences resulting in a large standard deviation (24.82 hours) between the two storm events, April 7 and August 1, 2014 that make up this pathway.

Table 4-9: Summary of storm and baseflow mean time.

Pathway	Storm Mean Time (hrs)	Standard Deviation	Baseflow Mean Time (hrs)	Standard Deviation
Inlet to Start M1	35.02	24.82	23.39	8.42
Start M1 to End M1	4.24		7.80	
Inlet to End M1	31.98	16.26	53.87	22.45
End M1 to End M2	9.68	0.95	27.94	
End M2 to Outlet	8.68		29.58	
End M1 to Outlet	19.83	8.16	43.66	14.98
Inlet to Outlet	48.59	18.98	96.01	13.50

Overall, these travel times provide greater insight into treatment efficiency at the CSW. The concept of a longer HRT resulting in better water quality removal can now be numerically proven for the CSW. However, there is the expected variability in travel times due to the limited amount of dye tracer tests performed. Additional storm and baseflow tracer tests are recommended in order to increase the sample size, allowing for more confidence in the average hydraulic residence time.

CHAPTER 5 STORM FLOW RESULTS AND DISCUSSION

5.1: Introduction

The results for this chapter consist of peak flow and volume analysis for storm events. Statistical evaluations and hydrographs will provide an understanding to the overall and seasonal hydraulic performance of the CSW. From the data analyzed, it was determined that the CSW functions very well during storm events. It should be noted that the hydraulic performance varies by season, with the best peak flow reduction occurring in the summer and the most volume reduction during the spring.

5.2: Volume and Peak Flow Reduction

For research purposes, data was analyzed only for peak flow rates and volumes during the selected sampling period (March 2013 to December 2014). The two years were shown separately and then presented together to provide a more in depth analysis of peak flow and volume reductions.

Table 5-1 depicts peak flow results for representative storm events at the CSW. The number of storm events evaluated is indicated by (n), with inlet west supplemented SWMM flows (m) and inlet main supplemented SWMM flows (k). SWMM flow data was necessary due to bad flow data or nonoperational flow meters at the inlet. The peak inflow and outflow each storm event from March 2013 to December 2014 can be found in Table C-1 in the appendix .

Table 5-1: Peak flow analysis from inlet to outlet for CSW 2.0

PEAK FLOW ANALYSIS	Mar'13 to Dec'13 (n=59, m=7)	Jan'14 to Dec'14 (n=73, m=33, k=1)	Mar'13 to Dec'14 (n=132, m=40, k=1)
In vs. Out – Statistically different?	Yes (<0.00001)	Yes (<0.00001)	Yes (<0.00001)
Average Storm Size (inches)	0.79	0.65	0.71
Average Storm Intensity (in/hr)	0.30	0.24	0.26
Average Peak Inlet (cfs)	8.63 (±7.50)	7.06 (±4.58)	7.76 (±6.04)
Average Peak Outlet (cfs)	2.14 (±1.10)	2.21 (±1.12)	2.18 (±1.11)
Peak Reduction	75.2%	68.7%	71.9%

n = number of storm events, m = inlet west SWMM supplemented flows, k = inlet main SWMM supplemented flows

The flows during the study period presented statistically different data between peak flows in and out of the CSW. This difference is an indication of peak flow reduction. Also, the difference between average peak inflows for 2013 and 2014 is correlated to the average storm size and intensity; the larger the average storm size and intensity, the larger the average peak inflow. However, the average peak outflows do not portray a similar trend. The reason behind this is the peak outflow is less dependent on the precipitation amount and intensity and more dependent on the hydraulic residence time (HRT). The HRT is highly influenced by factors related to the water balance in a wetland, such as evapotranspiration (ET), infiltration, and vegetation. The seasonal analysis additionally demonstrate the impact these parameters have on peak outflow rates.

Table 5-2 indicates the total volume reductions observed at the CSW during storm events. Table C-2 in the appendix provides the inflow and outflow volume for each storm used in the analysis. As stated previously, statistically different data between the volumes in and out demonstrates the volume reduction. For example, the p value for 2013 is slightly larger than 2014, thus resulting in a smaller percentage of volume reduction in 2013 compared to 2014.

Even though there are two months missing from 2013, the amount of volume entering and exiting the CSW in for 2014 is over double of 2013. The large inlet volume for 2014 is due to larger snowfall (and subsequent snowmelt) during that year. According to the National Oceanic and Atmospheric Administration (NOAA), the total snowfall from January to December 2013 at the Philadelphia International Airport was 19.1 inches. The following year had nearly 57 inches of snowfall. Nonetheless, the CSW performed much better in the context of volume reduction in 2014. Maturity and establishment of vegetation at the CSW, as well as infiltration rates and ET could be the influencing factors. A seasonal analysis is presented in the next section to further relate these parameters to volume reduction.

It should be noted that the inlet west SWMM supplemented data was a result of an inaccurate flow meter from June 9 to December 4, 2014. Though the SWMM program provides modeled data by using the curve number infiltration and loss method, it does not take into account air temperature influences on infiltration rates. As a result the modeled inlet data could have larger flows then what would be observed during the warmer months where infiltration rates are the highest.

Table 5-2: Storm volume reduction from inlet to outlet at CSW 2.0

VOLUME ANALYSIS	Mar'13 to Dec'13 (n=59, m=7)	Jan'14 to Dec'14 (n=73, m=40, k=1)	Mar'13 – Dec'14 (n=132, m=47, k=1)
In vs. Out – Statistically different?	Yes (0.002)	Yes (0.0009)	Yes (0.00003)
Total Precipitation* (inches)	46.38	47.24	93.62
Volume In (CF)	4,457,736	9,600,012	14,057,748
Volume Out (CF)	3,309,455	6,271,376	9,580,831
Volume Reduction	25.8%	34.7%	31.8%

n = number of storm events, m = inlet west SWMM supplemented flows, k = inlet main SWMM supplemented flows
* Precipitation is rainfall only and excludes snowfall

5.3 Seasonal Storm Flow Analysis

Rainfall amount and intensity are not the only influencing parameters of peak flow and volume reduction at the CSW. As stated previously, there is also the effect of ET, infiltration, and vegetation. These three parameters are highly variable among the four seasons; summer, fall, winter, and spring. A seasonal analysis for storm events from June 1, 2013 to May 31, 2014 was performed to justify the other factors' influences.

Table 5-3 depicts peak flow data analysis on a seasonal basis. The Summer of 2013 was a very wet season with over 22 inches of rain, and as a result presented the highest average peak inlet and outlet flows. For the Philadelphia region the average total precipitation for the summer months according to National Oceanic and Atmospheric Administration is 14 inches. The average peak outlet flow did not increase as much as the inlet peak flow based on the high total precipitation and storm intensity. Figure 5-1 illustrates the random variability of peak inflows in comparison to peak outflows. The peak outflow is dependent on the storage volume of the CSW, which is influenced by ET and infiltration. Due to research limitations, numerical justification of these factors is not provided. From previous researches and common knowledge, the suspected reason behind a lower peak outlet during the summer is due to denser vegetation in the meanders and the warmer air temperatures, which increase ET and infiltration rates. It is notable that the peak outflow rate for each storm is never greater than 5 cfs. The design of the outlet structure is the suspected cause of the limiting outflow rate. During high periods of flow when the water level is above the v-notch weir, the flow is to travel into the T-shaped weir. These weirs constrain the flow rate and result in ponding upstream.

Table 5-3: Seasonal peak flow analysis for storm events

SEASONAL ANALYSIS	Summer (n=21, m=5)	Fall (n=12)	Winter (n=18, k=1)	Spring (n=15)
Total Precipitation* (inches)	22.14	9.94	11.71	18.84
Average Storm Intensity (in/hr)	0.46	0.23	0.17	0.24
Average Peak Inlet (cfs)	12.97 (±9.44)	6.45 (±4.23)	6.00 (±3.98)	10.4 (±7.27)
Average Peak Outlet (cfs)	2.52 (±1.09)	1.88 (±1.17)	2.07 (±1.22)	2.46 (±1.20)
Peak Reduction	80.6%	70.8%	65.5%	76.3%

n = number of storm events, m = inlet west SWMM supplemented flows, k = inlet main SWMM supplemented flows
 Precipitation is rainfall only and excludes snowfall.
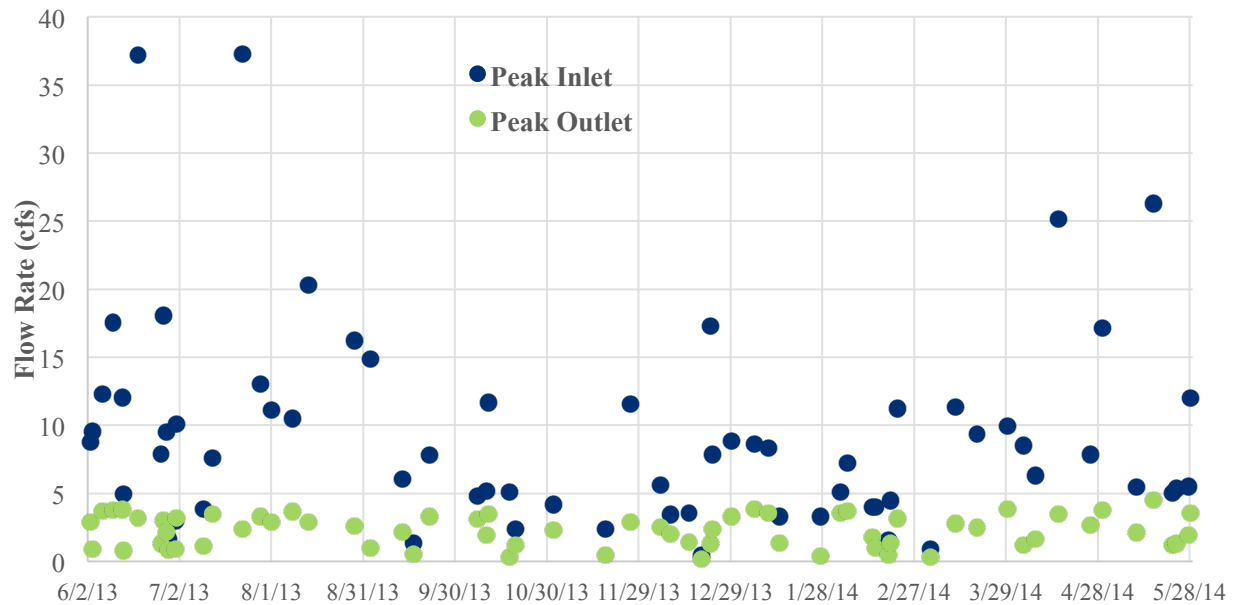
Figure 5-1: Peak inflow and outflow for various storm events.

To better comprehend the influence of precipitation and storm intensity on a per season basis, a linear regression analysis was performed. Table 5-4 illustrates the coefficient of determination (R^2) obtained from a linear trend line fit of peak inlet and outlet flow data. Appendix C contains the linear regression graphs that provided these values. The minute R^2

values for the summer storms illustrate that storm intensity and precipitation have little effect on peak inlet and outlet flows. The lowest linearity numbers regarding peak inflows in the summer and fall is an indication that other factors are influencing the runoff rate; such factors consist of infiltration capacity, soil moisture, and vegetation cover. The winter months demonstrated the storm intensity having the most influence on the peak inflow. Low infiltration rates because of frozen ground results in higher peak outflow rates with more precipitation as volume retention is diminished; there could also be less resistance from vegetation, which is less dense than in the summer. Spring storms showed the greatest precipitation influence on both peak inflow and outflows.

Table 5-4: Linear regression analysis on peak inflows and outflows

PEAK FLOW LINEARITY (R^2)	Summer (n=21, m=5)	Fall (n=12)	Winter (n=18, k=1)	Spring (n=15)
Storm Intensity vs. Peak Inflow	0.2027	0.1047	0.4608	0.4496
Storm Intensity vs. Peak Outflow	0.0562	0.4342	0.0059	0.4345
Precipitation vs. Peak Inflow	0.1283	0.3262	0.0275	0.5883
Precipitation vs. Peak Outflow	0.2881	0.4697	0.4049	0.617

n = number of storm events, m = inlet west SWMM supplemented flows, k = inlet main SWMM supplemented flows

Besides peak flow reduction, there is also seasonal variation among volume control at the CSW. Table 5-5 displays the seasonal data analysis based on volume reduction. The inlet and outlet volumes presented a slightly different correlation compared to the peak flows. Even though summer has the highest total precipitation and intensity, its inlet volume was not the highest of all seasons. Winter and spring had the highest inlet and outlet volumes, which is a result from snow accumulation and melt. Fall had the least amount of storm volume reduction. Such small volume reduction could be attributed to decaying plants that allows for flow to push

by faster, in addition to lower ET and infiltration rates between storm events. Winter and spring presented the most storm volume reduction. The longer average event durations during the winter and spring are the suspected cause of greater volume reduction. As stated in the methodology section, the end of a storm event is dictated by the outflow being less than 0.10 cfs. The reason behind the longer event durations in the winter and spring is primarily due to lower ET and infiltration rates in the CSW.

Table 5-5: Seasonal analysis for storm volume reduction

SEASONAL ANALYSIS	Summer (n=21, m=5)	Fall (n=12)	Winter (n=18, k=1)	Spring (n=15)
Average Event Duration (hrs)	31.1	17.9	45.6	71.6
Total Volume In (CF)	2,070,079	725,290	2,895,838	4,715,424
Total Volume Out (CF)	1,353,339	513,449	1,775,129	2,574,025
Volume Reduction	34.6%	29.2%	38.7%	45.4%

n = number of storm events, m = inlet west SWMM supplemented flows, k = inlet main SWMM supplemented flows

5.4 Extreme Storm Events

In this section, a selected few storm events are analyzed in order to show the CSW's performance during extreme events. Table 5-6 provides storm flow analysis for four different extreme storm events; one selected per season from the sample size in the previous section. The July, October, and February storms are close to a one year event. The May 16th storm was more representative of a 10 year event.

Table 5-6: Seasonal extreme storm event results

EXTREME EVENTS	July 22, 2013	October 11, 2013	February 13, 2014	May 16, 2014
Total Precipitation* (inches)	1.34	1.99	1.89	4.23
Average Storm Intensity (in/hr)	0.73	0.29	0.15	0.48

Volume Reduction (CF)	30,000	56,000	180,571	250,000
Volume % Reduction	37%	33%	49%	43%
Peak Reduction (cfs)	34.9	8.2	2.20	21.8
Peak % Reduction	93%	70%	55%	83%

* Precipitation is rainfall only and excludes snowfall

On July 22, 2013 there was a significant storm event that produced one of the highest inlet flows seen at the CSW (Figure 5-2). The peak inlet flow was 37.3 cfs. The CSW demonstrated its capability of detaining a high peak inflow with only a 2.34 cfs peak outflow. Such reduction in peak flow can be attributed to the large storage volume of the CSW at that time. The amount of storage volume is primarily influenced by infiltration and ET rates within the CSW, and the annual water balance. The storage volume also resulted in a peak lag time of only 3.25 hours. In addition to peak flow reduction, the peak outflow is spread out over a longer period of time meaning it is not as peaky as the inflow.
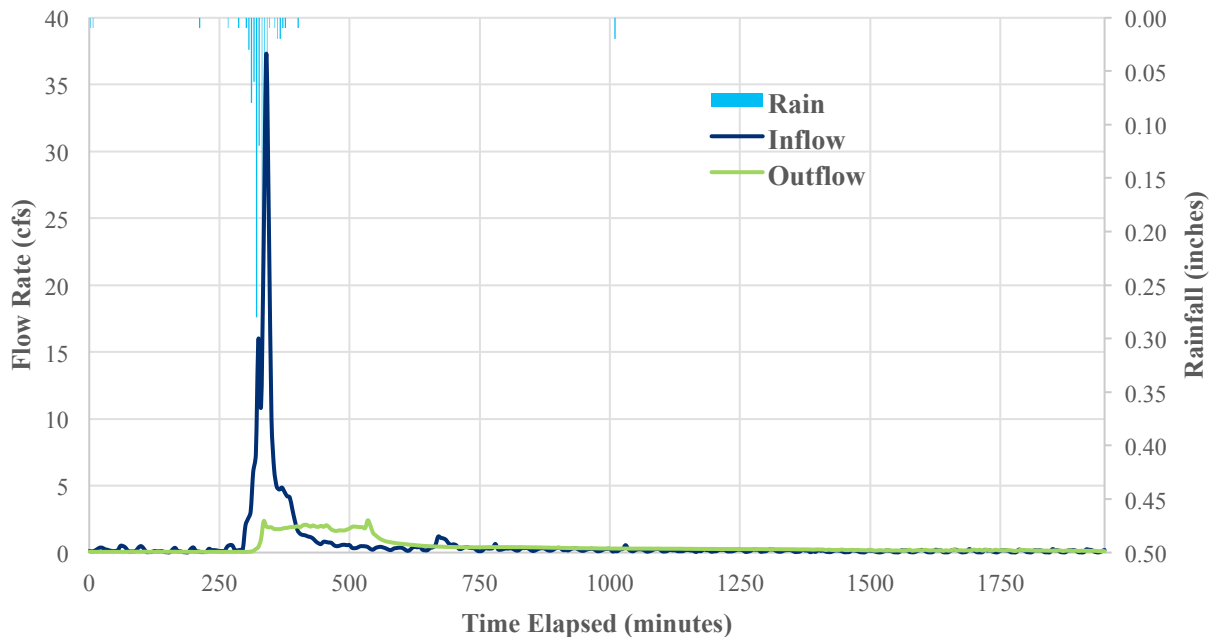
Figure 5-2: July 22, 2013 storm hydrograph with inflow and outflow

Though Fall 2013 did not produce as many storms as the other seasons, there was still one event that reached over an inch of precipitation within 12 hours. On October 11, 2013 the

CSW received almost a 2 inch storm event (Figure 5-3). This particular storm did not produce an extremely high peak inflow (11.66 cfs) like that of the July 22, 2013 storm; primarily due to its much lower rainfall intensity. The peak outflow for this storm was much higher than that from the July storm; 3.46 cfs. Reasons for the elevated peak outflow and lower storm volume reduction are reduced volume capacity due to previous rainfall, decreased infiltration and ET rates as well as decaying plants in the CSW. The peak lag time for this event, 9.92 hours, was much longer than that of the July storm. Suspected influences for the differences in peak lag time are due to lower rainfall intensity and duration.
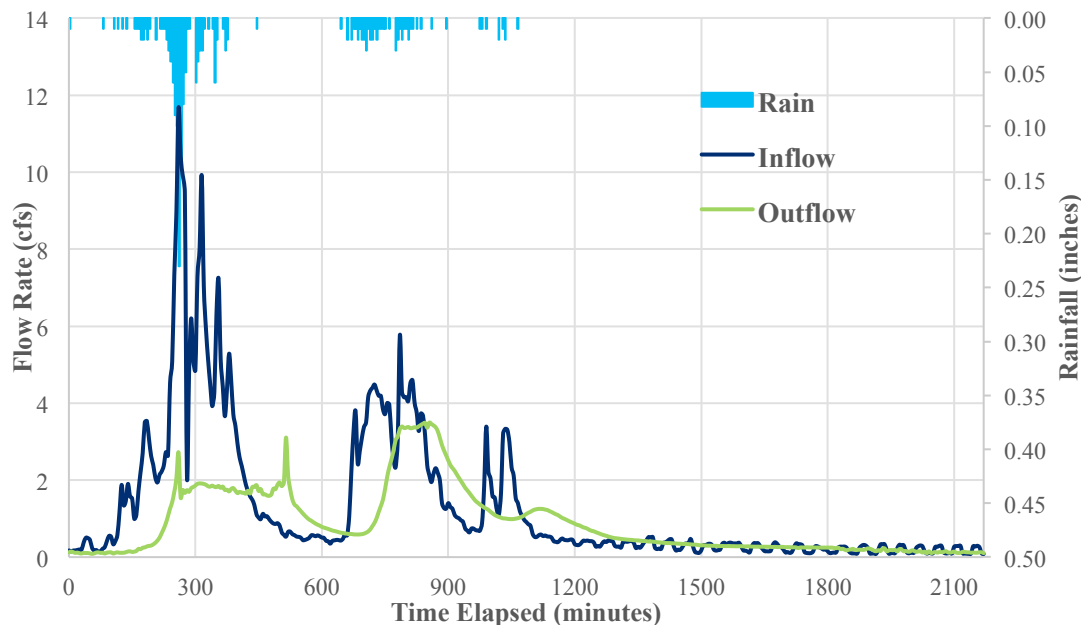
Figure 5-3: October 11, 2013 storm hydrograph with inflow and outflow

May 16, 2014 had the most rainfall intense event of the year, with over 4 inches of rain in 10 hours (Figure 5-4). The peak inflow reached 26.3 cfs, and after 10.5 hours of lag time the outlet attained a peak flow rate of 4.50 cfs. The long peak lag time is indicative of successful flow rate mitigation through the CSW's meanders. Though the peak flow reduction is not as great as the July event, the amount of reduction is still substantial in relation to the intensity and

71

duration of the storm. Isolated spikes (smaller peaks not caused by storm event) for the inflow could be due to air conditioning discharge, leaky pipes, groundwater seepage, or other water related campus activities.
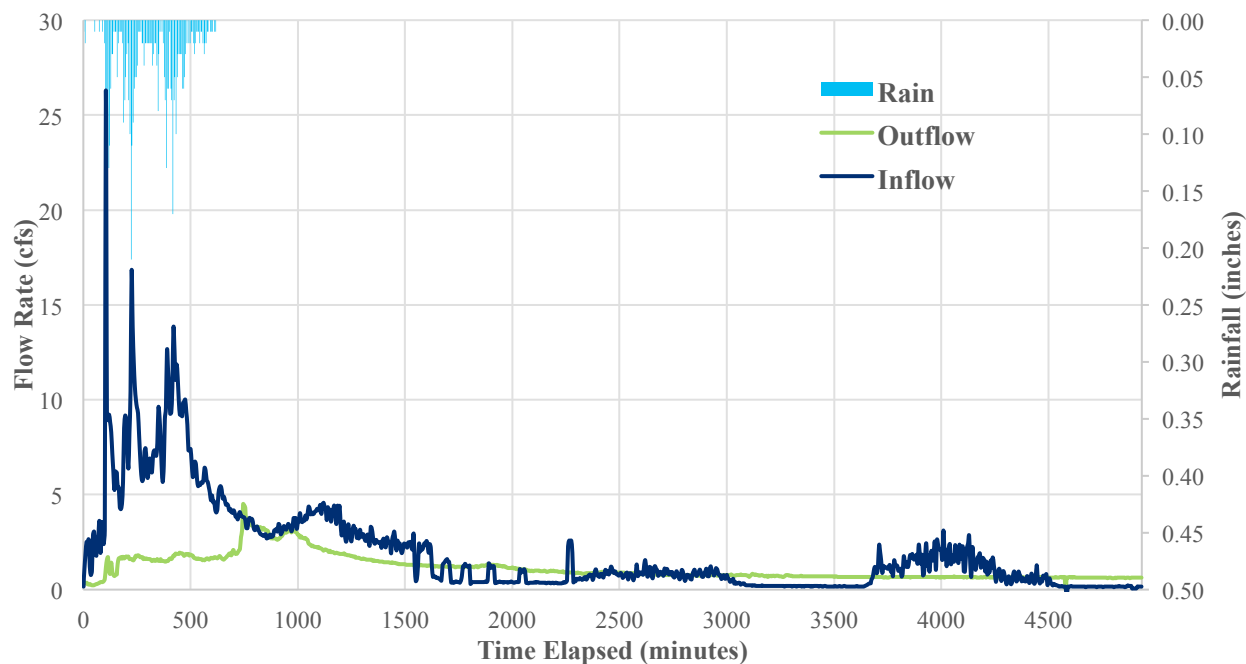
Figure 5-4: May 16, 2014 storm hydrograph with inflow and outflow

Though not an extreme event based solely on rainfall intensity or precipitation; the February 2014 snow storm depicted intriguing high inflows. The snowfall and melt event occurred from February 13 to the end of February 18. The rain gauges on campus are not heated, therefore they do not accurately account for snowfall. As a result, snow precipitation data was retrieved from NOAA Atlas at the Philadelphia International Airport. The storm began with slightly over 10 inches of accumulated snow by the end of February 13, 2014. The following day brought only 1 inch of snowfall to the area. Over the next three days there was little snowfall or rain accumulation, however, the influence of sunlight and campus salting caused melting snow. On the last day, February 18, about 3 inches of snow accumulated in the region. With a complete

understanding of the weather conditions for the duration of the snow event in February, a better analysis can be performed on the flow data. Figure 5-5 illustrates the hydrograph for the February event. Unlike the previous hydrographs that combined the inlet main and inlet west flow rates, for this event it is helpful to show the two as separate inflows. It should be noted that the cyclic motion of the flow at inlet west is a result of back currents at the inlet pond on windy days. The peak inflow occurred not on a snowfall event, but instead during a likely snow melt at 4.01 cfs at 12:15 on February 16. However, the outlet was not highly influenced by the snowmelt since its peak outflow of 1.77 cfs occurred during the snow storm on February 13 at 22:15. In retrospect, the associated peak inflow for the February 13th event was 3.97 cfs, which amounts to a 55% peak flow reduction.
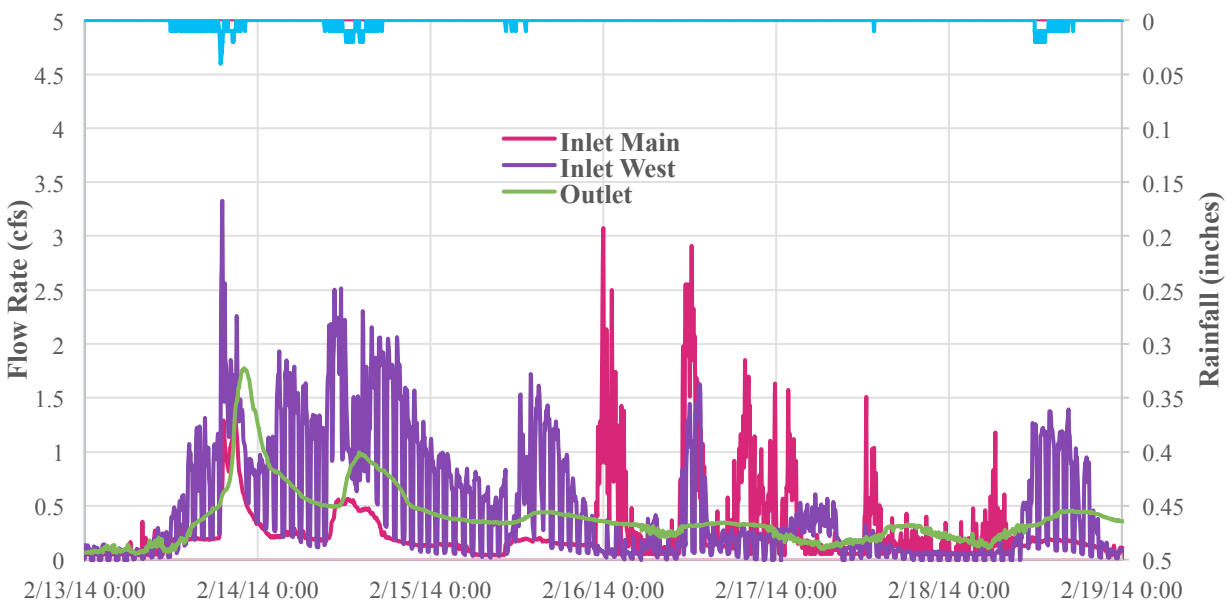
Figure 5-5: February 13, 2014 snow storm hydrograph with inlet main and west inflows and outflow

Taking a closer look at the February 16th and 17th inflow peaks reveal the impact snow melt has on runoff, particularly with main campus. Since the ground is partially frozen during snow events, stormwater runoff is not infiltrated as much as it would be during the warmer

seasons. About 50% of the 16.42 acres main campus drainage area is impervious, while the 26 acres of west campus is nearly 72% impervious. Typically, inlet west maintains higher flow rates then inlet main due to its drainage area. However, this was not the case for the two snow melt peaks. It is suspected that when the main campus is cleared of snow from the roads and pathways, the snow is stacked at certain locations. Snow piles result in more runoff then anticipated since now there is a larger volume of precipitation then what was recorded.

CHAPTER 6 TEMPERATURE RESULTS AND DISCUSSION

6.1: Introduction

Stormwater runoff not only contributes to higher flow rates in receiving waterways, but these systems, such as constructed stormwater wetlands, are also susceptible to temperature spikes. These temperature spikes are attributed to heated stormwater runoff entering the CSW and the progression of temperature through the CSW was analyzed. The CSW also has thermal stratification at the meander 1 plunge pool during the warm summer months (Figure 6-9). As anticipated, the CSW acts as a source of thermal pollution due to open water and slow flow rates.

6.2: Storm Events

Table 6-1 breaks down the storm events analyzed from April 2014 to February 2015 in order to illustrate the influence of air temperature and rainfall on the CSW's water temperature during an event. In addition, other factors also influence the CSW temperature, which will be discussed later. The outlet temperatures (Temp4Out and PT_OutTemp), correlated directly with the average air temperature, meaning that as the air temperature increased, so did the outlet water temperatures and vice versa. The inlet temperature sensors (Temp2IN and TempIMOut) did not present a similar relationship to the air temperatures. A possible explanation is the total rainfall and intensity effects the temperature at the inlet, which is then moderated as flow moves through the CSW. For example, the average storm air temperature in August is about 1.5°C cooler than July, however, the Temp2IN sensor yielded slightly warmer temperatures, possibly due to the lower average rainfall intensity. An additional hypothesis is the average event length being short in August (50.7 hours) in comparison to July (54.3 hours). The longer the event length, the more time the inlet water temperature has to cool.

Table 6-1: 2014-2015 Monthly storm events air and water temperatures statistics (Figure 3-2 illustrates the locations of temperature sensors).

Month	Total Rain (inches)	Avg. Rainfall Intensity (in/hr)	AVERAGES (°C)				
			Air	Temp2 IN	TempIM Out	Temp4Out	PT_OutTemp
April	8.32	0.24	10.34	13.17	--	13.99	12.76
May	11.13	0.31	16.97	16.17	--	19.27	18.13
June	2.94	0.26	21.33	18.24	19.48	23.75	22.68
July	4.05	0.41	22.90	19.69	21.80	25.09	24.07
August	4.17	0.38	21.45	19.75	21.20	22.96	22.11
September	1.16	0.27	19.13	18.65	20.15	20.30	19.33
October	2.93	0.18	14.10	16.27	16.65	14.25	13.91
November	2.97	0.15	5.24	9.28	9.79	--	5.55
December	3.09	0.14	4.00	7.71	8.46	--	4.36
January	0.76	0.16	-0.52	--	6.85	--	0.47
February	1.62	0.12	-5.37	--	5.86	--	-1.22

To address the influence of heated stormwater runoff, the maximum five minute temperature change at the inlet for each storm event was determined (Table 6-2). The time elapsed was the average amount of time passed from the start of the storm event up until the maximum five minute temperature change was reached. The maximum five minute temperature change, or temperature spike, is a key indicator of thermal pollution entering the CSW. For example, July being the warmest month resulted in having the highest average inlet temperature spike in the quickest amount of time. During the winter it would be expected that these spikes would not be as prominent, however, this was not the case for TempIMOut in November and December. The temperature spikes for TempIMOut could be a result of other heated sources, such as drainage from a boiler, are resulting in thermal runoff entering the CSW.

Table 6-2: 2014-2015 Monthly storm events average inlet temperature spikes statistics.

MONTH	Avg Air Temp (°C)	Avg. Rainfall Intensity (in/hr)	AVG. MAXIMUM 5 MINUTE CHANGE (°C) & TIME ELAPSED (MINS)			
			Temp2IN	Time Elapsed	TempIMOut	Time Elapsed
April	10.34	0.24	0.38	931.25	--	--
May	16.97	0.31	0.91	347.14	--	--
June	21.33	0.26	0.96	199.55	1.60	183.18
July	22.90	0.41	1.83	39.29	2.04	38.57
August	21.45	0.38	1.18	192.50	1.35	177.50
September	19.13	0.27	1.37	315.00	0.94	85.00
October	14.10	0.18	0.24	360.00	0.95	470.00
November	5.24	0.15	0.25	170.00	1.66	372.00
December	4.00	0.14	0.11	260.00	1.73	220.63
January	-0.52	0.16	--	--	0.69	105.00
February	-5.37	0.12	--	--	0.45	462.00

Temperature hydrographs provide an excellent illustration of the temperature spikes occurring in the CSW. Due to the large number of storms between April 2014 and February 2015, only a select number of events were chosen (Table 6-3).

Table 6-3: Storm events for temperature analysis statistics.

Storm Date	Rainfall (in)	Event Duration (hr)	Intensity (in/hr)	ADT* (hr)	Previous 24hr Avg. Air Temp (°C)
5/16/2014	4.23	143.4	0.48	126	21.66
6/19/2014	0.14	12.25	0.17	130	28.07
7/14/2014	0.97	21.83	0.90	16.25	25.84
12/5/2014	0.19	15.75	0.13	53.42	4.36

*Antecedent Dry Time (ADT)

Beginning with an extreme storm event that occurred at 6:30 on May 16, 2014, Figure 6-1 depicts the temperature fluctuation at the inlet and outlet of the CSW during the entire event.

There was a maximum temperature spike of nearly 1°C at the inlet that occurred 110 minutes after the storm began, therefore it can be concluded that heated runoff was present. Though the air temperature cools considerably through the event, the influence of an almost 6 day ADT, as well as high rainfall intensity, are contributing factors to the inlet temperature spike. The antecedent dry time allows for constant heating of impervious surfaces. The outlet temperature does not experience this kind of spike as a result of a long travel time from inlet to outlet, in addition to a cooling factor occurring from the rain itself.
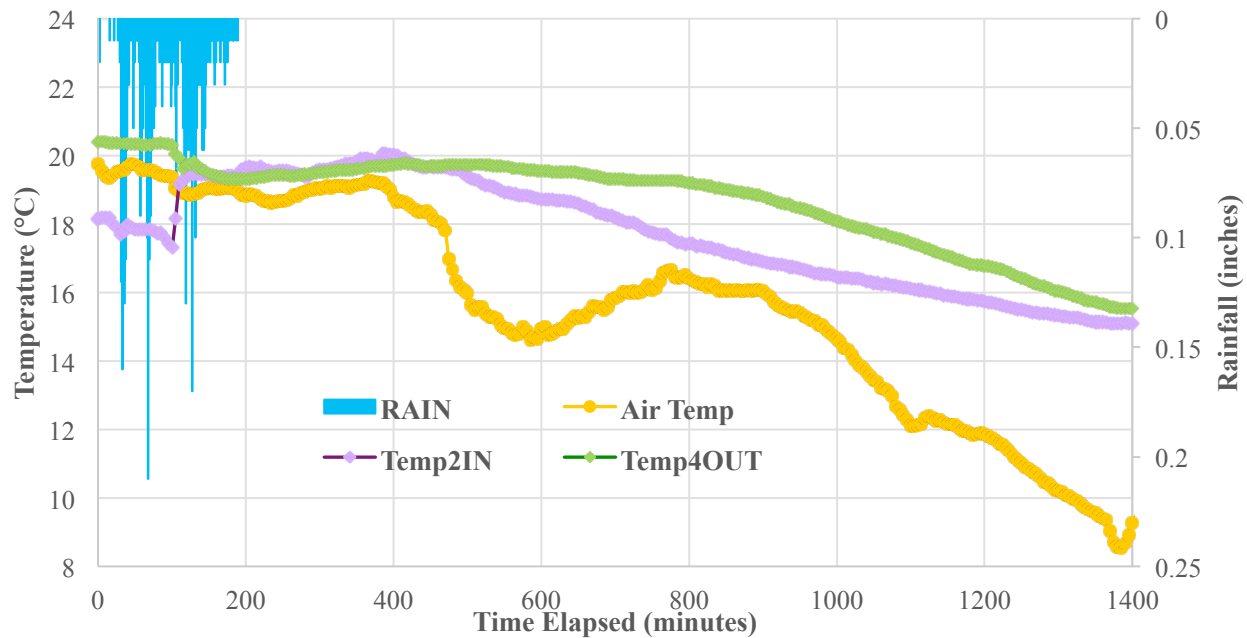
Figure 6-1: May 16, 2014 storm event temperature hydrograph.

Figure 6-2 indicates the intense thermal impacts from impervious surfaces during a summer storm in July. Even though the ADT is less than one day, the very warm air temperature previous to the storm along with high rainfall intensity is the suspected cause of a 3.32°C inlet spike within 130 minutes of the storm. As discussed previously, the sudden temperature drop at the outlet indicates the cooling effect from the rain. The outlet also illustrated an increase in temperature that correlated with the air temperature after about 9.5 hours once the rainfall ended.
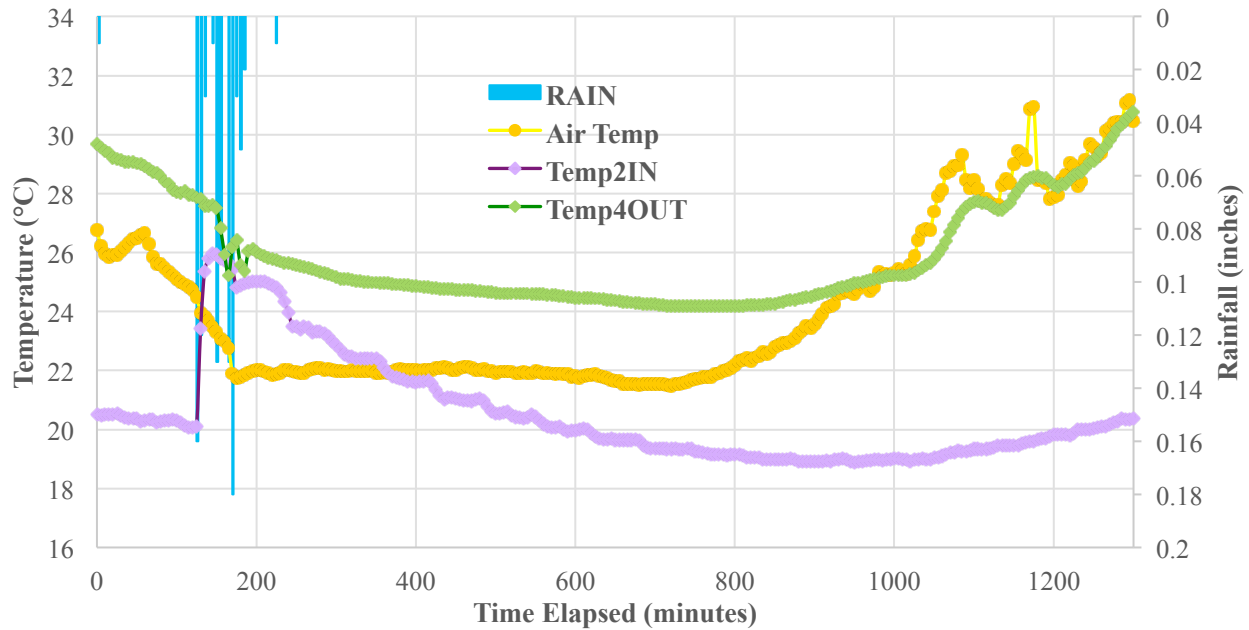
Figure 6-2: July 14, 2014 storm event temperature hydrograph.

The previous two storms demonstrated the effect of high rainfall intensity runoff on visible temperature spikes caused heated stormwater runoff. A small storm on the late evening of June 19, 2014 illustrates the thermal influence of a lower intensity storm (Figure 6-3). Though the event began slightly after midnight, it would be presumed that impervious surface temperature was still above atmospheric temperature due to the very warm temperatures the previous day. Only a 0.78°C inlet temperature spike was seen within 35 minutes of the start of the storm. The low rainfall intensity and the cooler air temperatures at night allowed for the stormwater runoff to cool before entering the CSW.
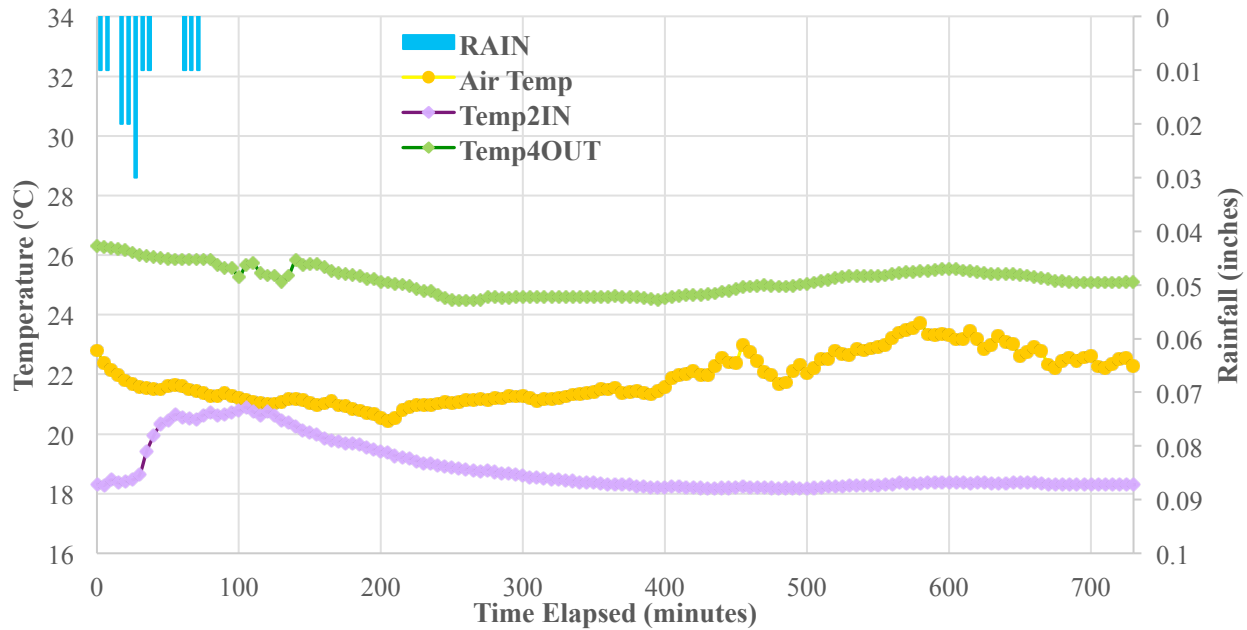
Figure 6-3: June 19, 2014 storm event temperature hydrograph.

Temperature data was monitored during the winter months as well. As suspected, the outlet temperature is cooler than the inlet. However, the presence of inlet temperature spikes was unexpected, particularly for the December 5, 2014 storm event (Figure 6-4). For TempIMOut there was a 2.40°C spike within 115 minutes (0.05 in of cumulative rain) and at Temp2IN (0.14 in of rain) it was 0.24°C after 345 minutes. The previous 24 hour average air temperature is considered cold (4.36°C), therefore the spikes are not attributed to heated pavement runoff. There is clearly another form of thermal pollution entering the CSW during the winter months. Possible sources could be boiler drain lines or ponded water that is being heated within the stormwater drains. It should be noted that are no visible temperature increases present for baseflow conditions. Nonetheless, the issue of winter storm temperature spikes remains inconclusive for the time being. Further research will be investigated to address the matter.
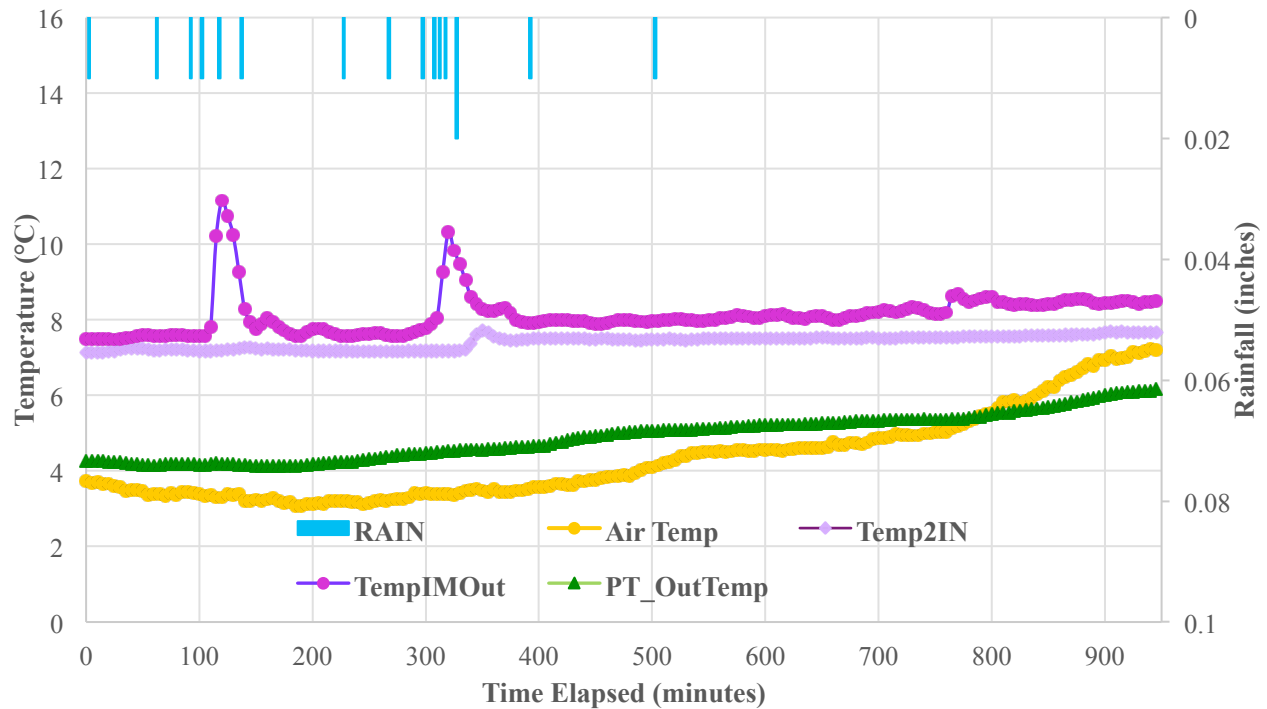
Figure 6-4: December 5, 2014 storm event temperature hydrograph.

A linear regression analysis was performed on selected storm events to demonstrate how rainfall intensity (Figure 6-5), the amount of precipitation, and previous 24 hour air temperate effect the inlet temperature spikes (Temp2IN). To maintain similar air temperature among the storms, only events from June to September 2014 were used in the linearity study. The graphs for the rainfall amount and air temperature influence are presented in Figure D-1 and D-2 in the appendix. The low R^2 value of 0.15 portrays the small impact the amount of rainfall has on runoff temperature spikes. Rainfall intensity appears to have a much greater influence on temperature spikes at the CSW as opposed to the rainfall amount. Surprisingly, the previous 24 hour average air temperature does not have a large effect on inlet temperature spikes ($R^2 = 0.22$).
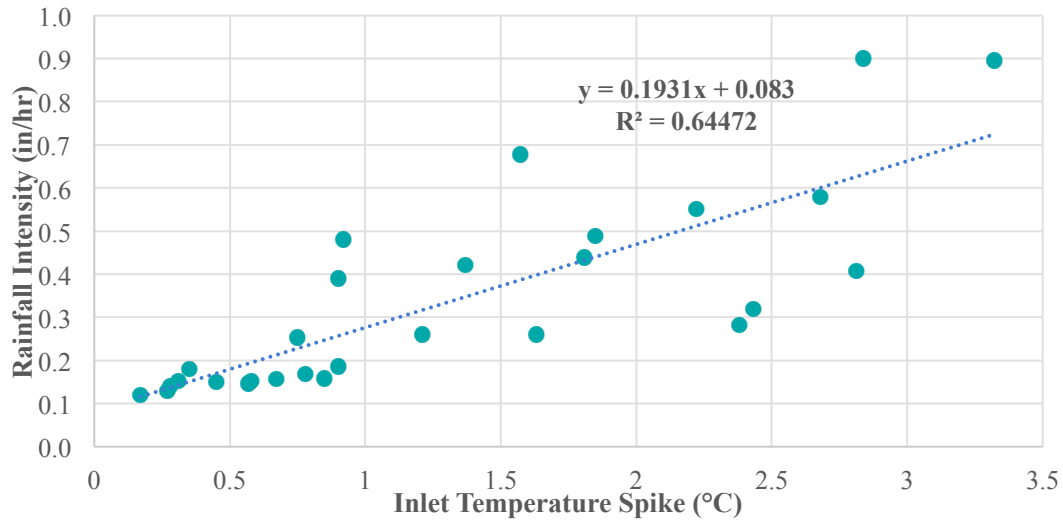
Figure 6-5: Rainfall intensity vs. inlet temperature spike linearity analysis.

To further analyze air temperature effects on runoff temperature spikes, the storm data was limited to only events with intensities greater than 0.20 in/hr. As a result, the dataset was reduced from 28 to 16 events. Figure 6-6 illustrates that the previous 24 hour average air temperature has a more predominate effect on the temperature spike for higher intensity events. Nonetheless, it still is below the rainfall intensity R^2 of 0.64 which could be due to other factors such as ADT, solar radiation, relative humidity, wind speed, and infiltration rates.
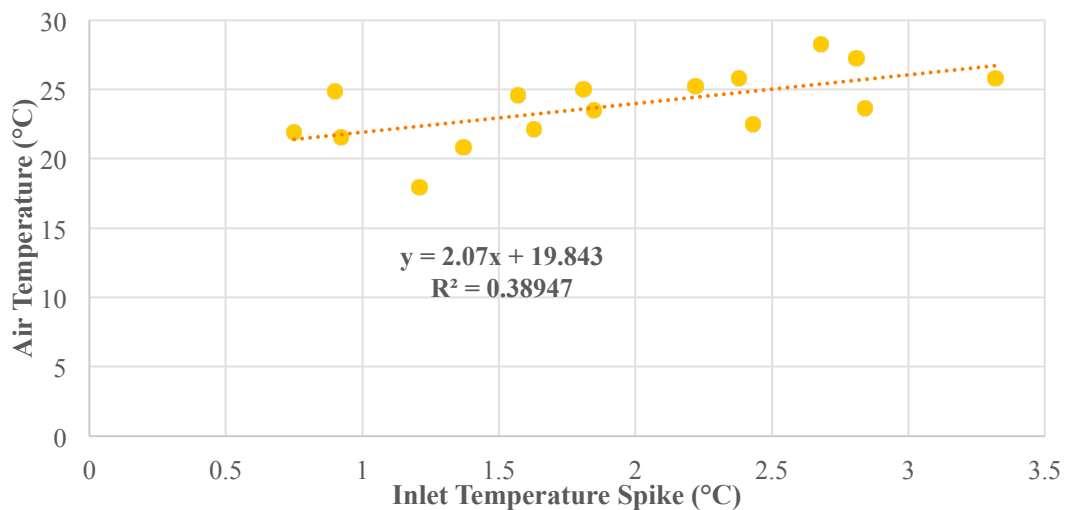
Figure 6-6: Air temperature vs. inlet temperature spike for high rain intensity events linearity analysis.

82

6.3 Monthly Statistical Analysis

To study the differences between inlet and outlet temperatures, a monthly analysis for 2014 was performed. The inlet temperature refers to Temp2IN and the outlet is PT_OutTemp. The most appropriate option for displaying the data was by a box and whisker plot (Figure 6-7). For each month the number of days (n) and total rainfall (m) were accounted for. The blue hatch marks represent the 25th percent quartile, while the green hatch marks are the 75th percent quartile. The lower error bar depicts the minimum five minute temperature and the upper bar is the maximum. Also displayed on Figure 6-7 is the average monthly air temperature.
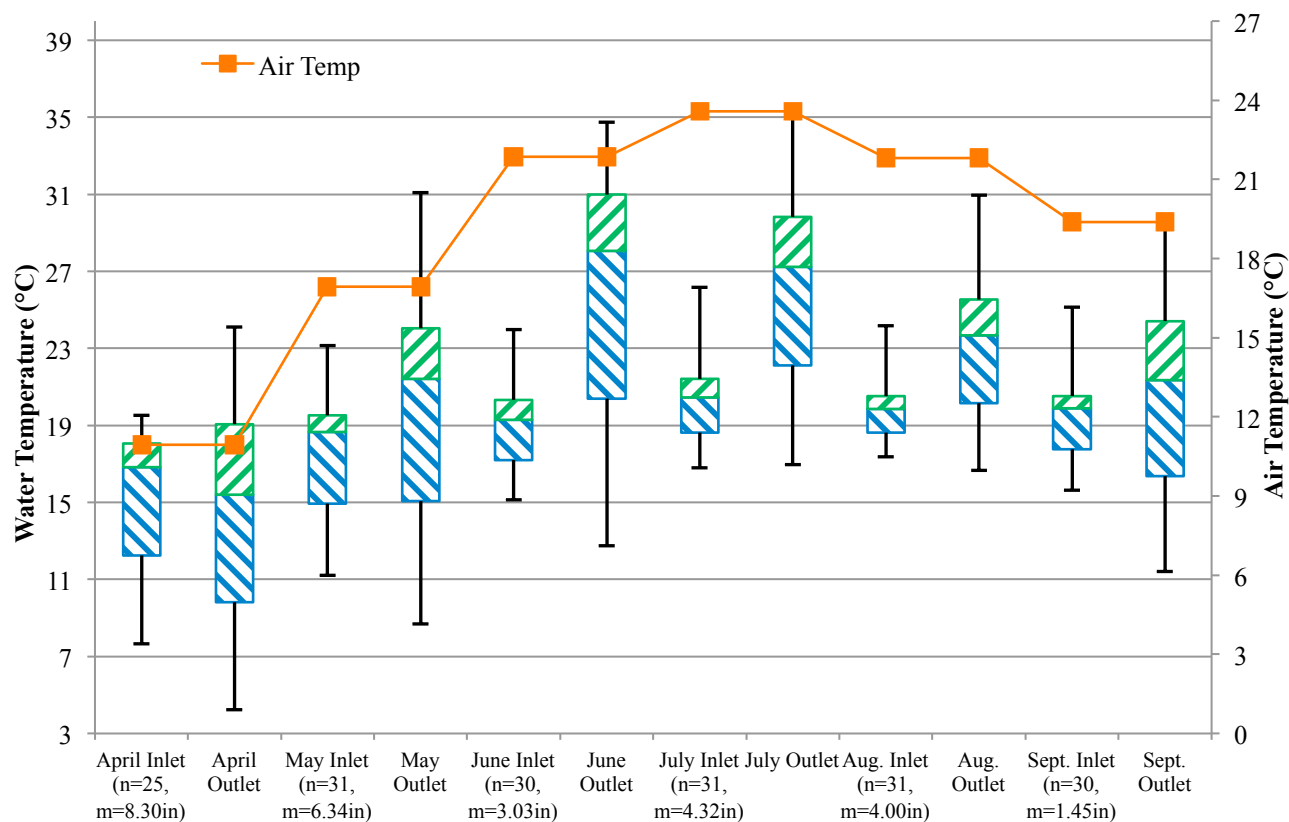
Figure 6-7: 2014 Monthly temperatures box and whisker plot.

As expected, the maximum outlet temperature consistently exceeds the inlet maximum. Interestingly, the minimum for the outlet is much smaller than the inlet temperature except during July when the minimum outlet (16.96°C) is slightly warmer than the inlet (16.79°C). The spread of the statistical data for the inlet and outlet temperature presents a unique trend. From April to August 2014 the maximum and minimum temperature range of the outlet decreases. The relationship, however, is not observed at the inlet as it appears to fluctuate more often. Nonetheless, the difference between the maximum and minimum for the inlet is significantly smaller than the outlet for each month. The difference between the 25th and 75th percent quartile ranges also is different from inlet to outlet. The outlet temperature quartile range decreases steadily from April to August 2014, while the inlet difference decreases to May and then slightly inclines at June and finally shows a decreasing trend through August. For the inlet and outlet, the quartile and maximum and minimum differences both increase going from August to September. The small amount rainfall (1.45 in) in September is the suspected influence.

The most interesting relationship is the strong statistical difference between the inlet and outlet temperatures for each month. The statistical difference values can be found in Table D-3 in the appendix. As previously mentioned, the inlet data has less variability than the outlet. The location of the inlet temperature probe is nearly 6 to 12 inches below the water surface, while the outlet is only under 1 to 3 inches of water. The implications of the outlet temperature sensor being in shallow water is the exposure and influence of air temperature, wind, and solar radiation that the inlet temperature sensor may be insulated from. However, the outlet was statistically different from the air temperature for each month.

6.4 Fishery Analysis

Temperature data is also analyzed on a daily average to account for thermal thresholds regarding fisheries. Table 6-4 tabulates the percentage of days within the specified range in which the outlet temperatures exceed the regulated daily average temperatures for warm water fishes (WWF) and trout stocking fisheries (TSF). The maximum temperature thresholds for the WWF and TSF are portray in Chapter 2 (Table 2-4). Temp4Out was the designated outlet temperature at the CSW.

Table 6-4: Percent exceedance of CSW outlet temperature in comparison to WWF and TSF maximum temperature thresholds (see Chapter 2.6 for temperatures).

Date Range	Percent Exceeding WWF Temperatures	Percent Exceeding TSF Temperatures
April 6-15	90%	90%
April 16-30	46.7%	46.7%
May 1-15	46.7%	46.7%
May 16-31	12.5%	26.7%
June 1-15	0%	93.3%
June 16-30	0%	100%
July 1-31	0%	90.3%
August 1-15	0%	0%
August 16-31	0%	0%
September 1-15	0%	0%
September 16-30	0%	0%
October 1-15	0%	0%
October 16-31	0%	0%

Trout have a much lower threshold for warm waters, resulting in higher percent temperature exceedance during the summer months. However, the months of August and September resulted in much cooler water temperatures than expected. Figure 6-8 illustrates a graph which depicts reasoning behind a 90.3% temperature exceedance for July and 0% for August. The average air temperature for the month of July (23.6°C) is slightly higher than

August (21.8°C), but the TSF temperature criterion is greater during August (26.7°C) than in July (23.3°C), thus yielding temperatures in compliance with the standard in August that were not met in July.
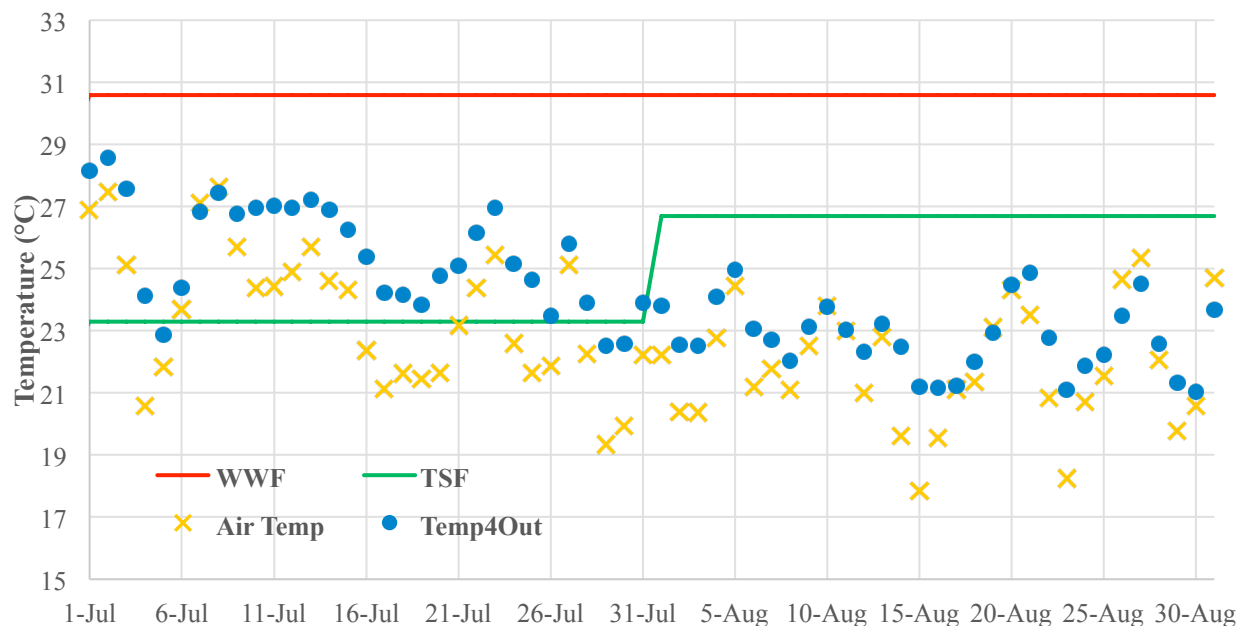
Figure 6-8: Daily average outlet water temperature in relation to WWF and TSF thresholds.

6.5 Meander 1 Thermal Stratification

The layering of water temperatures, or thermal stratification, is commonly seen in stagnant deeper pools of water. Thermal stratification is prominent in the summer, while in the spring and fall there is typically complete mixing of the stagnant water due to wind and cooler temperatures. The CSW has numerous locations with slow-moving ponded areas; referred to as plunge pools. Towards the end of Meander 1 (M1) there is a low flow pool about 24 to 36 inches in depth that demonstrates stratification.

Figure 6-9 illustrates the large temperature differences during July 2014 on the basis of one month, one week, and one day. The one month graph reveals the strong temperature

fluctuation at the surface (Temp1), as well as the influence of rainfall on complete mixing in the M1 pool. The storm events resulted in the bottom temperature (Temp3) mixing with the surface causing a drastic increase in the water temperature.
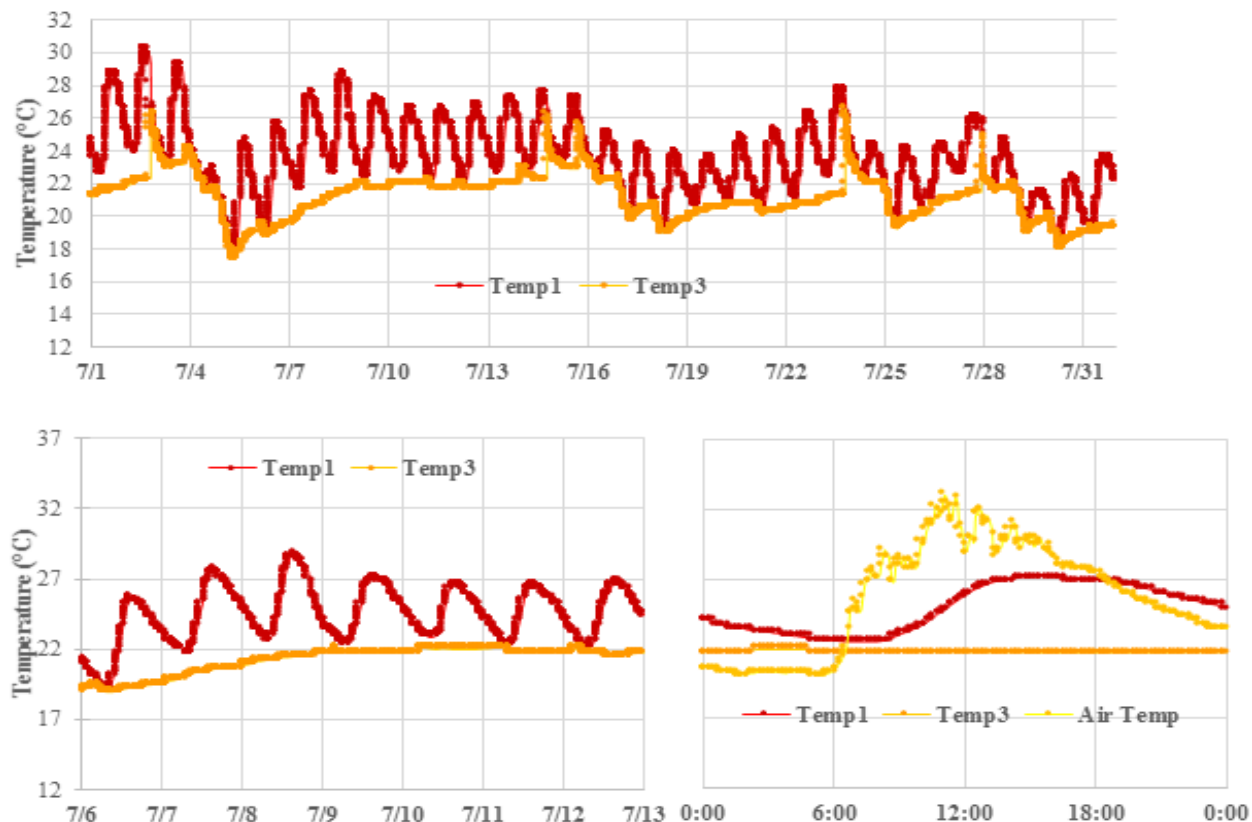
During the week long duration graph, there are time frames where Temp1 and Temp3 are

Figure 6-9: July, 2014 meander 1 temperatures for one month (top), one week (bottom left) and one day (bottom right).

similar in temperature without the effect of rainfall. The 24 hour depicts that the temperature at

the surface and the bottom are almost reaching equilibrium right before sunrise (7:00 to 8:00).

The equilibrium behavior is due to the cooling of the surface temperature through the night,

while the bottom remains steady. Once the sun has risen and the air temperature increases, the

surface water also follows a similar rising trend. The surface water reaches its peak temperature

typically between 15:00 and 16:00 and then begins to slowly decrease as a result of the air

temperature declining as well. To statistically determine the influence of air temperature on the

surface water, paired t-tests were performed. For the month of July 2014, the air and surface

water temperatures were not significantly different ($p = 0.093$). Of the 31 days in July, eleven

indicated strong similarity between the air and surface water temperature (p > 0.05). The water surface and near bottom temperatures were significantly different through the entire month (p ≪ 0.0001).

The month of October 2014 was selected to demonstrate the effects of cooler air temperature and higher wind speeds on the water temperature at M1. In Figure D-3 of the appendix are the month, week, and day graph for October. The cooler temperatures and stronger wind speed allowed for circulation at the M1 pool, resulting in little to no thermal stratification. From statistical analysis, Temp1 and Temp3 were still statistically different, but with a much larger p value (0.0074) than in July. Only one day presented statistically similar temperatures between the surface and bottom waters. Unlike July where the surface and air temperature were similar, the month of October was statistically different (p = 0.038) with only 2 out of 31 days being similar.

Discussed previously about the influence of rainfall on mixing, Figure 6-10 illustrates the July 14, 2014 storm event with reference to air temperature, Temp1, and Temp3. Interesting to note is the air temperature being cooler than the surface water at the beginning of the storm. As the rainfall intensified, Temp1 spiked in temperature until it reached equilibrium with Temp3, which lasted for two hours. The two hour time frame indicates the presence of high storm flows resulting in complete mixing at the M1 pool.
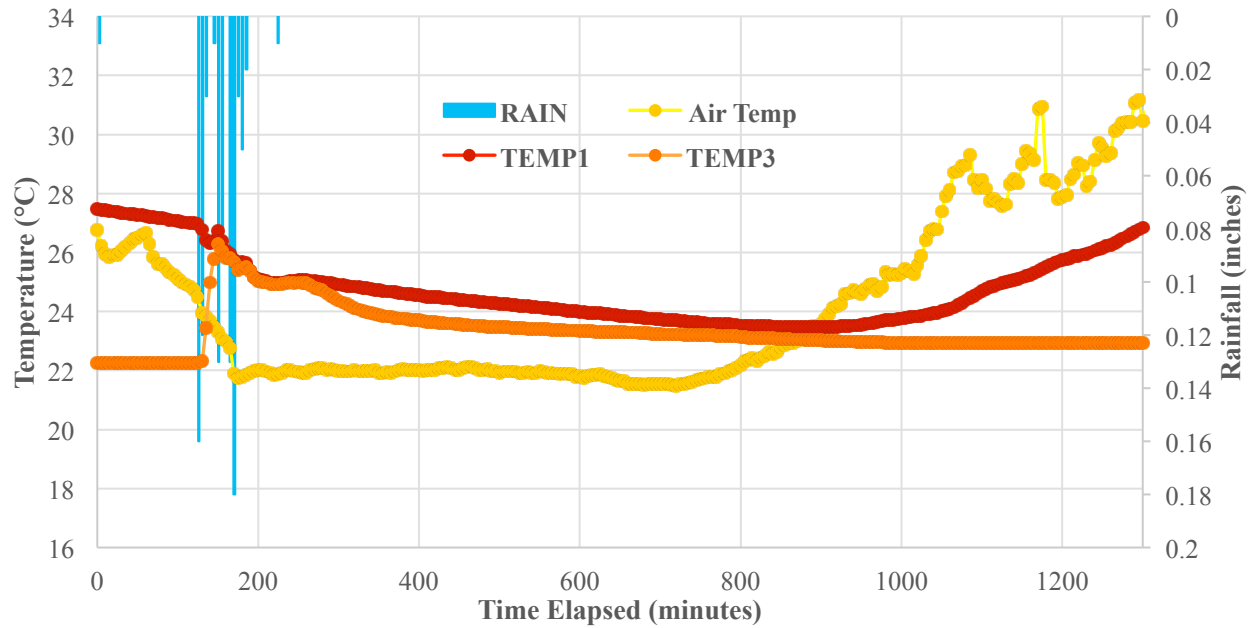
Figure 6-10: July 14, 2014 Storm event meander 1 temperatures hydrograph.

6.6 CSW Temperature Mitigation

Outlet temperatures typically exceeded the inlet during the summer months. The difference in temperature implies that the CSW is a source of thermal pollution. Though it is hypothesized that the large inlet forebay and smaller outlet sedimentation pond is the cause, installing temperature probes through various locations in the meanders will support or deny this theory. Figure 6-11 illustrates the air and water temperatures throughout the CSW for one day. August 27th, 2014 was selected as the day since it was during baseflow conditions and a very warm day with a high of 32.07°C.

90
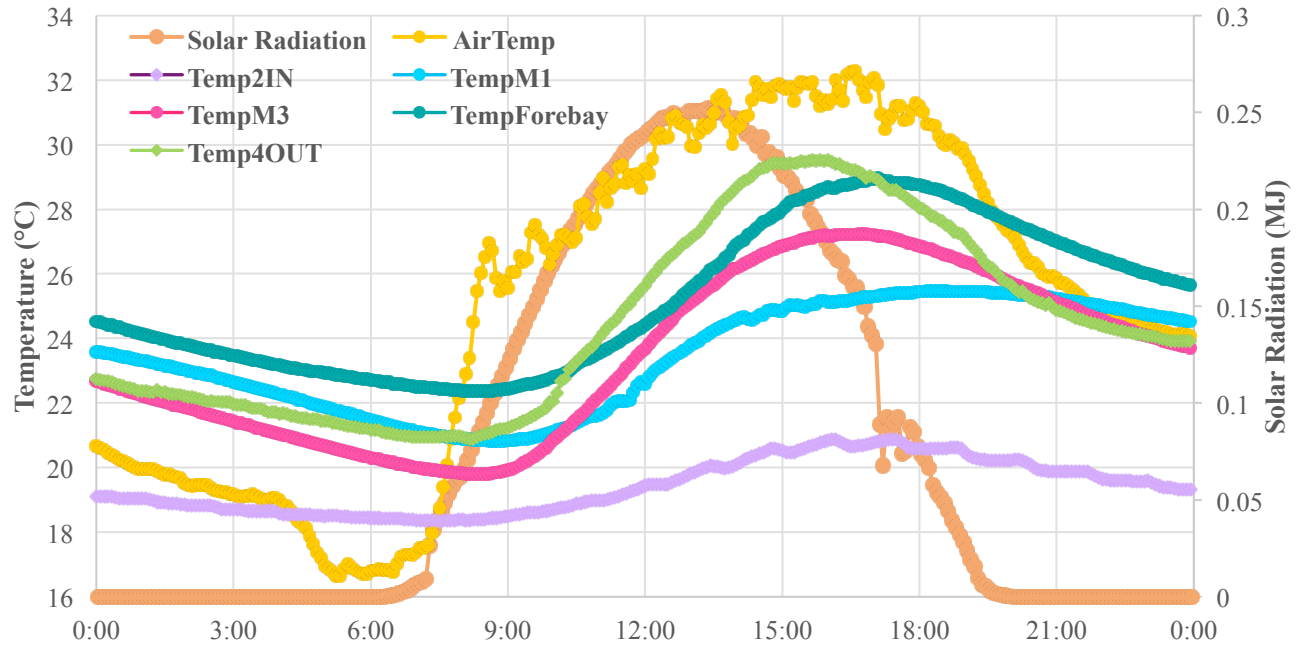
Figure 6-11: Baseflow on August 27, 2014 water temperatures through the CSW

Beginning at midnight, the air temperature begins to gradually cool, where from 4:15 to 7:15 the inlet water temperature is warmer than the air. About an hour later, the outlet temperature starts to exceed TempM1. The influence of the sun rising and the air temperature increasing are suspected to be the cause. At 10:30, TempM3 increases past the temperature at TempM1, in addition to the outlet temperature surpassing the TempForebay. Interestingly, TempM1 and TempForebay become almost equal around 12:45, which is near the peak time for solar radiation. Even though the solar radiation begins to decrease at 13:00, the water temperatures do not follow this trend. Instead, they appear to decline with relation to the air temperature. Around 20:10, TempM1, TempM3, and Temp4Out begin to reach temperature equilibrium with each other. However, an hour later TempM1 does not mimic the stronger falling temperatures and thus becomes warmer than TempM3 and Temp4Out up until the end of the day.

Besides the individual trend of each temperature, another interesting phenomenon is the gap between the various temperature sensors in the CSW. For instance, the continuously large difference between TempM1 and Temp2IN. The smallest temperature gap was 2.30°C at 9:20, while the largest (5.39°C) was at 20:40. The differences indicate that the inlet forebay acts as a thermal pollution source at the CSW. Also the gap between TempM3 and TempForebay reveals the outlet sediment forebay is a source of thermal influence on the outlet temperature.

As illustrated previously in this section regarding temperature during storm events, Figure 6-12 demonstrates the thermal mixing throughout the CSW. One inch of rainfall and an intensity of 0.15 in/hr occurred on August 12, 2014. Between 13:50 and 15:10 the inlet temperature sharply increased, while the other temperatures gradually decreased. Though there was not a large temperature spike (0.45°C), the increasing flow rates resulted in the water completely mixing at the inlet. About 90 minutes after the rainfall concluded, the temperatures at end of M1, M3, outlet forebay, and the outlet were almost at equilibrium with each other. The similar temperatures continued for approximately three hours. The temperature equilibrium can be strongly attributed to high storm flow through the meanders.
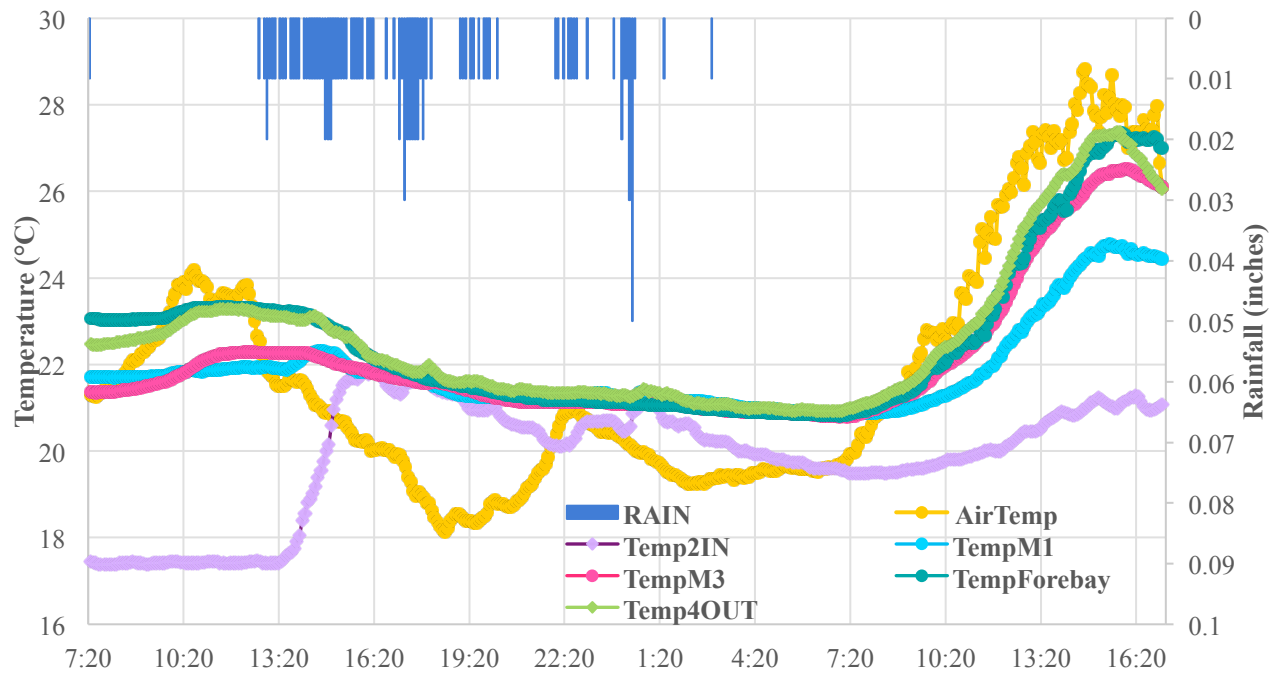
Figure 6-12: August 12, 2014 Storm event temperature mitigation hydrograph.

CHAPTER 7 WATER QUALITY PERFORMANCE RESULTS AND DISCUSSION

7.1: Introduction

Water quality performance at the CSW was analyzed for both storm and baseflow events based on concentration from 2011-2014. A seasonal analysis was also performed in order to further understand each water quality parameter's removal process and numerically validate the large standard deviations. Storm events that utilized autosamplers were evaluated separately from storm grab samples. The nitrogen concentrations and mass loadings from the autosampler event on April 30th, 2014 were analyzed based on the first flush phenomena and the influence of rainfall amount.

7.2: Concentration Based Performance

Water quality treatment performance at the CSW was analyzed based on concentrations. Tables 7-1 and 7-2 summarize the storm and baseflow averages for each water quality pollutant at the inlet and outlet, including sample size and standard deviations. Sample sizes for the water quality constituents vary as a result of quality control and assurance protocols at the Villanova Water Resources Laboratory. In addition, the standard deviations for some parameters are higher than the mean concentration. This is suspected due to strong seasonal variation, which will be analyzed later within this chapter. For storms the large standard deviations could be the cause of variable flow rates per event. Baseflow conditions typically have an outflow of less than 0.10 cfs, whereas the storm outflows vary between 0.3 and 4.0 cfs.

94

Table 7-1: Summary of baseflow water quality parameters.

Parameter	Unit	n	INLET		OUTLET		Removal
			Mean	SD	Mean	SD	
pH	--	33	7.36	0.56	7.58	0.51	---
Conductivity	μS/cm	33	958	303	989	507	---
TSS	mg/L	32	17.7	23	16.9	21	4%
TDS	mg/L	33	636	246	683	405	-7%
NO_3	mg/L	27	1.78	0.98	0.469	0.465	74%
NO_2	mg/L	31	0.067	0.045	0.030	0.037	56%
TKN	mg/L	21	1.11	0.63	0.78	0.72	30%
TN	mg/L	18	2.71	0.80	1.21	0.86	55%
PO_4	mg/L	24	0.078	0.076	0.043	0.052	44%
TP/TKP	mg/L	24	0.24	0.22	0.13	0.22	45%
Cl^-	mg/L	28	374	326	413	393	-10%

Though the CSW was not designed for water quality treatment during baseflow conditions, data has proven it to be successful at removing certain pollutants. As suspected, total dissolved solids (TDS) and chlorides (Cl^-) increase in concentration from inlet to outlet and total suspended solids (TSS) have a marginal decrease (4%) (Table 7-1). Chloride is a conservative parameter, therefore it is not removed through any biological, chemical or physical processes. TDS and TSS primarily rely on physical processes such as particle settling through slow enough velocities. During storms there is removal, on average, of all pollutants, which is most likely due to a combination of biological, chemical and physical processes, as well as dilution.

Table 7-2: Summary of storm water quality parameters.

Parameter	Unit	n	INLET		OUTLET		Removal
			Mean	SD	Mean	SD	
pH	--	37	7.06	0.4	7.19	0.3	---
Conductivity	μS/cm	37	742	836	485	470	---
TSS	mg/L	36	16.4	20	13	11	21%
TDS	mg/L	37	533	555	362	451	32%
NO_3^-	mg/L	21	1.58	2.44	0.595	0.51	62%
NO_2^-	mg/L	31	0.051	0.029	0.041	0.026	19%
TKN	mg/L	24	1.13	0.96	1.04	1.17	8%
TN	mg/L	17	2.77	2.74	1.75	1.53	37%
PO_4	mg/L	26	0.066	0.057	0.053	0.041	19%
TP/TKP	mg/L	33	0.27	0.23	0.21	0.18	23%
Chloride	mg/L	30	362	504	207	344	43%

7.2.1: Nitrogen

Figure 7-1 illustrates total nitrogen (TN) storm and baseflow removal moving downstream from the inlet of the CSW with standard deviations as the error bars. The progression of total nitrogen concentration through the CSW gives insight into the removal or accumulation of the water quality constituent. Though the two inlet baseflow and storm TN values are very similar (2.71 and 2.77 mg/L respectively), the 55% baseflow removal is greater than the 37% removal for storms. Both storm and baseflow events show an average decrease in concentration from inlet to M3. However, from baseflow M3 (1.64 mg/L) to the outlet (1.21 mg/L) there is a greater reduction than opposed to storm M3 (1.87 mg/L) to outlet (1.75 mg/L). The higher removal of TN in baseflow is likely tied to longer hydraulics retention times (HRTs) (see Chapter 4). The much higher standard deviations of TN for storm events in comparison to baseflow could also be attributed to the lower storm percent removal. A seasonal analysis will investigate the reason behind these extreme standard deviations.
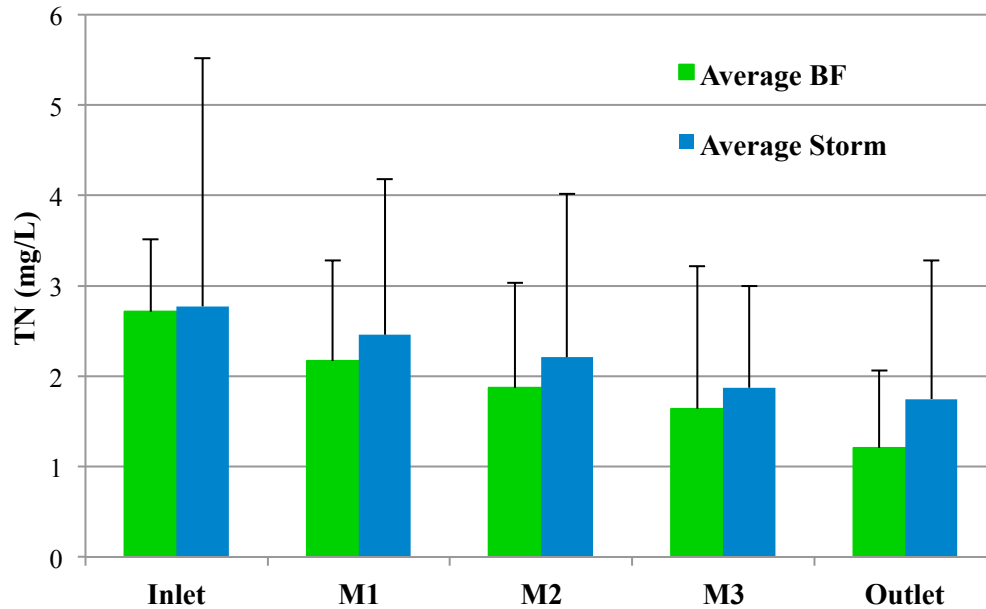
Figure 7-1: Total nitrogen by sampling location.

In addition to analyzing water quality dynamics at different sampling locations in the CSW, percent exceedances are also reported. A Gumbel distribution was used to sort and rank the observed concentrations; inlet and outlet points with the same percent exceedance are not necessarily from the same sampling event. The purpose of a percent exceedance plot is to demonstrate the differences and similarities between baseflow and storm concentrations and their corresponding distributions and yield an understanding of how the system performs over time.

Figure 7-2 is the percent exceedance plot for TN and the stream water quality standard of 4.91 mg/L from PA Code Chapter 25 is used as a reference value for comparison. Of the 17 storm events at the CSW, only one inlet concentration and one outlet concentration exceeded the standard, and the outlet concentration was 4.97 mg/L, slightly greater than the standard (4.91 mg/L). Generally, the further away the influent and effluent concentrations curves are from each other, the greater the improved performance (greater reduction from inlet to outlet), and vice versa. The tighter grouping of the storm data sets demonstrates overall less reduction from inlet

to outlet. The greater gap between the observed influent and effluent concentrations for baseflow indicates greater removal through the CSW. Additionally, the reduction observed for baseflow is relatively consistent. This percent exceedance analysis supports the observations presented in Tables 7-1 and 7-2 and Figure 7-1. Also, the influent TN concentrations for storm and baseflow are similar, although the baseflow effluent is overall lower than the storm effluent
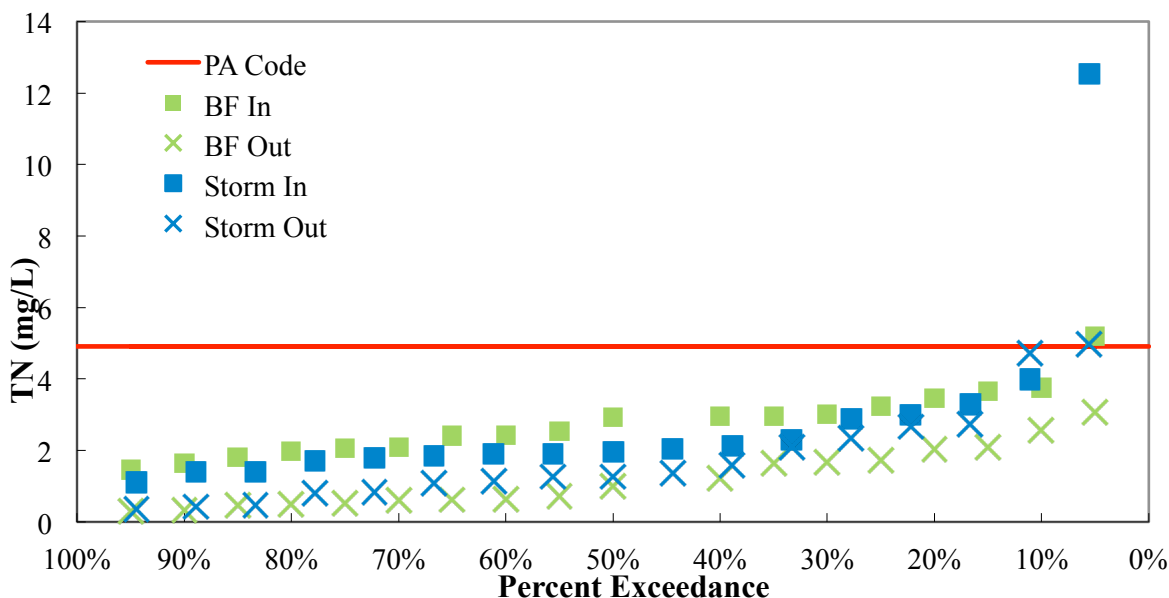
Figure 7-2: Total nitrogen percent exceedance graph

Total nitrogen represents the inorganic (nitrate and nitrate) and organic (total kjedahl nitrogen) forms of nitrogen. Each nitrogen species relies on a different removal process. In order to understand TN removal as a whole, the three components that comprise it should be analyzed separately. The primary steps of the nitrogen cycle are to oxidize ammonium (NH_4^+) to nitrite (NO_2^-) and then to nitrate (NO_3^-). However, NH_4^+ can also be removed as NH_3 through ammonia volatilization. These concepts should be kept in mind when analyzing nitrite concentrations at the CSW.

Though nitrite is an intermediary process in the nitrogen cycle, there still should be evidence of reduction from inlet to outlet since there is no known point sources of nitrogen entering through the meanders. Figure 7-3 illustrates an interesting trend in NO_2^- concentrations for both storm and baseflow events through the CSW. Even though inlet baseflow has higher nitrite concentrations then a storm, its reduction is over double the amount in comparison to storms. The influence of HRT is suspected to be the result of greater reduction. From baseflow M1 (0.052 mg/L) to M2 (0.055 mg/L) and storm inlet (0.051 mg/L) to M1 (0.054 mg/L) there is a statistical difference between the increasing average concentrations. The increase in concentrations could be due to outside sources of nitrogen entering through the meanders as opposed to at the inlet (e.g. direct runoff, additional inlet pipes and animals).The standard deviations being nearly double or over the mean concentrations for each location can be attributed to seasonal fluctuations (see Chapter 7.3.1).
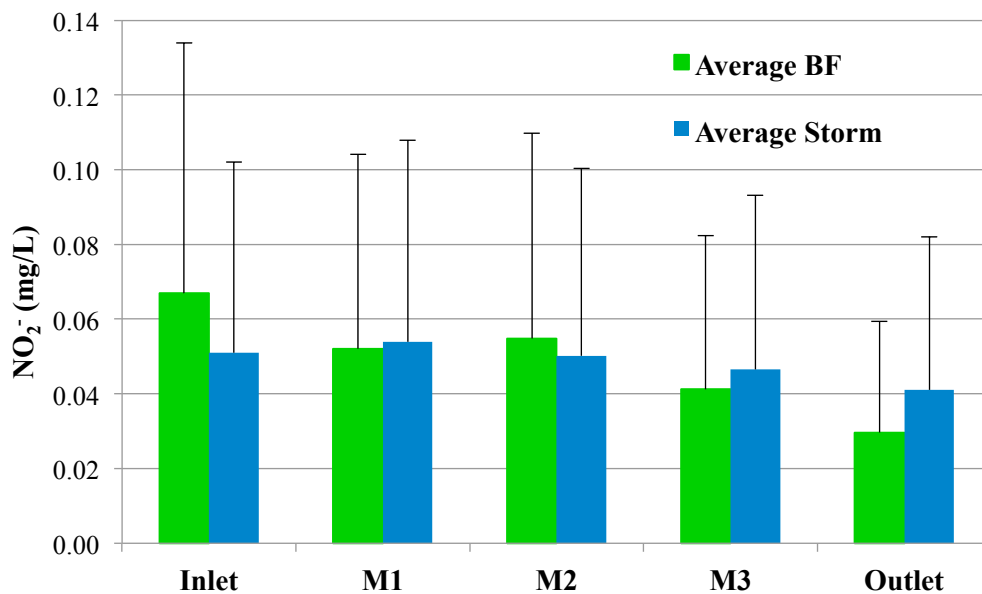
Figure 7-3: Nitrite concentration by sampling location

Whereas nitrite concentrations fluctuated going from inlet to outlet, nitrate levels only showed decreasing trends (Figure 7-4). Of all constituents measured, nitrate has the greatest average removal during both baseflow and storm conditions. The most removal occurred from the inlet to M1 (i.e. 41% for baseflow and 34% for storms). The combination of long HRT and uptake through plants could be the contributing factors to high nitrate reduction. Furthermore, nitrate can diffuse into soil, unlike nitrite, which is only removed through bacteria. The reductions observed for nitrate can also be explained through flow through the shallow meanders and deep plunge pools, which potentially allows for aerobic and anaerobic conditions in the CSW. The additional cycling pathways through diffusion and variable aerobic zones may explain why nitrate has greater concentration reduction through the CSW than nitrite.
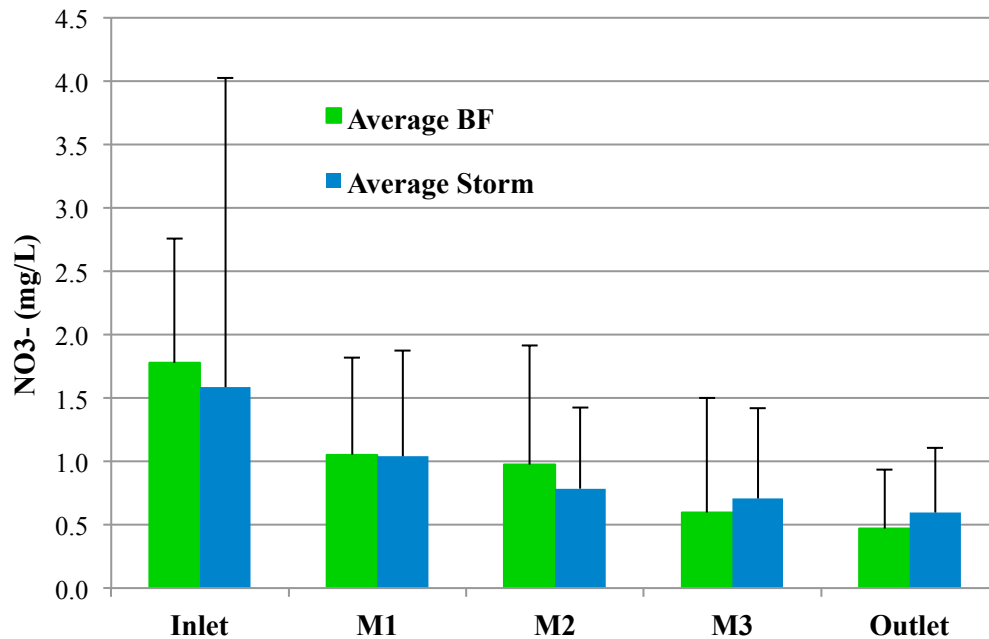
Figure 7-4: Nitrate concentration by sampling location.

Total Kjeldahl nitrogen (TKN) is both the inorganic (ammonium and ammonia) and organic forms of TN at the CSW. Organic nitrogen is transformed through biological processes to the ammonium form, which is then proceeded to nitrite and nitrate through nitrification.

However, it is important to note that algae and aquatic species utilize nitrate and ammonium to convert the nutrients back to organic nitrogen forms. Figure 7-5 illustrates the difficulty in removing TKN as a result of the CSW's ability to accumulate organic nitrogen. Total Kjeldahl nitrogen increases 10% from M2 to M3 for baseflows and from 8% for inlet to M1 and 6% for M3 to outlet for storms. Besides accumulation from animal waste and plants, the increase may also be attributed to the CSW soil having some attached organic-N. In addition, the high TKN concentrations could be due to samples not being filtered before digestion and thus allowing for organic content to pass through. Without further knowledge on the soil chemistry in the CSW a definite conclusion cannot be made for the increases in TKN concentrations.
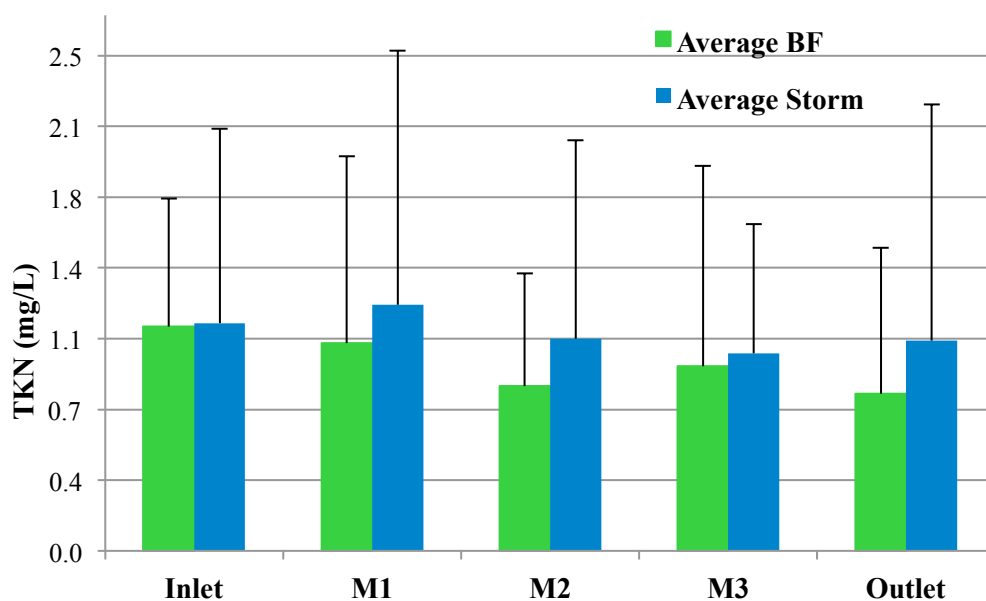
Figure 7-5: TKN concentration by sampling location.

Though ammonia was not individually analyzed because of limited number of samples, an event in which all nitrogen species were successfully obtained can provide insight into the nitrogen cycle (Table 7-3). Organic nitrogen (organic-N) was calculated by subtracting TKN from NH_3. The duplicate samples are presented to show the influence of organic matter on

101

measured concentration, for example, the difference in TKN and NH_3 for M1-1 and M1-2. Examining concentrations from inlet to M1 shows that NH_3, TKN, and organic-N all increase while the other constituents decrease. Assimilation and ammonification are the possible processes contributing to increases in organic-N and NH_4^+. Based on averages, from M1 to M3 all the nitrogen species decrease, which indicates successful nitrogen removal processes of ammonification, nitrification and denitrification. However, the reductions could also be attributed from NO_3^- and NH_4^+ diffusion into the soil or nitrogen uptake by vegetation. Finally, from M3 to the outlet the concentrations of NH_3 and NO_3^- increase. The ammonification process, which converts organic-N to ammonium, could be the reason behind NH_3 increasing and thus TKN and organic-N decreasing. In the context of NO_3^- increasing from M3 to outlet is postulated to be a result of decaying plant matter near the outlet.

Table 7-3: November 4, 2014 baseflow nitrogen parameters by sampling location.

	NH_3	NO_2^-	NO_3^-	TKN	Organic-N	TN
IN1	0.018	0.024	1.289	0.325	0.307	1.638
IN2	0.025	0.026	1.243	0.692	0.667	1.961
M1-1	0.146	0.005	0.699	3.842	3.696	4.545
M1-2	0.057	0.005	0.669	0.718	0.661	1.391
M3-1	0.025	0.005	0.045	0.334	0.309	0.384
M3-2	0.054	0.005	0.104	2.511	2.458	2.621
OUT1	0.068	0.005	0.045	0.100	0.032	0.150
OUT2	0.061	0.005	0.343	0.100	0.039	0.448
% Removal from IN1 to OUT1	-289%	79%	97%	69%	90%	91%

7.2.2: Phosphorus

Particularly for storm events, phosphorus posed as a difficult water quality parameter to remove at the CSW (Figure 7-6). Phosphorus removal strongly relies on HRT, hence the most removal is observed during baseflow conditions. The greatest reduction in baseflow total phosphorus (TP) concentrations occurred from M1 (0.201 mg/L) to M2 (0.133 mg/L), even though it is suspected that the HRT is lower from M1 to M2 than other longer pathways (27.94 hours, n = 1); other phosphorus removal processes may be greater between the meanders. Dissolved phosphorus removal through microbes is a rapid process, and in a long enough time span phosphorus can be released again by cell death.
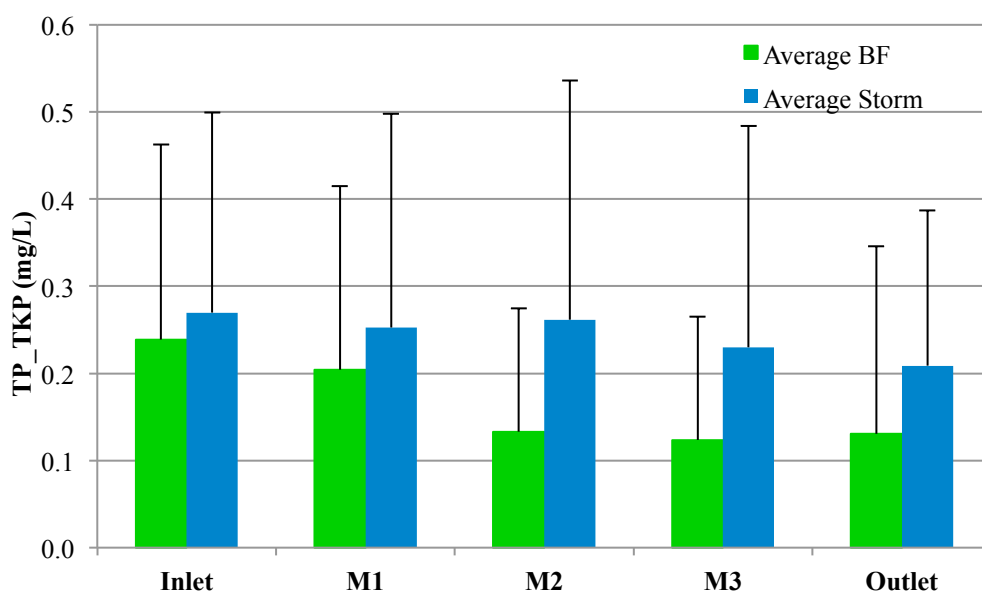
Figure 7-6: Total phosphorus by sampling location.

Figure 7-7 depicts the percent exceedance for TP, using the PA Code water quality limit (0.14 mg/L) as a reference. Total phosphorus exceeds the PA Code limit at the outlet approximately 24% of the time for baseflow and 55% of the time for storm observations. However, nine of the 16 outlet exceedance events occurred in 2011, prior to the CSW being

considered fully established, as construction was during the Summer of 2010. Uptake of phosphorus through vegetation is an important removal process. Plants need longer than one year to become mature, thus resulting in very little to no removal of TP through vegetation in 2011. Further, as plants mature and coverage becomes denser, there is greater hydraulic resistance to promote settling. Interestingly, for the higher 50% exceedance observations (0.5-1 in Figure 7-7) the influence concentration is similar for baseflow and storm. However, for the lower 50% exceedance observations, the storm TP influent concentration is substantially higher than the baseflow influent concentration.
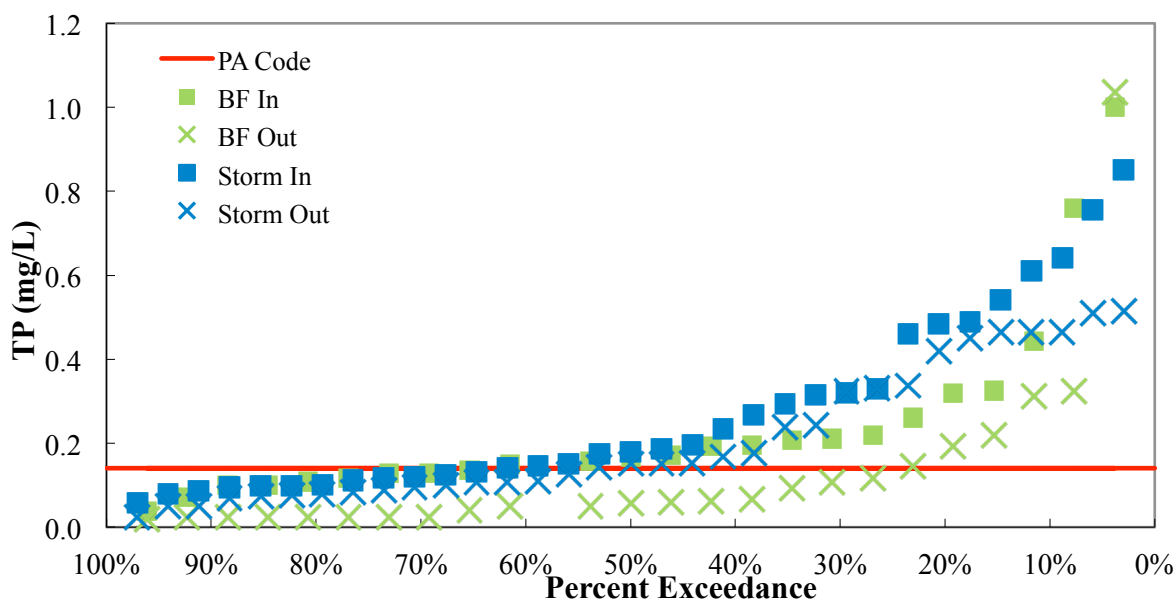
Figure 7-7: Total phosphorus percent exceedance graph.

Orthophosphate (PO_4^{3-}), a soluble inorganic form of phosphorus, is also tested and analyzed at the CSW (Figure 7-8) and has similar trends to TP. The similarities consist of the greatest removal occurring between M1 (0.078 mg/L) and M2 (0.048 mg/L) for baseflow and from M2 (0.075 mg/L) to M3 (0.057 mg/L) for storms, with approximately double the percent removal during storms than baseflow (Tables 7-1 and 7-2). A study on the phosphate

concentrations in the CSW sediment could provide greater insight into the key removal processes.
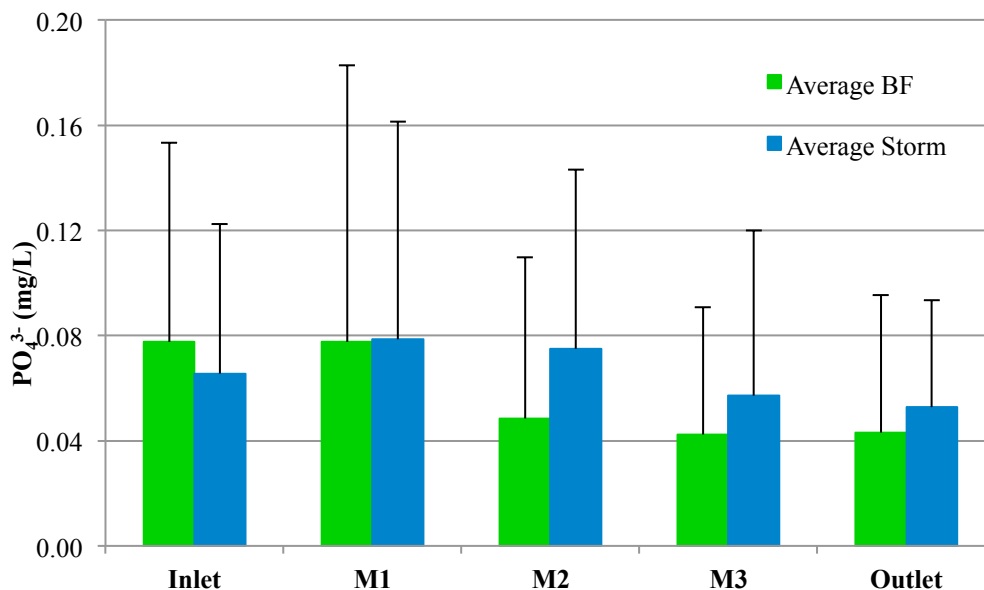
Figure 7-8: Orthophosphate concentration by sampling location.

7.2.3: Chlorides

Chlorides presented to be a difficult parameter to remove from the CSW, especially during baseflow conditions (Figure 7-9); chloride is known to be conservative, so this finding is expected, albeit disappointing. The standard deviations, represented as error bars, are extremely large and exceed the average values. A seasonal analysis performed in section 7.3.3 will explain the large standard deviations. Storm concentrations showed a gradual decreasing trend from inlet to outlet. The decreasing trend is suspected to be a result of dilution from stormwater flow. Since there is little volume reduction from inlet to outlet during baseflow conditions, chloride concentrations rarely decreased on an event-by-event basis. The increase in baseflow concentrations at M2 and outlet are due to natural chlorides or other sources entering the CSW.
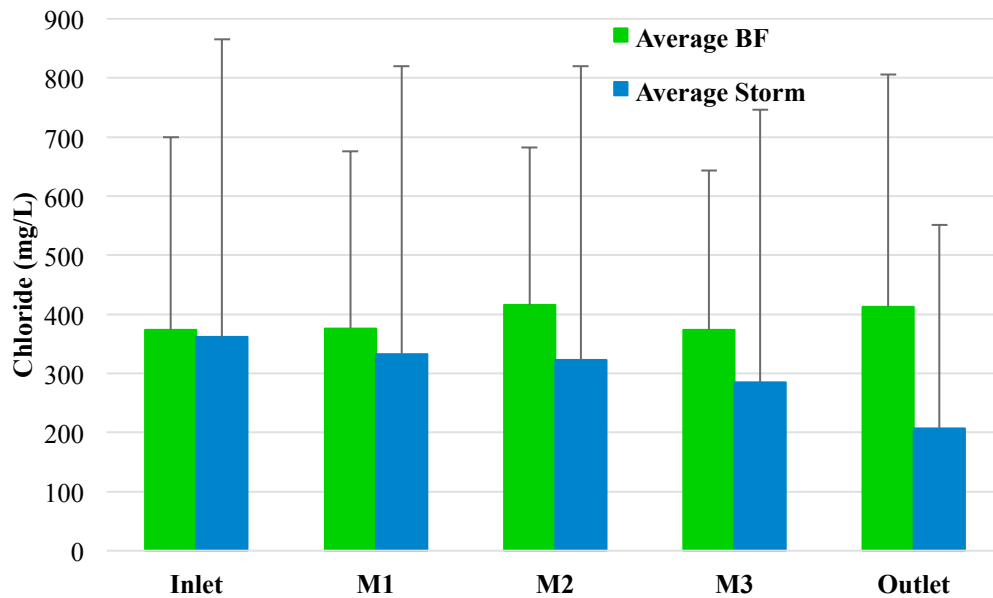
Figure 7-9: Chloride concentration by sampling location.

Figure 7-10 illustrates the percent exceedance plot for chlorides during baseflow and storm events with reference to the PA Code limit of 250 mg/L. About 50% of baseflow outlet concentrations exceeded the 250 mg/L limit, while only 17% of storm event effluent concentration were above the maximum. As the baseflow outlet concentrations showed a gradual increase in concentration with less percent exceedance, the storm events jumped from 234 mg/L to 530 mg/L.
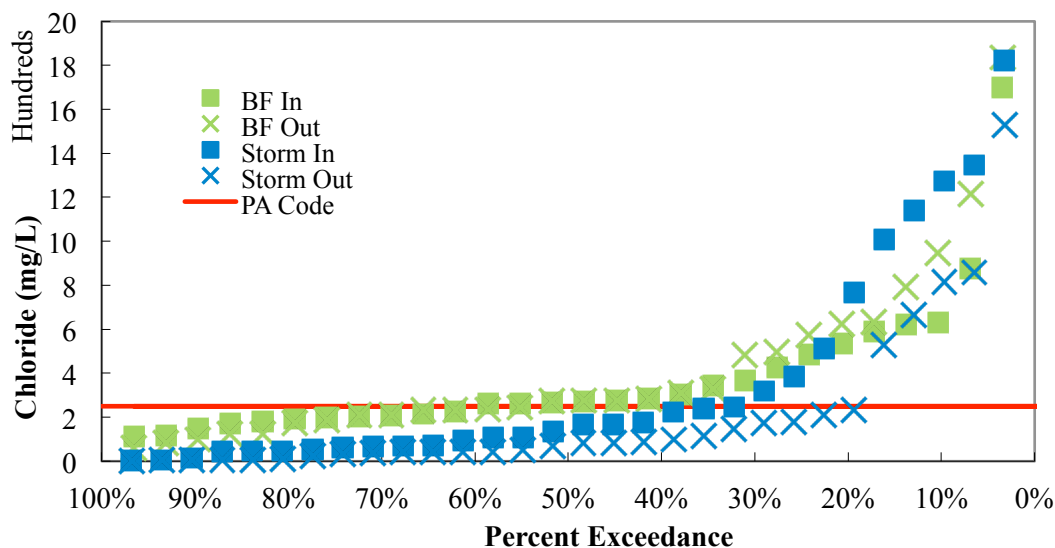
Figure 7-10: Chloride percent exceedance graph with reference to the PA Code limit.

7.2.4: Total Suspended Solids and Total Dissolved Solids

Similar to chlorides, TSS and TDS display little to no treatment due to no biological or chemical removal processes. Figure 7-11 and 7-12 illustrate the average TSS and TDS concentrations and standard deviations for each sampling location. From inlet to M1 during baseflow, TSS decreases while TDS increases. The low flow and longer HRT from inlet to M1 benefits TSS by allowing for adequate settling time. The increase in TDS can be partially related to the chloride concentration trend. It is difficult to directly interpret TDS removal or accumulation since the concentration depends on the amount of cations and anions.
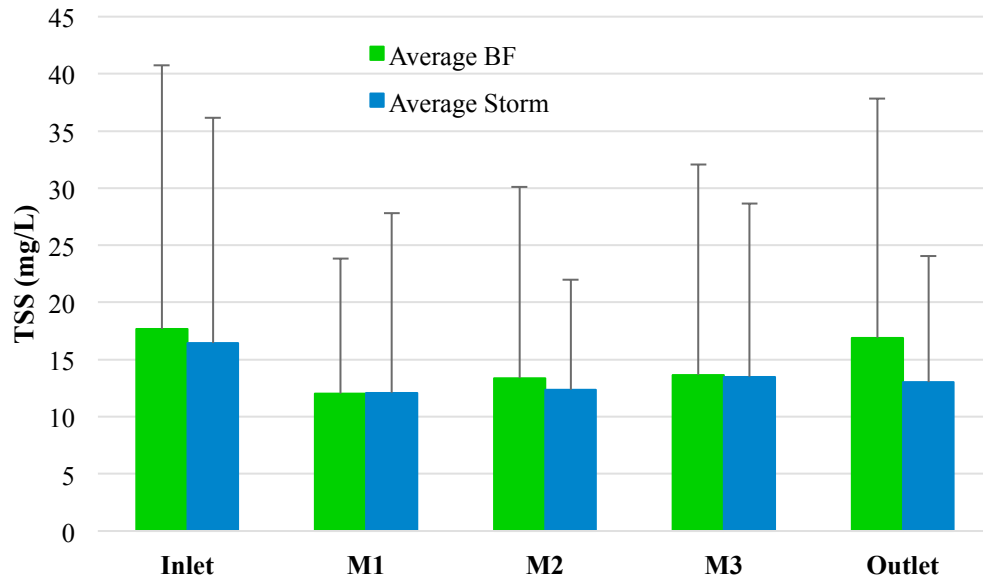
Figure 7-11: Total suspended solids by sampling location.
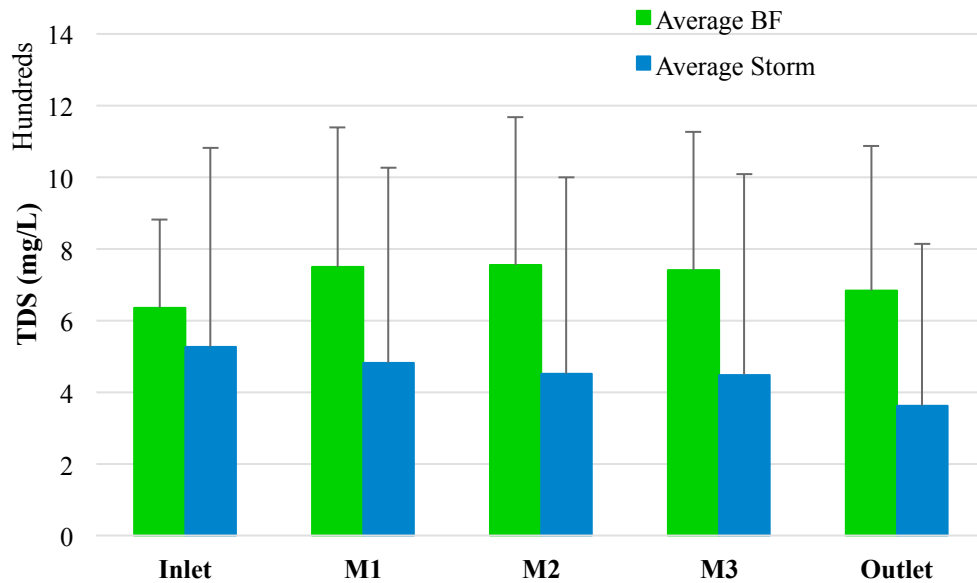
Figure 7-12: Total dissolved solids by sampling location.(y axis scale in hundreds)

From M3 to the outlet there is a large sediment forebay, which is supposed to create ideal settling conditions. However, the TSS increase between these two locations provides indication of a possible failing sediment forebay. On the opposite spectrum, during storm events the TSS

decreases on average from 13.5 mg/L at M3 to 13.02 mg/L at the outlet. Even though storm flow rate is much higher than the baseflow rate and should resuspend the solids, this was not observed. It is hypothesized that because the samples are collected the following morning after a storm there is enough time allowing for the particles to settle. The relationship of TSS between these two locations also supports an explanation behind the TP concentrations. Since suspended solids can contain nutrients, the increase in baseflow TP concentration and decrease in storm TP concentration from M3 to the outlet dictate that phosphorus is dominant in the particulate form.

7.3 Seasonal Performance

The next step in understanding the removal processes of water quality parameters is a seasonal based analysis. The Villanova University CSW is situated in eastern Pennsylvania, where the climate typically experiences all four seasons. The seasons pertaining to this research are defined as the following; Summer (June 1 to August 31), Fall (September 1 to November 30), Winter (December 1 to February 28), and Spring (March 1 to May 31).

7.3.1: Nitrogen

Nitrogen species are known to be affected by temperature primarily due to biological processes. The warmer temperatures in the summer and fall depict the seasonal influence on nitrite reduction from inlet to outlet at the CSW (Figure 7-13). Inlet NO_2^- in the winter for baseflow conditions portrays the largest average concentration. Decaying vegetation that is releasing nutrients and groundwater leeching and infiltration of these nutrients are potential accounts for this large influent concentration. For storms, the largest average inlet NO_2^- concentration was present in the fall, but with winter being the next greatest value.

109
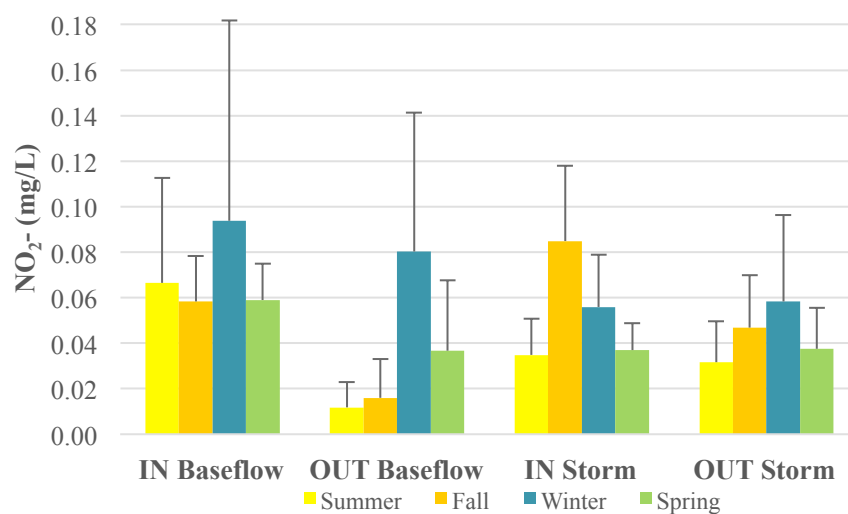
Figure 7-13: Nitrite seasonal average inlet and outlet concentrations.

Nitrite can only be transformed to NO_3^- through nitrification, which is a microbial mediated process. Warmer temperatures promote greater microbial activity that resulted in greater NO_2^- reduction during the summer and fall seasons as depicted in Figure 7-13 and Table 7-4. However, for storms in the fall there is much greater NO_2^- removal in comparison to the summer. Nitrification is also limited by dissolved oxygen (DO) levels since it is an aerobic process. The slightly cooler than summer temperatures in the fall may have higher DO to compensate for the temperature change.

Table 7-4: Nitrite seasonal average percent removal.

	Baseflow		Storm	
	% Removal	N	% Removal	N
Summer	82%	10	9%	10
Fall	73%	9	45%	6
Winter	14%	5	-4%	8
Spring	38%	7	-2%	7

Nitrate presented a similar seasonal reduction influence as a result of warm temperatures to that of nitrite (Figure 7-14). The only difference is the extremely high inlet storm NO_3^-

concentration for the winter. Plant decay entering the CSW from stormwater runoff is the suspected cause of the elevated NO_3^- concentration. Nonetheless, the CSW was capable of reducing the nutrient throughout every season (Table 7-5). During baseflow conditions in summer and fall, the warm temperatures promoting microbial activity are suspected to transform NO_3^- to atmospheric nitrogen through denitrification. However, this does not appear to be the case for storm events. The greatest storm NO_3^- reduction is in the winter and spring. Diffusion of nitrate into the CSW sediment could possibly explain the greatest storm removal in the winter and spring. In conclusion, it is difficult to assume NO_3^- presents seasonal trends due to multiple removal or transformation processes involved.
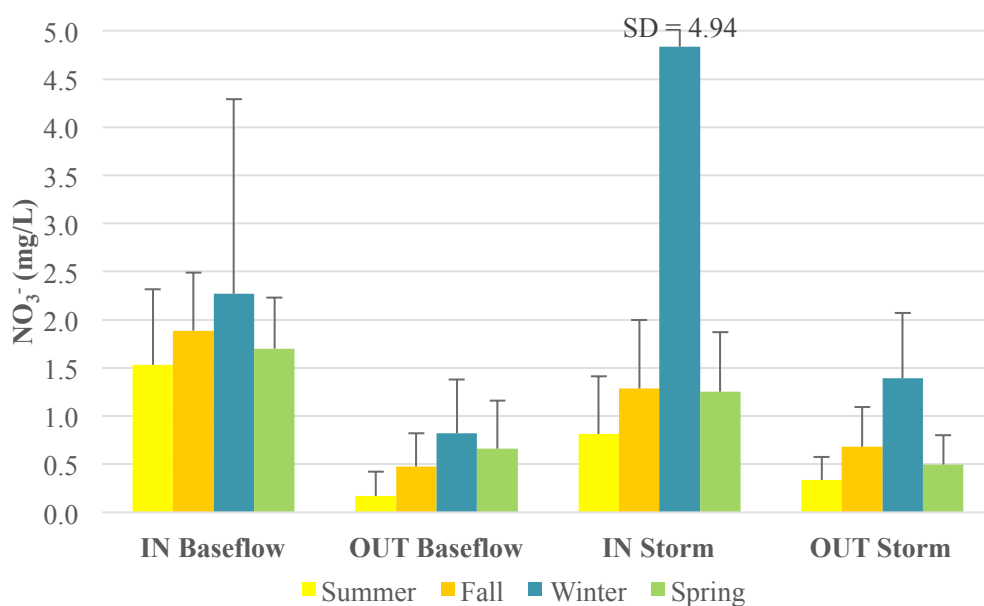
Figure 7-14: Nitrate seasonal average inlet and outlet concentrations

Table 7-5: Nitrate seasonal average percent removal.

	Baseflow		Storm	
	% Removal	N	% Removal	N
Summer	89%	8	59%	9
Fall	75%	9	47%	5
Winter	64%	3	71%	3

Spring	61%	6	60%	4

Total Kjedahl nitrogen is the final nitrogen specie analyzed for seasonal trends at the CSW. It is important to restate that TKN is primarily comprised of organic nitrogen with slight amounts of ammonia. Figure 7-15 illustrates that there is no clear seasonal trend of influent TKN concentrations during baseflow and storm events. However, it can be concluded that nitrate is the dominant form of influent nitrogen, except during summer storms where TKN is larger than NO_3^-. The dominant form is influenced by temperature, dissolved oxygen, and biochemical conditions. Organic nitrogen can be accumulated in more ways than removed, thus resulting in a portion of TKN always being present in the CSW. The removal of TKN also does not conclude a seasonal influence regarding temperature and vegetation (Table 7-6).
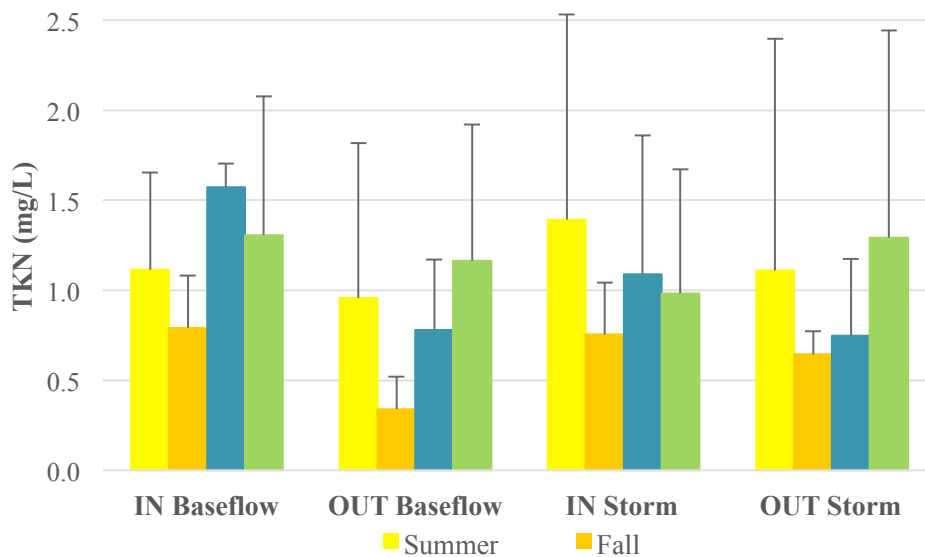
Figure 7-15: TKN seasonal average inlet and outlet concentrations.

Table 7-6: TKN seasonal average percent removal.

	Baseflow		Storm	
	% Removal	**N**	**% Removal**	**N**
Summer	14%	5	20%	8

Fall	57%	7	15%	2
Winter	50%	3	32%	6
Spring	11%	6	-32%	8

7.3.2: Phosphorus

Like total nitrogen, total phosphorus is comprised of different phosphate species; organic, orthophosphate, and polyphosphate. Orthophosphate is biologically available form of phosphates, thus is primarily removed through plants and microorganisms. Figures 7-16 and 7-17 illustrate the influent and effluent trends of TP and orthophosphate during baseflow and storm conditions. As expected, the highest inlet total phosphorus concentrations occurred during the summer and fall as a result of fertilizing on campus. However, for PO_4^{3-} this was not the case as the highest baseflow influents were the summer and winter. The summer can be explained through lawn fertilizers, but in the winter the high orthophosphates are suspected from decomposing plant matter on campus, or long term leaching and infiltration of phosphorus. Though organic phosphate is the form bound to plant tissue, it is transformed to orthophosphate after plant decomposition.

Figure 7-16: Total phosphorus seasonal average inlet and outlet concentrations.
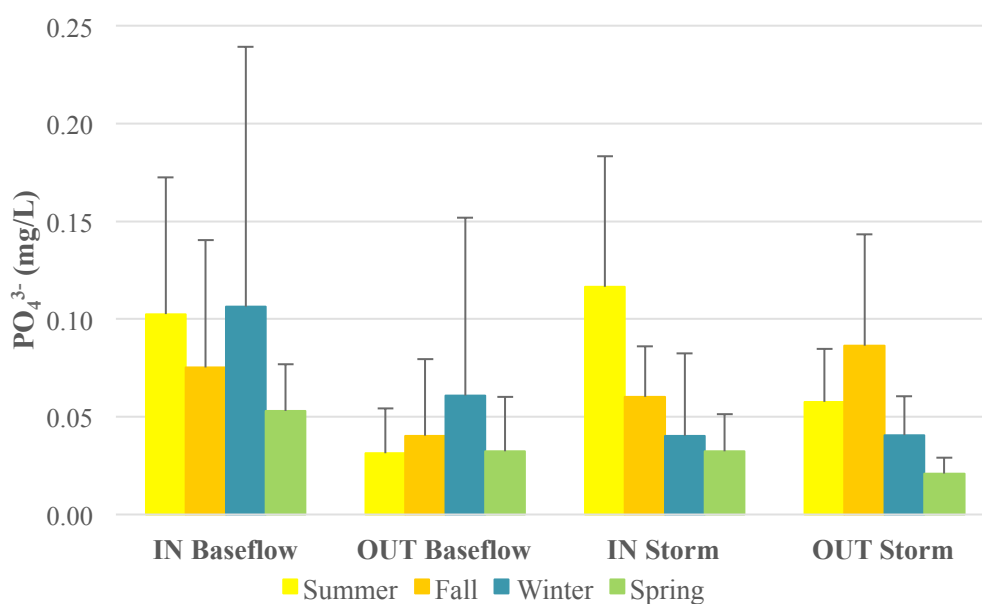
Figure 7-17: Orthophosphate seasonal average inlet and outlet concentrations.

Tables 7-7 and 7-8 show the percent removal of PO_4^{3-} and TP for each season of baseflow and storm events. During baseflow conditions, both parameters were sufficiently

removed for each season. Summer and fall were of course the highest orthophosphate removal due to strong influence from the biological community at the CSW. Total phosphorus baseflow reduction was the most during the summer and winter. The strong winter reduction can partially be attributed to the high removal of TSS during the winter (55%) as well. Since total phosphorus is composed of both particulate and dissolved forms, it is suspected that the main form of TP in the winter is particulate.

Table 7-7: Total Phosphorus seasonal average percent removal.

	Baseflow		Storm	
	% Removal	N	% Removal	N
Summer	65%	7	25%	11
Fall	28%	7	2%	7
Winter	66%	4	50%	9
Spring	33%	6	-17%	6

Table 7-8: Orthophosphate seasonal average percent removal.

	Baseflow		Storm	
	% Removal	N	% Removal	N
Summer	69%	6	50%	8
Fall	46%	8	-44%	6
Winter	43%	5	-1%	7
Spring	39%	5	35%	5

In regards to storm phosphorus reduction, the baseflow relationship presented previously applies to the TP more so than orthophosphate. Orthophosphate does illustrate most storm removal during the summer, however, the second highest reduction was in the spring. A possible reason could be due to the PO_4^{3-} being more predominant in the dissolved phosphorus form, since TDS storm removal was somewhat similar for the spring (27%).

7.3.3: Chlorides

Figure 7-18 portrays the anticipated high chloride concentrations at the inlet in the winter. The concentration is especially elevated during storm events, predominately due to runoff carrying deicing salts. The slightly higher influent baseflow chlorides in the spring indicates the water quality impact of snow melts.
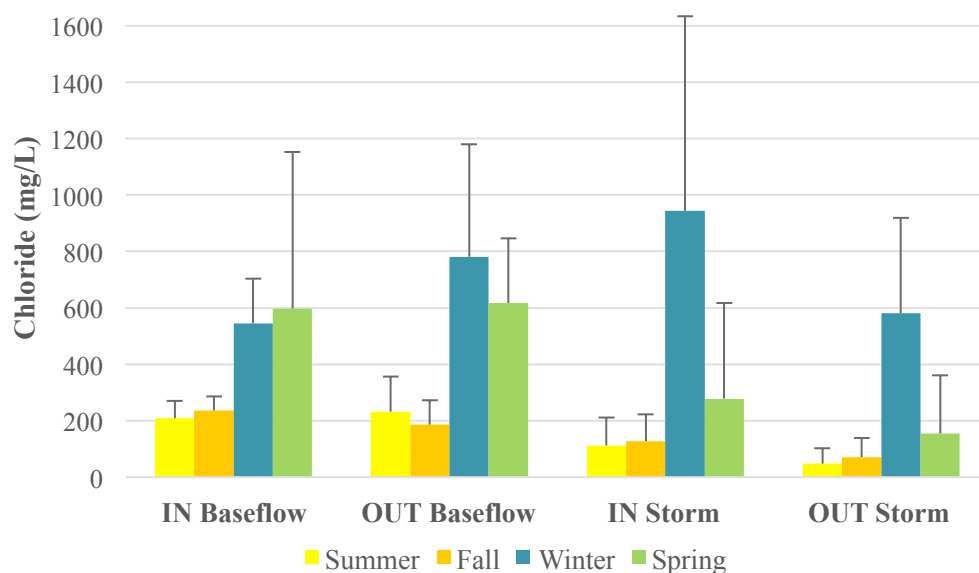
Figure 7-18: Chloride seasonal average inlet and outlet concentrations.

With regards to treatment efficiency of chlorides, Table 7-9 illustrates little to no seasonal trend. Since there are no biological or chemical processes governing chloride removal, the effect of temperature plays an extremely small role, nor does any resistance provided by dense vegetation. Dilution for reducing chloride concentrations is the primary removal for storm events. No seasonal trends for storms can be made because rainfall intensity and amount are the suspected influences on chloride removal. It was expected to be little to no removal of chlorides during baseflow conditions. However, the fall season exemplifies a decent amount of chloride reduction. A hypothetical explanation for this is evapotranspiration (ET) rates being smaller in

116

the fall in comparison to the summer. With lower ET rates is the more likely volume reduction through groundwater recharge. Salts, like chlorides, enter the groundwater through soil and organic material dissolution.

Table 7-9: Chloride seasonal average percent removal.

	Baseflow		Storm	
	% Removal	N	% Removal	N
Summer	-11%	9	58%	9
Fall	21%	8	45%	5
Winter	-43%	5	39%	7
Spring	-3%	7	45%	9

7.3.4: Total Suspended Solids and Total Dissolved Solids

Like chlorides, TSS and TDS removal do not rely on biological or chemical processes. Figures 7-19 and 7-20 depict the average seasonal concentrations for TSS and TDS during baseflow and storm conditions. High fall and summer inlet TSS concentrations for storms are anticipated due to runoff carrying debris and sediments from construction related activities on Villanova University's campus. However, this was not the case for baseflow events. Decaying plant matter in the winter is the suspected cause of elevated influent TSS concentrations during baseflow. In the winter, these solids are entering the CSW through snow melts. Total dissolved solids depict a similar seasonal influent trend to that of chlorides, which is expected.
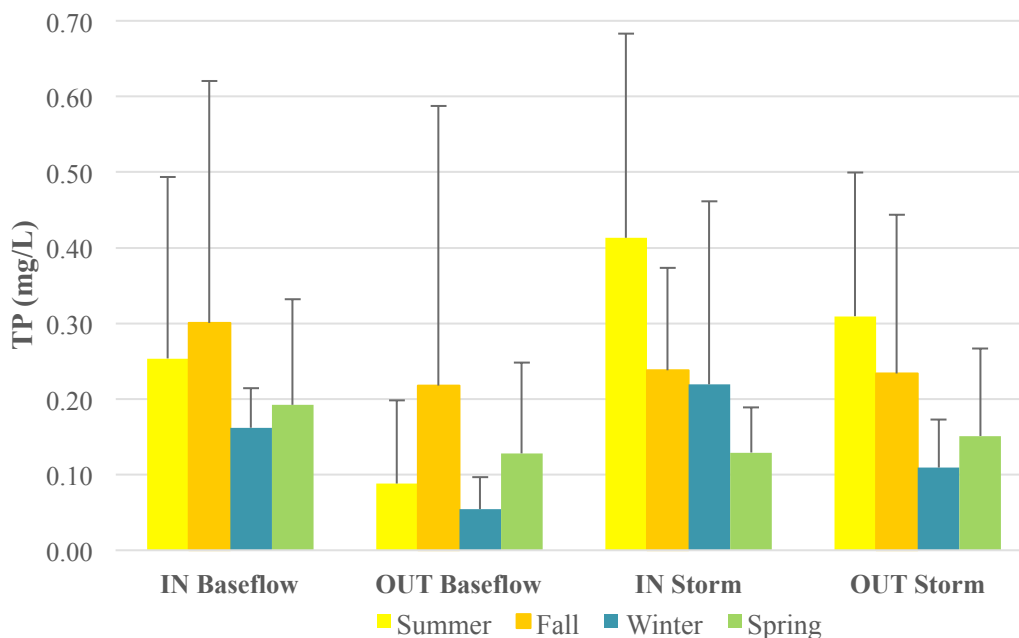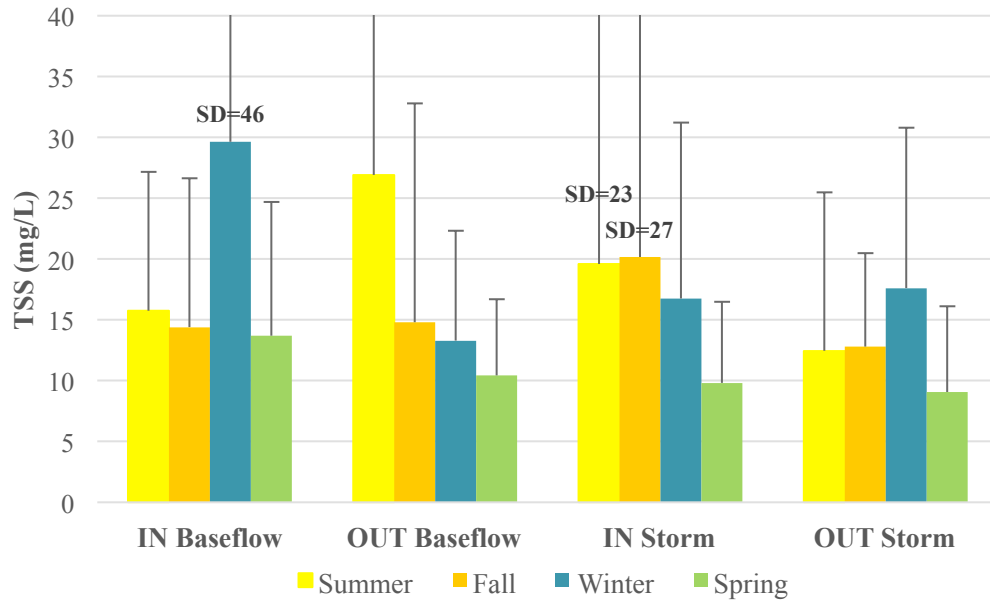
Figure 7-19: TSS seasonal average inlet and outlet concentrations.
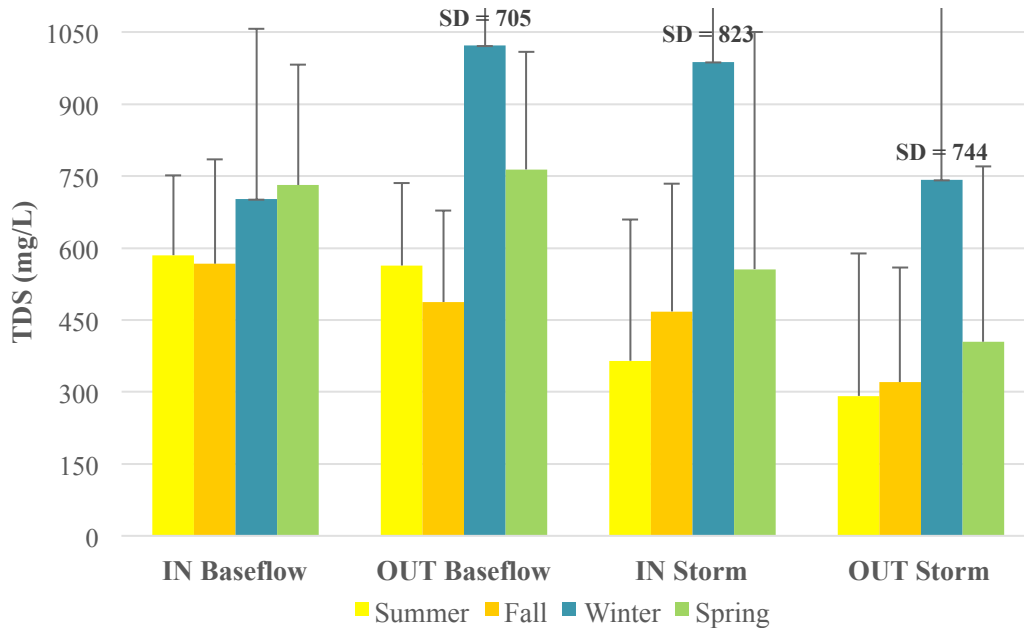
Figure 7-20: TDS seasonal average inlet and outlet concentrations.

A seasonal trend for treatment efficiency due to vegetation growth and temperature was present for TSS (Table 7-10). Algae is considered a suspended solid, thus removal in the summer and fall is non-existent for baseflow. The cooler temperatures and higher flows in the spring and winter do not allow for algal growth at the CSW, resulting in TSS baseflow reduction. In regards

to storm events, the previous influence of algae on TSS does not appear to apply. The summer and fall storms present the highest TSS treatment, which can be attributed to high plant density that allows for particles to settle by slowing the flow rates. Winter and spring do not have the abundance of vegetation, thus resulting in higher storm flows that do not allow for ideal particle settling conditions.

Table 7-10: TSS seasonal average percent removal.

	Baseflow		Storm	
	% Removal	N	% Removal	N
Summer	-71%	9	36%	12
Fall	-3%	9	37%	7
Winter	55%	7	-5%	9
Spring	24%	7	8%	8

Total dissolved solids removal did not mirror chlorides seasonal trends (Table 7-11). Since total dissolved salts comprise of more than just chloride ions, there is differences in the percentage of removal obtained. For example, chlorides were not removed in the summer baseflow events, while TDS concentrations were slightly reduced. With regards to baseflow TDS trends, the winter and spring only accumulated in dissolved solids. This can be attributed to the large amount of chloride ions present on campus, which could enter the CSW at points beyond the inlet.

Table 7-11: TDS seasonal average percent removal.

	Baseflow	Storm

	% Removal	N	% Removal	N
Summer	4%	10	20%	13
Fall	14%	9	32%	7
Winter	-46%	7	25%	9
Spring	-5%	7	27%	8

7.4 Autosampler Storm Events

The use of autosamplers during storm events began in April 2014. The idea behind automated samplers is to understand the first flush phenomena and pollutant removal throughout a storm event. For the April 30, 2014 storm, the nitrogen species illustrated first flush characteristics through the highest inlet concentration being IN-1S (Table 7-12). The primary cause of the high concentration is a result of buildup of the constituents on the impervious surfaces, which are then released in the beginning of the storm event. Though the outlet samples are to be delayed 90 minutes after the inlet sample is taken, this is typically not the case due to high rainfall intensity. If another inlet sample is taken before the previous outlet, then the outlet sample is automatically triggered to compensate for the additional rainfall. Figure 7-21 depicts the time and corresponding flow rates in which each sample was taken. There are three samples per bottle and are colored coded as light blue is -1S, dark green is -2S, pink is -3S, and orange is -4S. It should be noted that the entire storm event hydrograph is not illustrated in order to show the inlet and outlet samples.

Table 7-12: Concentrations of nitrogen species for April 30, 2014 storm.

mg/L	NO$_2^-$	NO$_3^-$	TKN	TN
IN-1S	0.040	0.984	2.69	3.71
IN-2S	0.022	0.562	0.504	1.09
IN-3S	0.022	0.649	0.919	1.59
IN-4S	0.018	0.489	0.357	0.865
OUT-1S	0.049	0.932	0.633	1.61
OUT-2S	0.047	0.926	2.64	3.61

OUT-3S	0.048	0.969	0.808	1.82
OUT-4S	0.042	0.969	0.723	1.73
Average IN	0.026	0.671	1.12	1.81
Average OUT	0.047	0.949	1.20	2.20
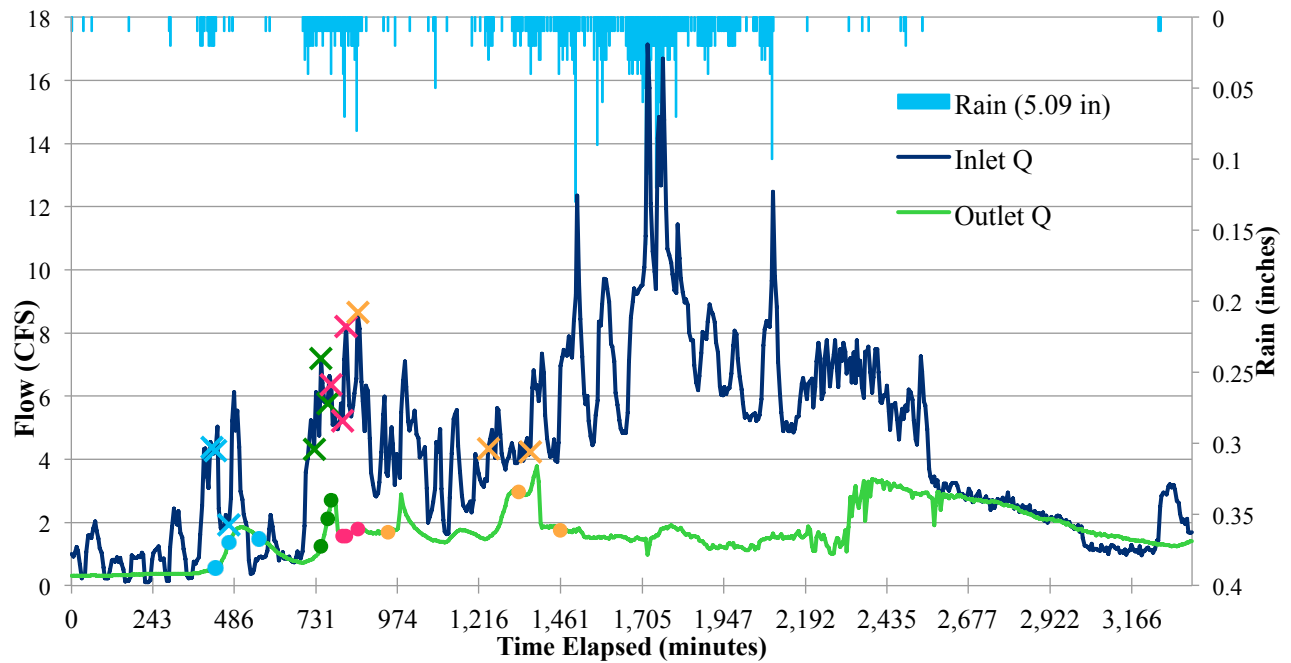
Figure 7-21: Condensed April 30, 2014 storm hydrograph with reference to the occurrence of inlet (X) and outlet (Circle) samples.

With regards to the outlet first flush concentration, it appears OUT-2S is more representative than OUT-1S. The reason is due to the first two OUT-1S samples taken 10 and 40 minutes after than two IN-1S samples. These times are not considered long enough HRTs from inlet to outlet. If considering percent removal based on IN-1S and OUT-2S, the NO_3^-, TKN, and TN are reduced 6%, 2%, and 3%, respectively. Though the reduction is not great, it is still important that the pollutant was treated, especially since nitrite accumulated by 17% possibly due to fast travel times from inlet to outlet as well as the colder temperature water.

Looking at the samples on an inlet and outlet average concentration resulted in no reduction in nitrogen. This demonstrates the importance of viewing water quality parameters on

a mass perspective, as well. Table 7-13 depicts the inlet and outlet volumes and masses with respect to each sample bottle and in total. The volumes of the first sample bottles (-1S) were calculated by taking the flow from the start of the storm up until the halfway point after the last -1S sample but before the first -2S sample. The -2S and -3S volumes were calculated in a similar manner. The last sample bottle (-4S) volumes started halfway after the last -3S sample was taken up until the end of the storm event. The duration for each inlet and outlet volume is depicted in Table E-1 in the appendix. Since the April 30th storm event took a long time (44 hours after rainfall ended) for the outflow to recede back to baseflow conditions (less than 0.10 cfs), the -4S volume was significantly larger than the other three volumes. Also, the total inlet and outlet mass loads were calculated by taking the corresponding average concentrations and multiplying by the total volumes. As a result, the sum of the -1S through -4S samples may not exactly add up to the corresponding total masses for each parameter.

Table 7-13: Volumes and nitrogen mass loadings for April 30, 2014 storm.

	Volume (L)	NO_2^- (kg)	NO_3^- (kg)	TKN (kg)	TN (kg)
IN-1S	1,515,084	0.060	1.49	4.08	5.63
IN-2S	865,680	0.019	0.486	0.437	0.943
IN-3S	645,480	0.014	0.419	0.593	1.03
IN-4S	27,634,360	0.507	13.5	9.88	23.9
OUT-1S	764,410	0.037	0.713	0.484	1.23
OUT-2S	306,281	0.014	0.283	0.809	1.11
OUT-3S	316,279	0.015	0.306	0.255	0.577
OUT-4S	11,649,021	0.487	11.3	8.42	20.2
Total Inlet	30,660,604	0.784	20.57	34.27	55.63
Total Outlet	13,035,992	0.606	12.37	15.66	28.64

The -1S nitrogen masses are not quite representative of being the largest, the -4S samples are the highest primarily due to the much larger portion volumes at the inlet and outlet. The most noticeable difference between concentrations and mass loading is the percent removal from inlet

to outlet. Though there was no reduction seen in the average concentrations, the total masses demonstrated significant removals for nitrite (23%), nitrate (40%), TKN (54%), and TN (49%). The stronger reductions were expected since the mass of pollutant loadings account for the flow rate and hydraulic efficiency of the system.

CHAPTER 8 CONCLUSIONS

Results from the dye tracer studies indicate that the CSW closely resembles completely mixed flow. For storm flow conditions, the hydraulic residence time (HRT) through the system was approximately 49 hours, while during baseflows the HRT was nearly double at 96 hours. Since the tracer tests were performed over the course of one year, evidence of seasonal and storm characteristics attributed to the differences in HRTs. The primary influences consisted of vegetation density and growth, precipitation amount and intensity, outflow rate, and wind speed. Continuing research on the hydraulic residence time will provide greater insight on the wetland flow and volume characteristics.

The CSW at Villanova University has proven to be an effective stormwater control measure on the premise of flood control. Evidence that the CSW reduces nearby and downstream flooding was seen in the high percentage of peak flow reduction. Though, constructed stormwater wetlands are not intentionally designed for volume reductions, the CSW demonstrated successful volume mitigation for storm events.

Aside from peak flow rates, temperature also illustrated to be an impact of stormwater runoff. Impervious surfaces reduce the amount of shading provided by plants, and as a result are significantly hotter than natural surfaces. The presence of heated stormwater runoff was confirmed through inlet temperature spikes during storm events at the CSW. It is important to maintain suitable water temperatures at the CSW in order to support fisheries. However, the effluent of the CSW often conveyed temperatures greater than the trout temperature threshold in July and August. Though, stormwater wetlands are greater for water quality and quantity reduction, their ability to cool the water proves to be much more difficult. A modified outlet

structure or shading by trees or taller vegetation could result in cooler effluent temperatures at the CSW.

Overall, the CSW reduces most water quality pollutants during both storm and baseflow events. The aerobic and anaerobic zones created by shallow meanders and plunge pools allowed for significant nitrogen reduction. Phosphorus posed as a more difficult constituent to remove in comparison to nitrogen primarily due to slower HRTs needed for removal. Additional understanding of nitrogen and phosphorus treatment was obtained through seasonal analysis. While nitrogen reduction was strongest in the fall and summer resulting from warmer temperatures, phosphorus did not depict any sort of seasonal trend. Lastly, the use of autosamplers for storms illustrated the high concentrations during the first flush as well as treatment efficiency differences between concentration and mass loadings. As opposed to concentrations, mass reductions increased the efficiency of nitrogen treatment throughout the April 30, 2014 storm event.

REFERENCES

Asaeda T., Vu, T. C. and Wake, A. (1996). "Heat Storage of Pavements and its Effect on the Lower Temperature." *Atmospheric Environment.* 30(3): 413-27.

Blansett, K. (2011). "Chapter 102 Erosion and Sediment Control and Stormwater Management Regulations: Changes you need to know." *Pennsylvania Housing Research Center Webinar Series*, Pennsylvania Housing Research Center, State College, PA.

Bois, B., Pieri, P., Leeuwen, C. V., and Gaudillere, P. J. (2005). "Sensitivity analysis of the Penman–Monteith evapotranspiration formula and comparison of empirical methods used in viticulture soil water balance." Institut National de la Recherche Agronomique de France.

Carpenter, S., Caraco, N. F., Corell, D. L., Howarth, R. W., Sharpley, A. N., and Smith, V. H. (1998). "Nonpoint Pollution of Surface Waters with Phosphorus and Nitrogen." *Issues in Ecology*. 3: 1-12.

Carson, H., Eaker, B., Gibson, P., and Randall, M. (2009). "Stormwater Problems & Impacts: Why All The Fuss?" *RiverLink, Inc.*

Chambers, P. A. and Mill T. "Dissolved Oxygen, Fish and Nutrient Relationships in the Athabasca River." *Northern River Basins Study Synthesis Report No. 5*.

Chang, N.B., Xuan, Z., and Wanielista, M. P. (2011). "A Tracer Study for Assessing the Interactions between Hydrualic Retention Time and Transport Processes in a Wetland System for Nutrient Removal." *Bioprocess Biosyst Eng*.

City of Puyallup. (2013). "8th Ave NW- Low Impact Development Retrofit." http://www.cityofpuyallup.org/services/public-works/stormwater-management/projects/8th-ave-nw-lid-retrofit/ (Dec. 10, 2013).

Department of Environment Resources. (1999). "Low-Impact Development Design Strategies." EPA 841-B-00-003. Prince George's County, MD.

Diaz, R. J. and Rosenberg, R. (1995). "Marine Benthic Hypoxia: A Review of its Ecological Effects and the Behavioral Responses of Benthic Macrofauna." *Oceanography Marine Biology Annual Review*. 33: 245-303.

Fisher, J., Stratford, C. J. and Buckton S., (2009). "Variation in Nutrient Removal in Three Wetland Blocks in Relation to Vegetation Composition, Inflow Nutrient Concentration and Hydraulic Loading." *Ecological Engineering*. 35(10): 1387-94.

Johnson D. (2013). "Lake Stratification." Action Wakefield Watersheds Alliance. http://awwatersheds.org/category/watershed-word-of-the-week/ (Dec. 3 2013).

Kadlec, R. H. and Reddy K. R. (2001). "Temperature Effects in Treatment Wetlands." *Water Environment Research*. 73(5): 543-57.

Kadlec, R. H. and Wallace, S. D. (2009).*Treatment Wetlands, 2ⁿᵈ Ed,.*CRC Press, Boca Raton, FL.

Messer, J. and Bresonik, P. L. (1984). "Laboratory Evaluation of Kinetic Parameters for Lake Sediment Denitrification Models." *Ecological Modeling* 21(4):277-286.

Mitch, W. J. and Gosselink, J. G. (1993). *Wetlands*, 2ⁿᵈ Ed, John Wiley, New York.

National Research Council (2009).*Urban Stormwater Management in The United States*. The National Academies Press, Washington, D.C.

New York Department of Environmental Conservation. (1996) "Module 2: Activated Sludge Operational Strategies for Nitrogen Removal." Long Island Sound Nitrogen Removal Training Program. http://www.dec.ny.gov/docs/water_pdf/module2.pdf (Dec. 19 2013).

Pennsylvania Code (PA Code). 2005. Title 25-Environmental Protection. Chapter 93-Water Quality Standards.

Pennsylvania Department of Environmental Protection (PA DEP). (2009). "Implementation Guidance for Temperature Criteria." DEP ID: 391-2000-017.

Persson J., Someo, N.L.G, and Wong T.H.F. (1999). "Hydraulic Efficiency of Constructed Wetlands and Ponds." *Water Science and Technology.* 40(3): 291-300.

Philadelphia Water Department. (2002). "Philadelphia Water Department – Belmont & Queen Lane Treatment Plants Source Water Assessment Report." PWSID #1510001. Philadelphia, PA.

Philadelphia Water Department. (2004). *The Schuylkill River Watershed Initiative*. Philadelphia, PA.

Philadelphia Water Department. (2013). "Schuylkill River Watershed History." http://www.phillywatersheds.org/your_watershed/schuylkill/history. (Nov. 20, 2013).

Queensland Department of Natural Resources and Mines. (2012). "Water Quality Assessment." http://kurrawa.gbrmpa.gov.au/reefed/exploring_wetlands/downloads/Information_Sheets.pdf. (Dec. 2nd, 2013).

Reddy, K. R. and Burgoon, P. S. (1996). "Influence of Temperature on Biogeochemical Processes in Constructed Wetlands—Implications to Wastewater Treatment." Paper presented at the *Symposium on Constructed Wetlands in Cold Climates*. Niagara-on-the-Lake, Ontario.

Reddy, R. R. and DeLaune, R. D. (2008). "Biogeochemistry of Wetlands: Science and Applications." CRC Press, Boca Raton, FL.

Shaw, G. R., Moore, D. P., Garnett, C. (2003). "Eutrophication and Algal Blooms." *Environmental and Ecological Chemistry*. 2.

Smith, K. (1997). "Constructed Wetlands for Treating Acid Mine Drainage." *Restoration and Reclamation Review*. 2 (7): 1-7.

United States Environmental Protection Agency (1999). "After the Storm: A Citizen's Guide to Understanding Stormwater."EPA 833-B-03-002. Washington, D.C.

United States Environmental Protection Agency. (2003). "America's Wetlands: Our Vital Link Between Land and Water." Washington, D.C.

United States Environmental Protection Agency. (2003). "Protecting Water from Urban Runoff." EPA 841-F-03-003. Washington, D.C.

United States Environmental Protection Agency (2005). "National Management Measures to Control Nonpoint Source Pollution from Urban Areas." EPA 841-B-05-004. Washington, D.C.

United States Environmental Protection Agency. (2013). "Monitoring and Assessing Water Quality—Volunteer Monitoring." http://water.epa.gov/type/rsl/monitoring/ (Dec. 20, 2013).

United States Environmental Protection Agency. (2013). "Nonpoint Source News-Notes." http://water.epa.gov/polwaste/nps/outreach/upload/94issue.pdf. (Nov. 15, 2013).

United States Environmental Protection Agency. (2013). "Wetlands." http://water.epa.gov/type/wetlands/ (Dec. 2, 2013).

University of New Hampshire Stormwater Center (UNHSC). (2010). "Investigation of Nutrient Removal Mechanisms of a Constructed Gravel Wetland Used for Stormwater Control in a Northern Climate." Durham, NH.

Valera, M. A. C. and Mara, D. (2009). "The Influence of Algal Biomass on Tracer Experiments in Maturation Ponds. *Desalin. Water Treat.*, 4: 89-92.

Wahl. M. D. (2010). "Quantifying the Hydraulic Performance of Treatment Wetlands." Ohio State University Master's Thesis.

The Water Planet Company. (2009). "Nitrification and Denitrification." http://www.thewaterplanetcompany.com/docs/WPC_Nitrification%20&%20Denitrification%20.pdf (Dec. 2013).

Water Resources Agency. (2013). "History of the Delaware River Basin." *University of Delaware*. http://www.wra.udel.edu/public-service/delaware-river-basin/history/. (Nov. 13, 2013).

Webster, J. R. and Benfield, E. F. (1986). "Vascular Plant Breakdown in Freshwater Ecosystems." *Annual Review of Ecology and Systematices*. 17: 567-94.

APPENDICIES

APPENDIX A
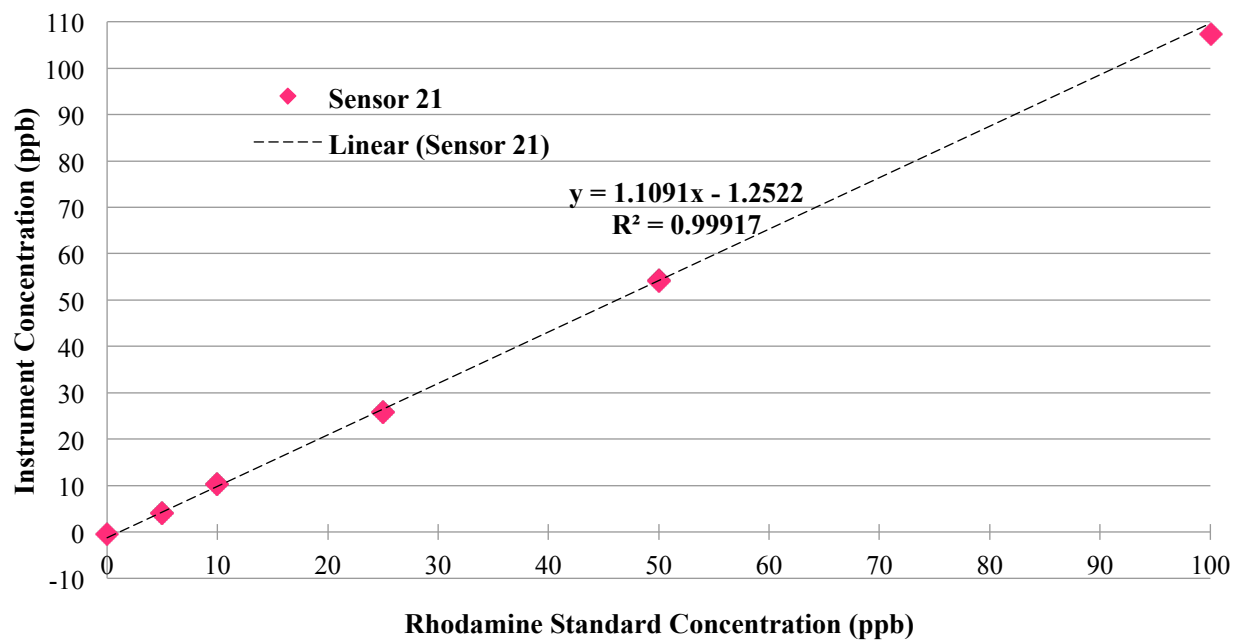
Figure A-1: Rhodamine sensor (S/N 21) calibration curve.
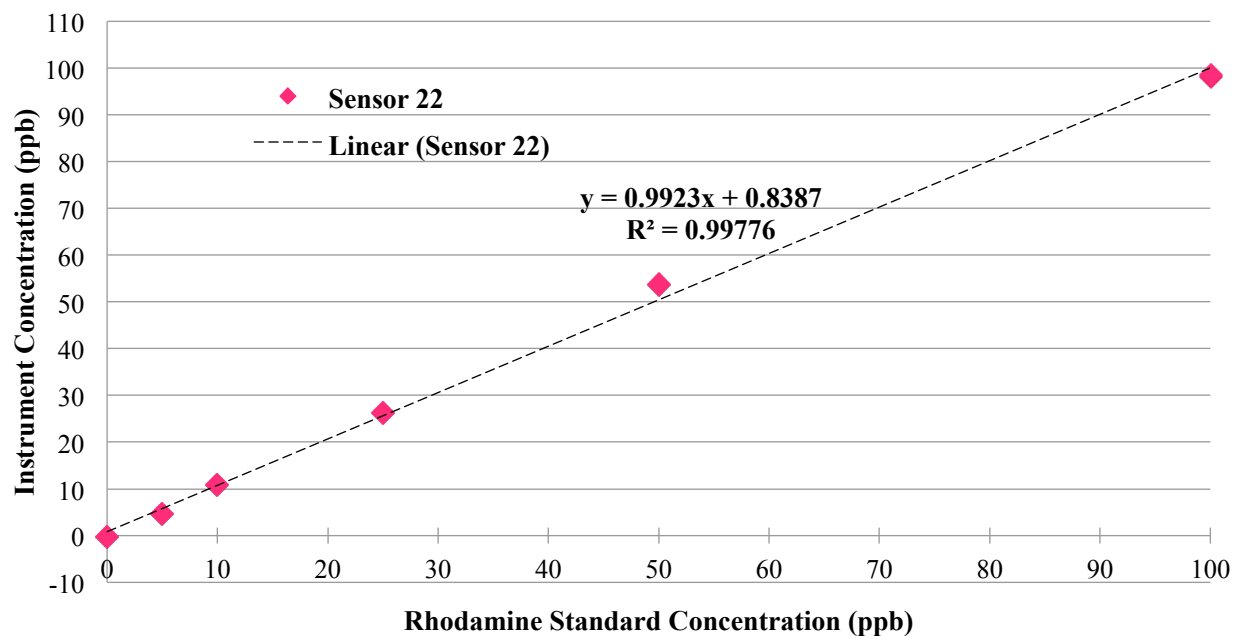
Figure A-2: Rhodamine sensor (S/N 22) calibration curve.

```
'New Inflow Sampling Routine based on Rainfall
'Reset the rainfall counter after 24 dry hours
If SWW_FLOW_DATA.timestamp - timelastrain > 21600.*4. Then   '21600 sec is 6 hr
        AS_PULSE = 0  'this variable just records whether a pulse was sent or not
    eventrain=0.0
        takesample=0
        sample1=0
        sample2=0
        sample3=0
        sample4=0
        sample5=0
        sample6=0
        sample7=0
        sample8=0
        sample9=0
        sample10=0
        sample11=0
        sample12=0
EndIf
' This routine takes makes a pulse when Rain reaches various rainfall depths
If Rain > 0 Then
        eventrain=eventrain+Rain
        timelastrain = SWW_FLOW_DATA.timestamp
    If (eventrain >= 0.20) AND (sample1=0) Then
        takesample = -1
        sample1 = -1
    EndIf
    If (eventrain >= 0.23) AND (sample2=0) Then
        takesample = -1
        sample2 = -1
    EndIf
    If (eventrain >= 0.25) AND (sample3=0) Then
        takesample = -1
        sample3 = -1
    EndIf
    If (eventrain >= 0.45) AND (sample4=0) Then
        takesample = -1
        sample4 = -1
    EndIf
    If (eventrain >= 0.5) AND (sample5=0) Then
        takesample = -1
        sample5 = -1
    EndIf
    If (eventrain >= 0.55) AND (sample6=0) Then
        takesample = -1
        sample6 = -1
```

```
    EndIf
  If (eventrain >= 0.6) AND (sample7=0) Then
        takesample = -1
        sample7 = -1
  EndIf
  If (eventrain >= 0.7) AND (sample8=0) Then
        takesample = -1
        sample8 = -1
  EndIf
  If (eventrain >= 0.8) AND (sample9=0) Then
        takesample = -1
        sample9 = -1
  EndIf
  If (eventrain >= 1.0) AND (sample10=0) Then
        takesample = -1
        sample10 = -1
  EndIf
  If (eventrain >= 1.25) AND (sample11=0) Then
        takesample = -1
        sample11 = -1
  EndIf
  If (eventrain >= 1.5) AND (sample12=0) Then
        takesample = -1
        sample12 = -1
  EndIf
EndIf

If test_AS_Command Then
  takesample = -1
  test_AS_Command = 0
  EndIf

If takesample Then
'Turn on power to switched 12 V port (Com Port)
        SW12(1)
        Delay(0,50,msec)
'a 50 millisecond 12V pulse to the autosampler, which is
'programmed to take one sample per pulse.
'Turn off power to switched 12 V port
        SW12(0)
        takesample = 0
 timelastsample = SWW_FLOW_DATA.timestamp
 AS_PULSE = AS_PULSE + 1
        If needM1sample Then
'Com port -10 is Com2 (C3 and C4)
```

```
SendVariables(commresultET,Com2,0,10,0000,100,"Public","needM1sample",needM1sample,1
)
    Delay(0,3,sec)
        If commresultET=0 Then
          needM1sample=0
        EndIf
        EndIf
  If needoutflowsample Then
    'Com port -10 is Com2 (C3 and C4)

SendVariables(commresultET,Com2,0,10,0000,100,"Public","needoutflowsample",needoutflows
ample,1)
    Delay(0,3,sec)
     If commresultET=0 Then
       needoutflowsample=0
        EndIf
    EndIf
needM1sample = -1
needoutflowsample = -1
EndIf

'variable needM1sample is sent to the SWW_ET CR1000
  If needM1sample AND (SWW_FLOW_DATA.timestamp - timelastsample > 60.*45.) Then
    'Com port -10 is Com2 (C3 and C4)

SendVariables(commresultET,Com2,0,10,0000,0,"Public","needM1sample",needM1sample,1)
    Delay(0,3,sec)
    If commresultET=0 Then
      needM1sample=0
    EndIf
    EndIf

'variable needoutflowsample is sent to the SWW_ET CR1000
If needoutflowsample AND (SWW_FLOW_DATA.timestamp - timelastsample > 60.*90.) Then
    'Com port -10 is Com2 (C3 and C4)

SendVariables(commresultET,Com2,0,10,0000,0,"Public","needoutflowsample",needoutflowsa
mple,1)
    Delay(0,3,sec)
    If commresultET=0 Then
      needoutflowsample=0
    EndIf
    EndIf
```
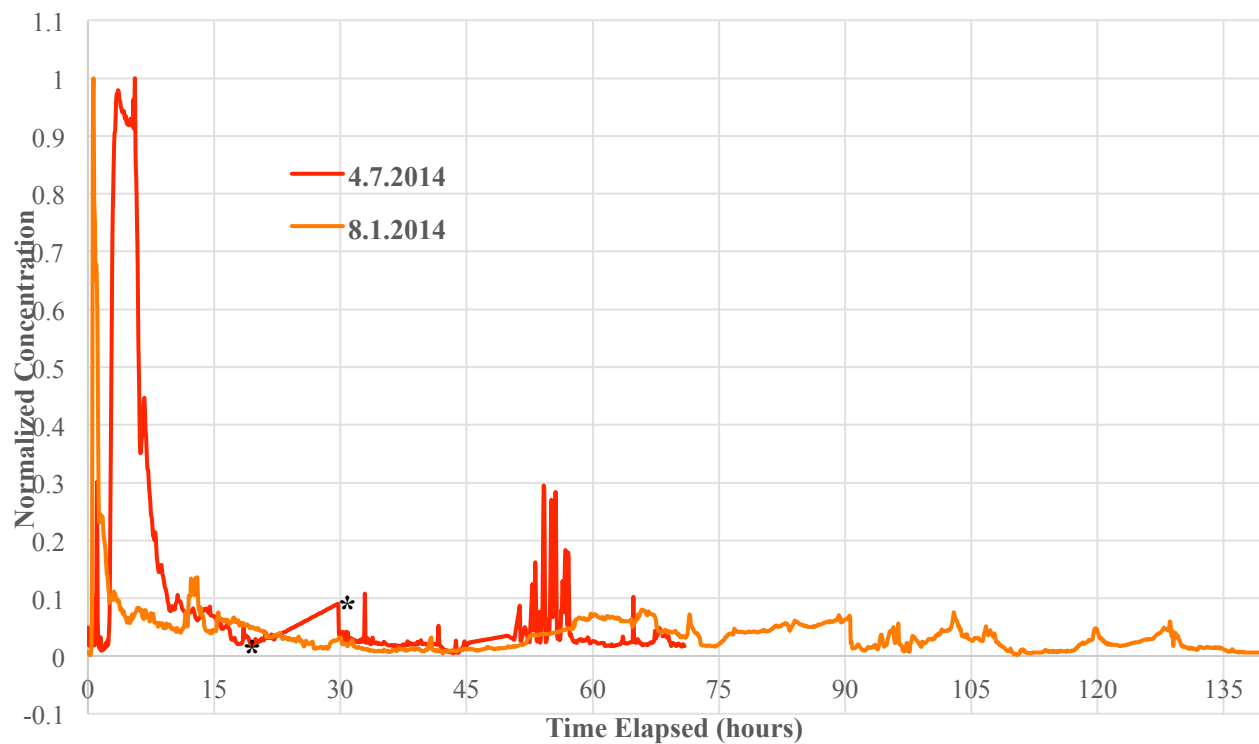
Figure B-1: Storm inlet to start of M1 residence time distribution curves(* indicates linear interpolation due to bad sensor readings).
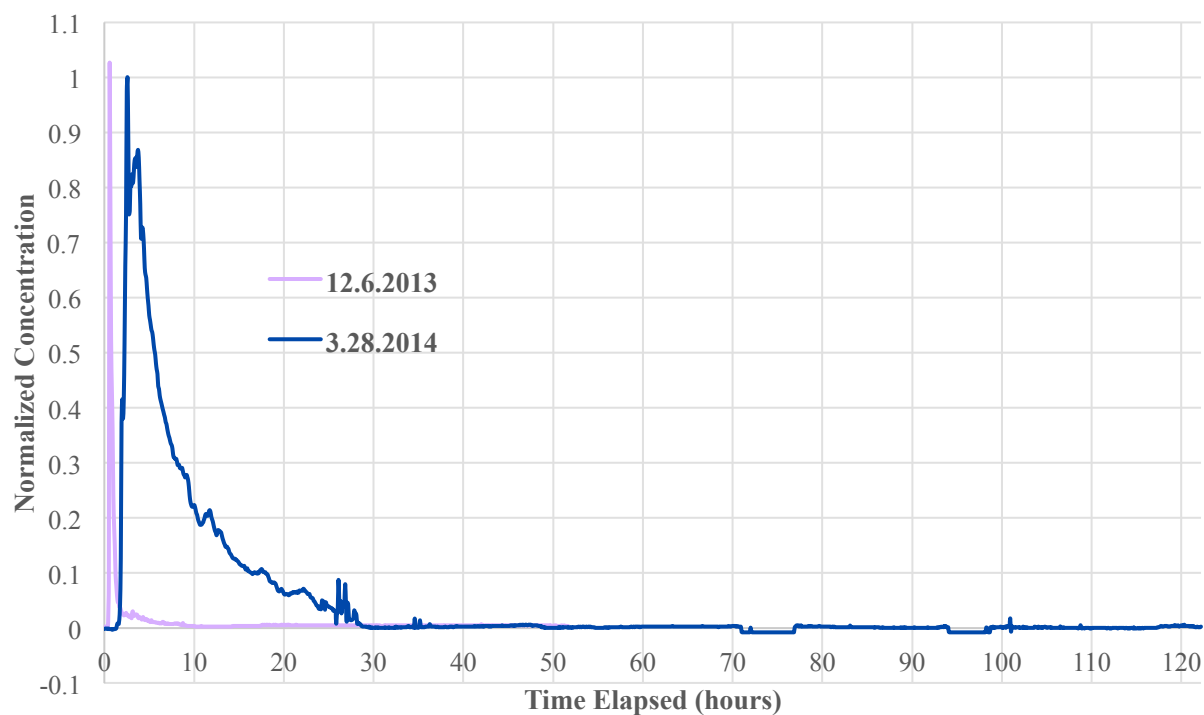
Figure B-2: Storm end of M1 to end of M2 residence time distribution curves.
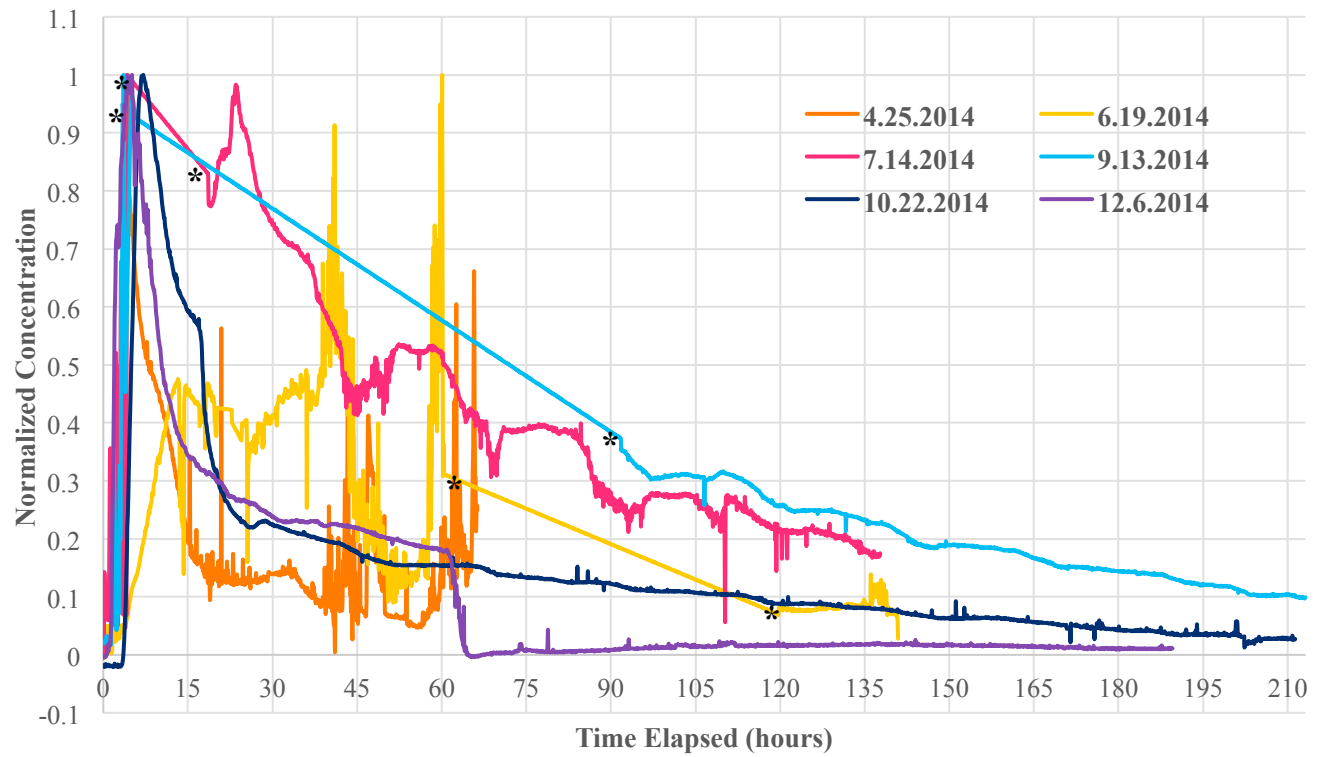
Figure B-3: Storm inlet to outlet residence time distribution curves. (*indicates linear interpolation due to bad sensor readings)
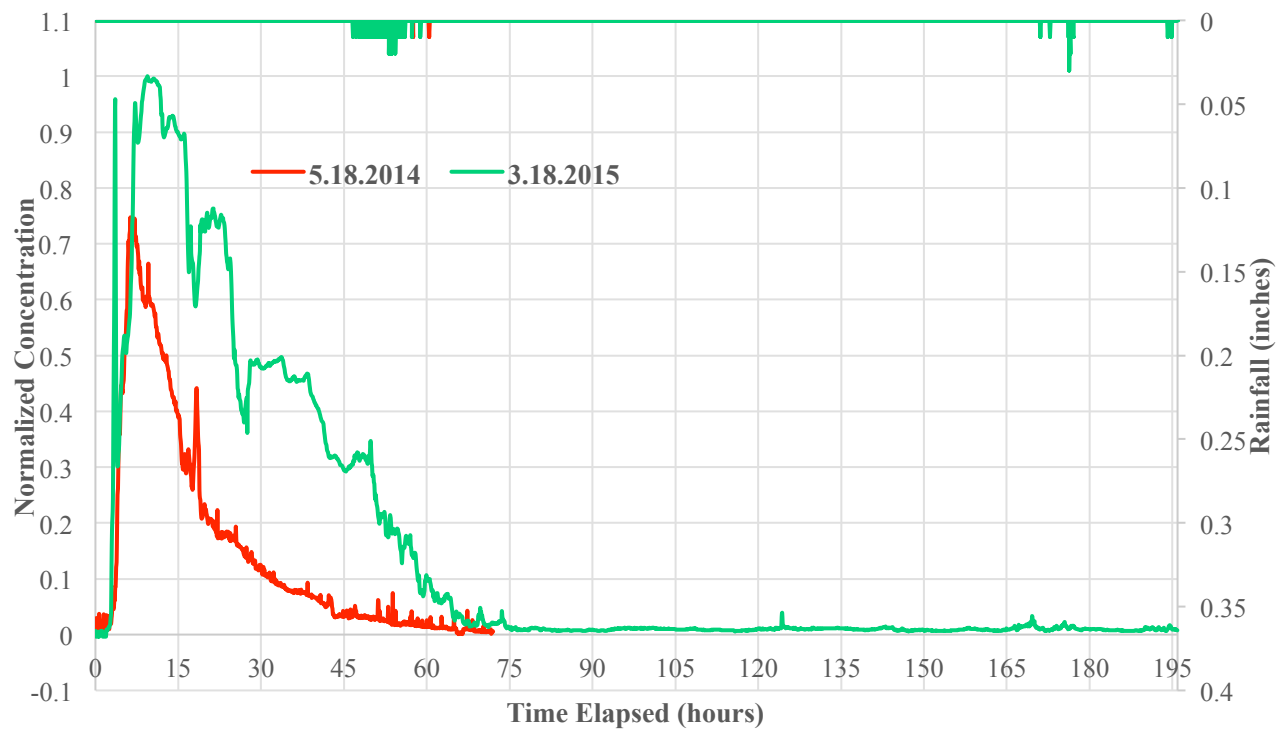
Figure B-4: Baseflow inlet to start of M1 residence time distribution curves.
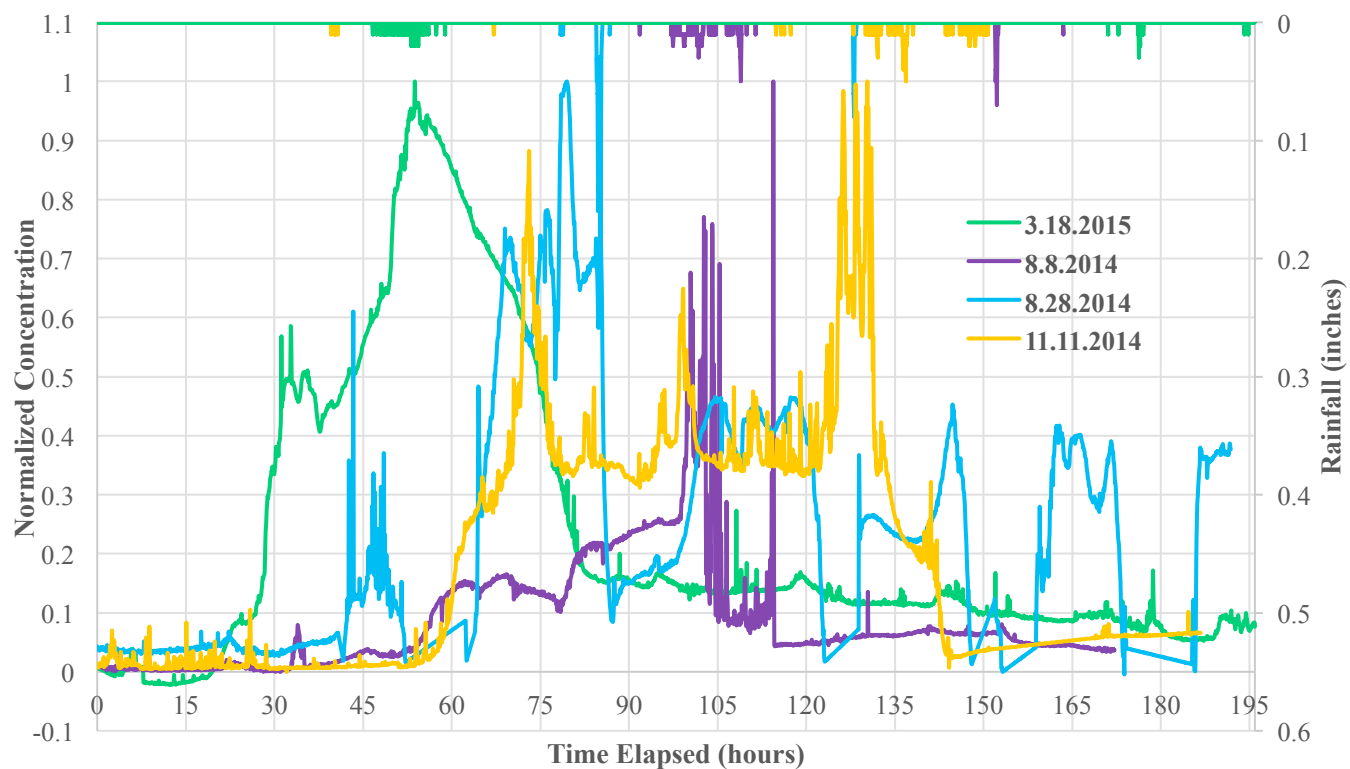
Figure B-5: Baseflow inlet to outlet residence time distribution curves.

136

APPENDIX C

Table C -1: Storm events peak flow and volume reduction.

Event Date	Total Rain (in)	Intensity (in/hr)	Peak Inflow (cfs)	Peak Outflow (cfs)	Peak Reduction	Volume In (ft3)	Volume Out (ft3)	Volume Reduction
3/6/2013	0.10	0.12	1.38	3.56	-158%	16,150	59,624	-269%
3/8/2013	0.12	0.14	0.41	3.27	-687%	9,193	51,985	-465%
3/12/2013	1.15	0.18	7.60	3.18	58%	133,703	98,733	26%
3/17/2013	0.22	0.12	0.38	0.19	50%	7,867	3,932	50%
3/18/2013	0.75	0.13	4.50	2.88	36%	129,722	102,606	21%
3/25/2013	0.64	0.13	1.55	0.79	49%	53,473	51,967	3%
4/10/2013	0.48	0.34	7.41	2.12	71%	33,234	37,930	-14%
4/12/2013	0.53	0.24	8.22	2.36	71%	50,076	37,394	25%
4/12/2013	0.40	0.37	8.52	2.82	67%	42,251	40,750	4%
4/19/2013	0.78	0.19	9.37	2.74	71%	66,743	62,018	7%
4/29/2013	0.54	0.12	2.92	1.70	42%	65,468	56,978	13%
5/7/2013	0.64	0.26	8.50	2.41	72%	56,074	48,619	13%
5/8/2013	0.33	0.17	4.24	1.44	66%	33,067	37,865	-15%
5/10/2013	1.24	0.33	11.82	2.80	76%	126,750	70,961	44%
5/11/2013	0.15	0.16	1.96	0.48	35%	20,533	19,603	5%
5/18/2013	0.30	0.13	3.16	0.64	80%	48,839	51,237	-5%
5/23/2013	0.77	0.58	22.35	2.87	87%	56,253	64,765	-15%
5/24/2013	0.17	0.15	2.87	0.66	77%	22,821	23,362	-2%
5/28/2013	0.37	0.12	5.04	0.97	81%	66,015	45,604	31%
6/2/2013	0.84	0.23	8.77	2.93	67%	60,256	40,138	33%
6/3/2013	0.12	0.48	9.56	0.88	91%	22,414	31,145	-39%
6/6/2013	4.41	0.23	12.32	3.70	70%	483,821	212,313	56%
6/10/2013	2.70	0.46	17.54	3.76	79%	295,713	171,675	42%
6/13/2013	0.50	0.46	12.06	3.81	68%	40,164	37,237	7%
6/13/2013	0.25	0.14	4.93	0.79	84%	50,869	40,159	21%
6/18/2013	1.15	0.45	37.20	3.18	91%	141,801	105,458	26%
6/25/2013	0.23	0.55	7.89	1.32	83%	18,177	26,015	-43%
6/26/2013	0.68	1.63	18.06	2.99	83%	75,666	38,142	98%
6/27/2013	0.48	0.44	9.48	2.15	77%	62,517	34,602	81%
6/28/2013	0.18	0.15	1.63	0.85	48%	44,965	73,233	-39%
6/30/2013	0.20	0.14	2.94	0.90	69%	26,842	19,553	37%
6/30/2013	0.73	0.27	10.13	3.18	69%	108,125	74,386	45%
7/9/2013	0.21	0.31	3.84	1.11	71%	22,220	24,239	-9%
7/12/2013	1.06	0.21	7.59	3.50	54%	97,121	78,991	19%
7/22/2013	1.34	0.73	37.30	2.41	94%	80,236	50,225	37%

7/28/2013	0.87	0.61	13.04	3.28	75%	49,381	55,769	-13%
8/1/2013	1.26	0.26	11.14	2.87	74%	108,896	78,287	28%
8/7/2013	0.36	0.54	10.47	3.69	65%	27,764	34,804	-25%
8/13/2013	3.25	0.74	20.32	2.92	86%	193,881	83,862	57%
8/28/2013	1.32	0.53	16.23	2.61	84%	59,250	43,108	27%
9/2/2013	0.22	0.24	14.88	0.97	94%	14,631	11,715	20%
9/12/2013	0.60	0.34	6.05	2.16	64%	33,657	39,768	-18%
9/16/2013	0.10	0.13	1.36	0.51	62%	6,792	7,961	-17%
9/21/2013	1.42	0.28	7.81	3.30	58%	85,100	52,784	38%
10/7/2013	0.76	0.28	4.81	3.10	36%	37,036	38,139	-3%
10/10/2013	0.57	0.14	5.19	1.92	63%	54,232	43,731	19%
10/11/2013	1.99	0.29	11.66	3.49	70%	171,123	114,798	33%
10/17/2013	0.11	0.16	5.08	0.31	94%	12,439	7,016	44%
10/19/2013	0.18	0.24	2.42	1.18	51%	9,836	12,260	-25%
11/1/2013	0.28	0.31	4.19	2.31	45%	16,145	21,551	-33%
11/18/2013	0.14	0.17	2.37	0.47	80%	8,949	8,352	7%
11/26/2013	3.57	0.22	11.58	2.88	75%	275,351	155,373	44%
12/6/2013	1.30	0.15	5.58	2.53	55%	141,746	117,432	17%
12/9/2013	0.44	0.12	3.43	2.03	41%	107,810	107,174	1%
12/15/2013	0.57	0.16	3.58	1.39	61%	65,956	50,282	24%
12/19/2013	0.27	0.12	0.42	0.19	54%	8,737	3,607	59%
12/22/2013	0.14	0.28	17.30	1.32	92%	34,757	28,815	17%
12/23/2013	0.72	0.15	7.85	2.38	70%	120,648	89,009	26%
12/29/2013	1.18	0.18	8.82	3.30	63%	144,482	80,416	44%
1/5/2014	1.41	0.20	8.62	3.83	56%	246,250	212,516	14%
1/10/2014	1.51	0.17	8.30	3.54	57%	287,623	232,680	19%
1/14/2014	0.31	0.11	3.29	1.37	58%	73,479	75,031	-2%
1/27/2014	0.20	0.27	3.28	0.38	88%	17,802	11,115	38%
2/3/2014	0.33	0.12	5.06	3.51	31%	178,191	119,878	33%
2/5/2014	0.79	0.19	7.24	3.72	49%	156,411	143,739	8%
2/13/2014	0.64	0.15	3.97	1.77	55%	97,997	55,256	44%
2/14/2014	0.69	0.13	4.01	1.00	75%	241,374	107,729	55%
2/18/2014	0.51	0.16	1.57	0.46	71%	32,740	28,555	13%
2/19/2014	0.30	0.17	4.47	1.38	69%	309,027	122,954	60%
2/21/2014	0.40	0.25	11.23	3.15	72%	631,809	188,940	70%
3/4/2014	0.12	0.14	0.89	0.34	62%	7,339	14,057	-92%
3/12/2014	0.42	0.20	11.32	2.79	75%	120,607	108,513	10%
3/19/2014	0.68	0.18	9.38	2.49	73%	165,869	116,567	30%
3/29/2014	2.94	0.18	9.91	3.86	61%	687,235	321,965	53%
4/3/2014	0.25	0.12	8.51	1.24	85%	246,081	98,646	60%
4/7/2014	0.37	0.13	6.30	1.64	74%	238,634	143,077	40%

4/15/2014	2.33	0.32	25.15	3.46	86%	532,001	206,662	61%
4/25/2014	0.60	0.21	7.86	2.68	66%	329,544	117,607	64%
4/29/2014	5.02	0.27	17.14	3.78	78%	1,082,769	460,362	57%
5/10/2014	0.24	0.17	5.44	2.13	61%	205,394	187,682	9%
5/16/2014	4.23	0.48	26.30	4.51	83%	591,497	337,181	43%
5/22/2014	0.17	0.19	5.01	1.20	76%	67,272	91,037	-35%
5/23/2014	0.31	0.29	5.35	1.30	76%	216,839	183,301	15%
5/27/2014	0.39	0.26	5.51	1.93	65%	49,261	62,474	-27%
5/28/2014	0.77	0.46	11.97	3.57	70%	175,082	124,894	29%
6/3/2014	0.16	0.32	3.25	1.34	59%	15,359	33,409	-118%
6/4/2014	0.14	0.15	4.02	0.86	79%	20,209	34,090	-69%
6/9/2014	0.15	0.18	3.73	1.16	69%	20,551	36,275	-77%
6/9/2014	0.68	0.33	9.86	2.78	72%	98,462	121,876	-24%
6/11/2014	0.12	0.12	11.92	1.08	91%	21,921	22,627	-3%
6/12/2014	0.39	0.16	11.44	3.77	67%	66,777	92,355	-38%
6/13/2014	0.13	0.26	5.73	2.89	50%	64,342	123,212	-91%
6/19/2014	0.14	0.17	2.46	1.31	47%	22,743	28,021	-23%
6/19/2014	0.17	0.15	2.39	2.27	5%	36,006	54,629	-52%
6/25/2014	0.13	0.39	2.98	1.55	48%	16,754	21,411	-28%
6/25/2014	0.73	0.44	8.92	4.15	53%	87,683	75,823	14%
7/2/2014	0.87	0.37	11.13	3.98	64%	98,880	161,839	-64%
7/13/2014	0.14	0.19	1.12	0.95	15%	26,550	27,832	-5%
7/14/2014	0.97	0.90	11.52	3.15	73%	94,766	41,895	56%
7/15/2014	0.24	0.15	5.88	1.56	74%	33,192	22,738	31%
7/23/2014	0.40	0.28	7.30	1.97	73%	46,491	33,470	28%
7/26/2014	0.19	0.25	4.98	1.07	79%	25,597	15,904	38%
7/27/2014	1.24	0.55	12.67	3.34	74%	122,867	53,121	57%
8/1/2014	0.30	0.90	10.96	3.32	70%	22,551	27,656	-23%
8/2/2014	0.48	0.14	5.84	2.52	57%	48,599	41,815	14%
8/2/2014	0.15	0.11	2.84	0.53	81%	21,538	16,756	22%
8/12/2014	1.00	0.15	6.57	2.66	59%	107,018	84,528	21%
8/14/2014	0.21	0.36	5.35	1.59	70%	26,706	26,327	1%
8/22/2014	0.57	0.49	7.83	3.06	61%	50,337	37,654	25%
8/23/2014	0.50	0.16	5.15	1.74	66%	58,995	53,936	9%
8/31/2014	0.96	0.68	13.45	2.89	78%	84,568	35,118	58%
9/2/2014	0.17	0.41	5.08	0.78	85%	19,746	13,290	33%
9/13/2014	0.37	0.26	7.22	2.87	60%	27,643	29,936	-8%
9/24/2014	0.62	0.13	7.25	2.04	72%	68,770	55,809	19%
10/3/2014	0.51	0.18	6.07	2.32	62%	47,122	50,486	-7%
10/7/2014	0.29	0.22	9.09	3.21	65%	31,245	30,055	4%
10/11/2014	0.40	0.13	7.67	2.14	72%	45,992	41,042	11%

139

10/15/2014	1.01	0.25	9.56	3.06	68%	112,123	86,695	23%
10/21/2014	0.72	0.13	8.06	1.01	87%	107,584	78,684	27%
11/1/2014	0.73	0.13	8.86	2.52	72%	73,263	68,314	7%
11/6/2014	0.45	0.12	6.27	1.39	78%	62,891	48,404	23%
11/13/2014	0.22	0.13	2.62	0.44	83%	32,239	19,556	39%
11/16/2014	0.94	0.16	5.50	2.85	48%	120,671	81,736	32%
11/24/2014	0.63	0.20	7.15	3.43	52%	73,348	48,176	34%
12/2/2014	0.24	0.13	2.66	1.47	45%	37,799	32,003	15%
12/3/2014	0.18	0.13	2.37	1.52	36%	29,501	29,075	1%
12/5/2014	0.16	0.13	2.27	0.84	63%	20,064	20,116	0%
12/6/2014	0.68	0.14	6.29	3.23	49%	86,599	86,829	0%
12/9/2014	0.76	0.16	5.22	3.56	32%	110,156	90,200	18%
12/16/2014	0.16	0.15	2.69	0.96	64%	19,979	23,096	-16%
12/22/2014	0.12	0.12	3.25	0.53	84%	25,619	22,143	14%
12/24/2014	0.79	0.14	4.20	2.95	30%	120,072	118,994	1%
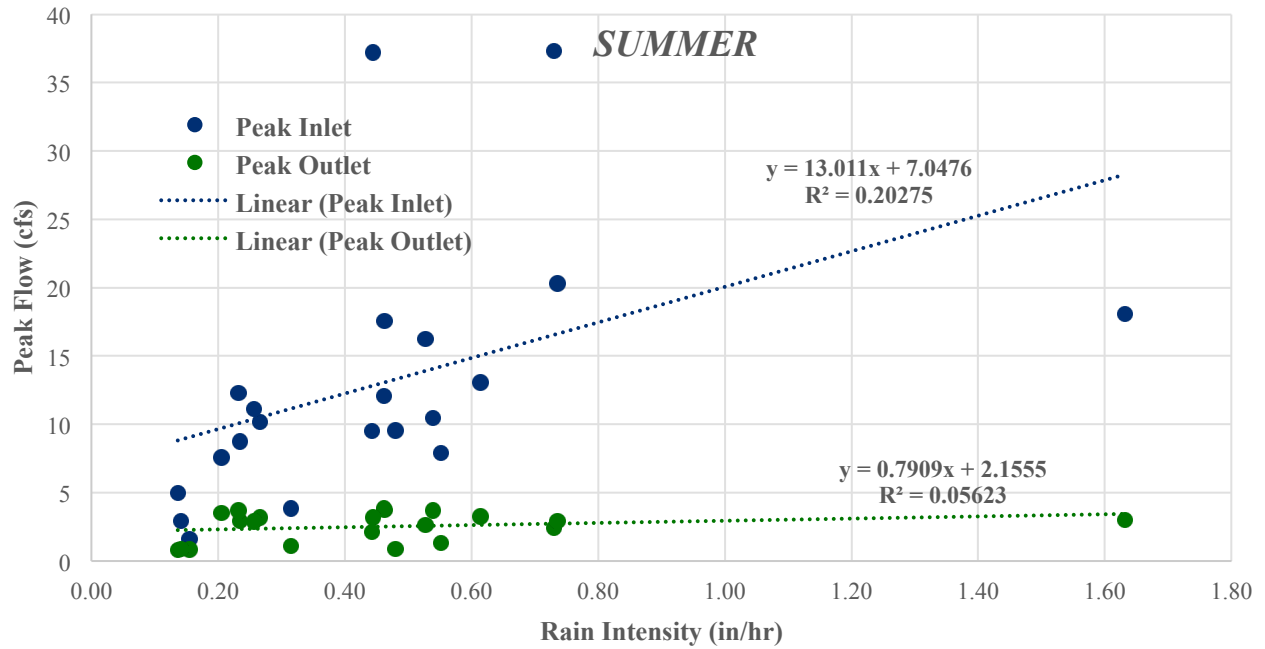
Figure C-1: Summer 2013 peak flows vs rainfall intensity
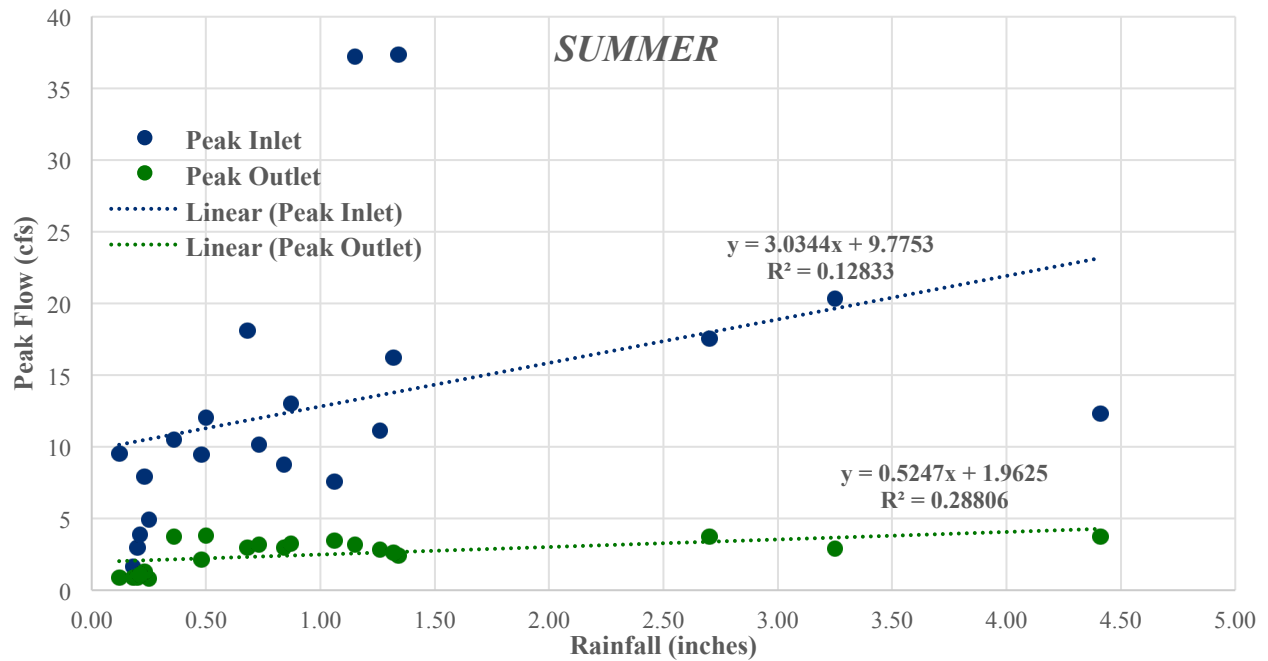
Figure C-2: Summer 2013 peak flows vs. rainfall amount
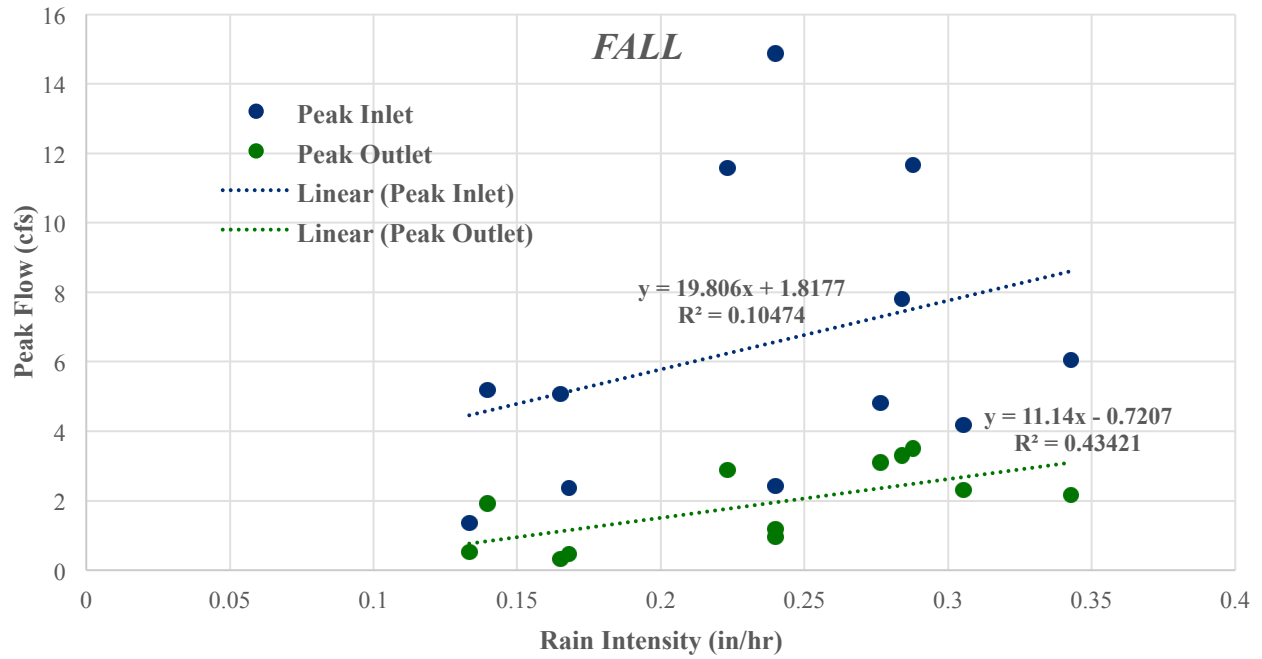
Figure C-3: Fall 2013 peak flows vs. rainfall intensity.
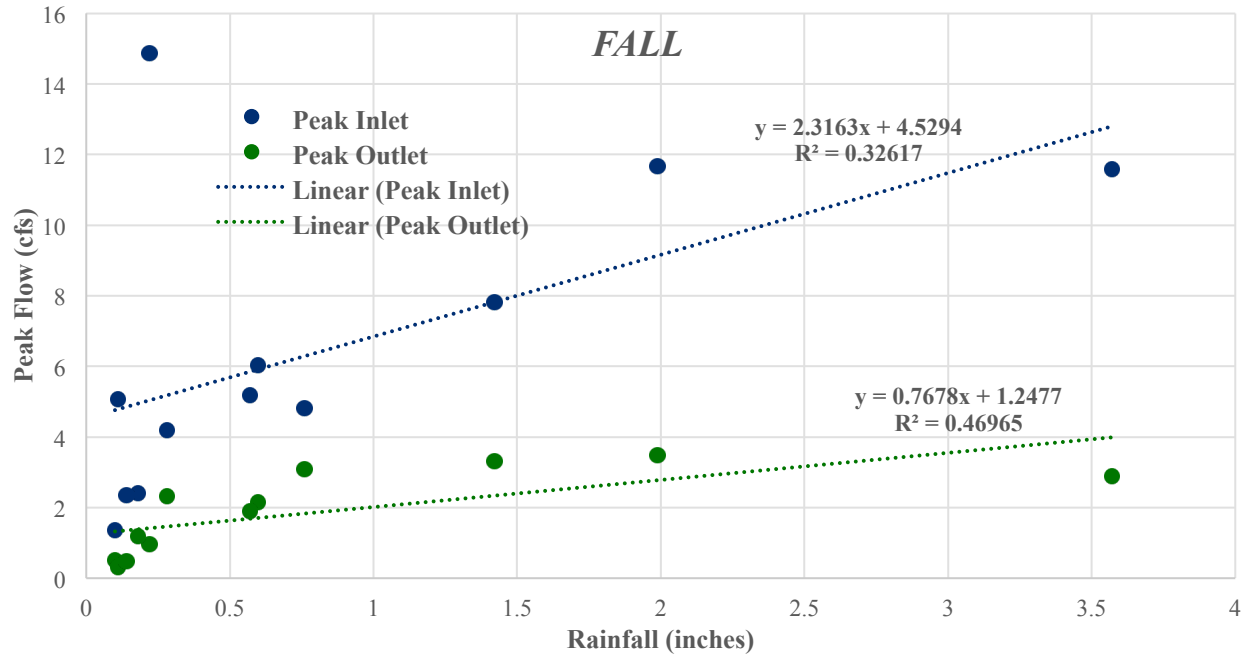
Figure C-4: Fall 2013 peak flows vs. rainfall amount.

142

Figure C-5: Winter 2013-14 peak flows vs. rainfall intensity.

Figure C-6: Winter 2013-14 peak flows vs. rainfall amount.

Figure C-7: Spring 2014 peak flows vs. rainfall intensity.
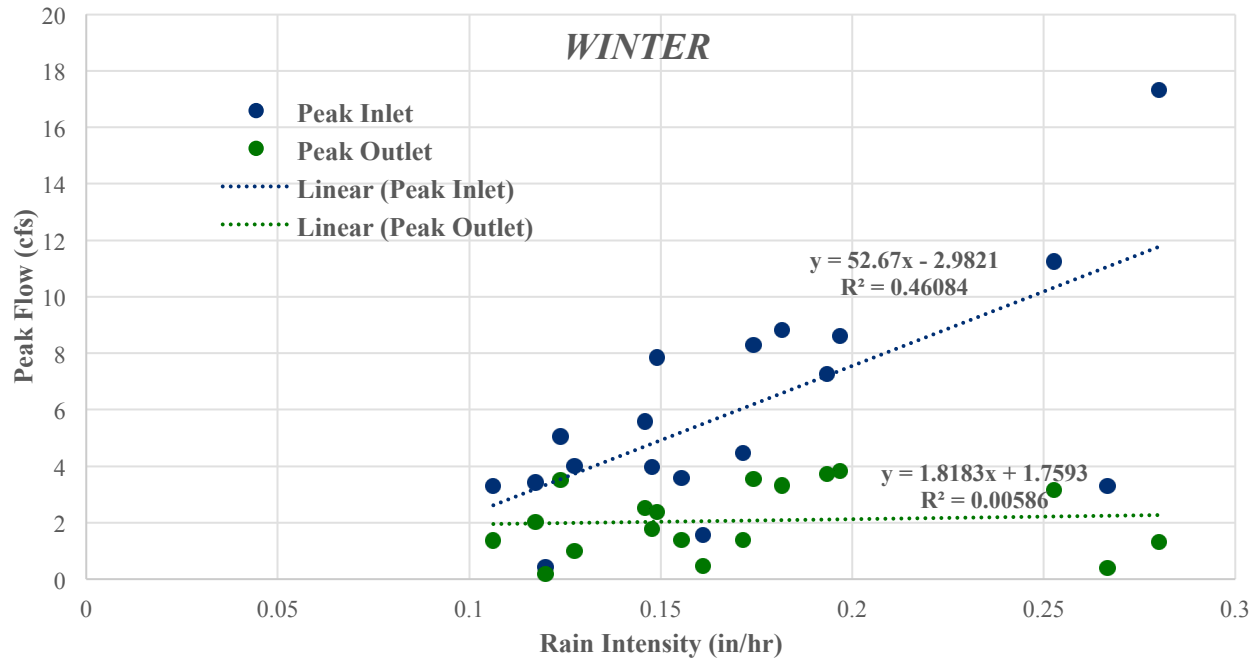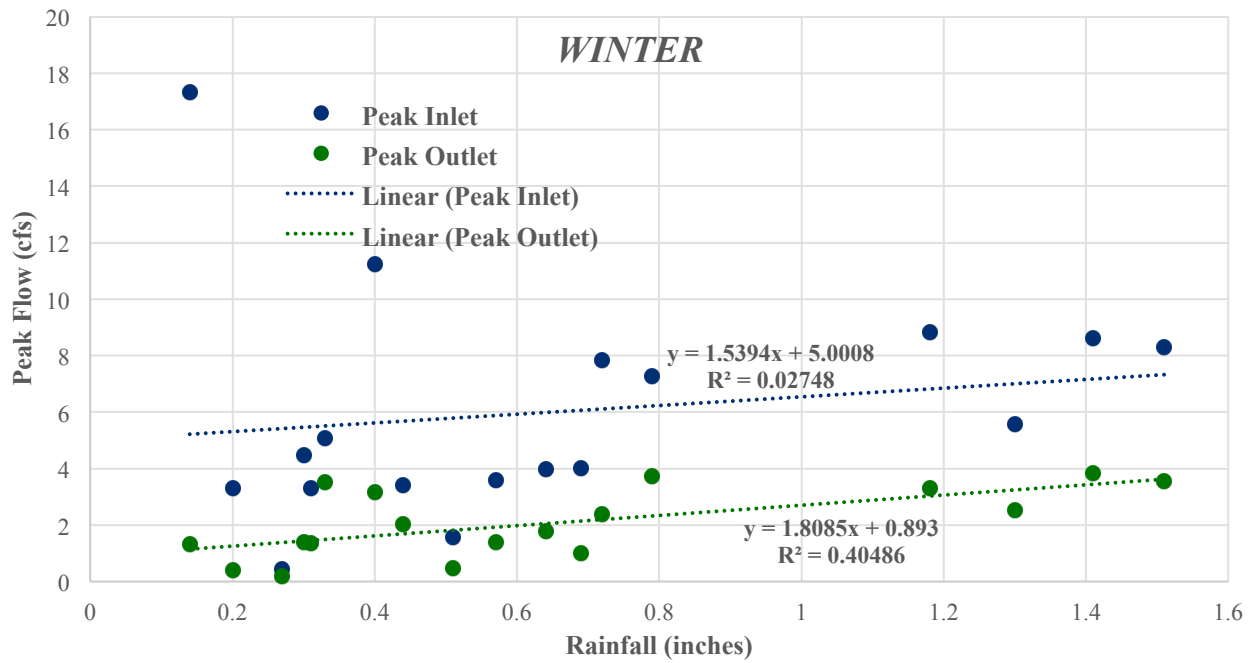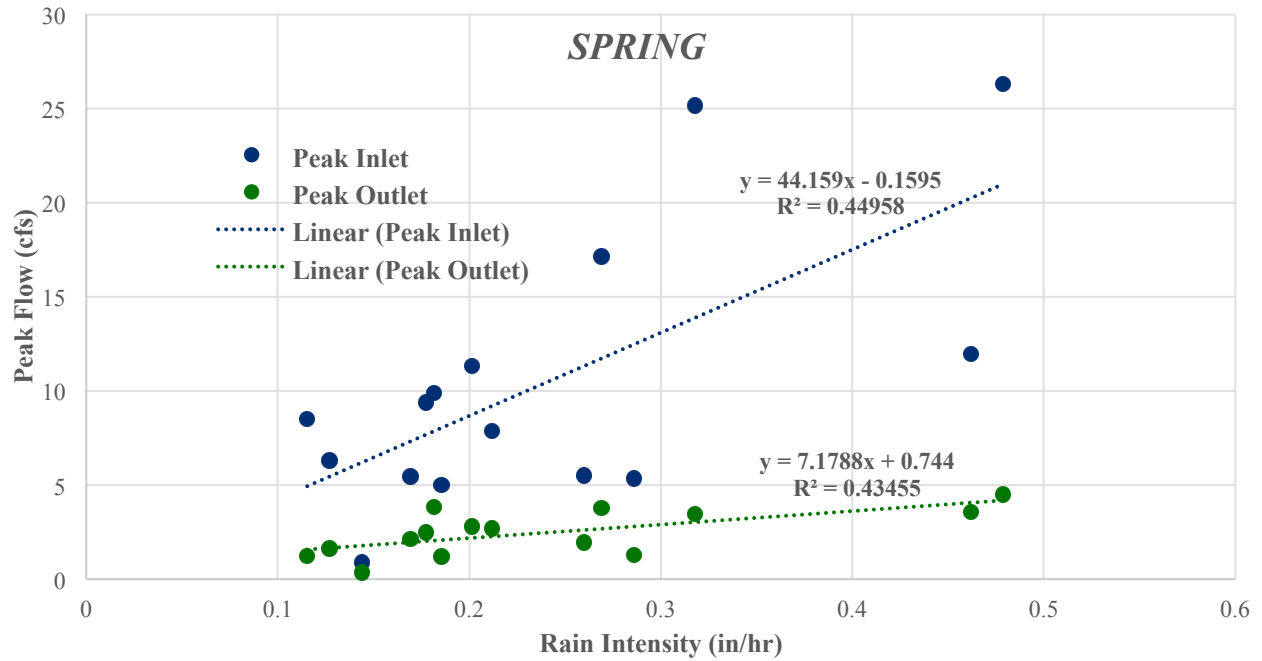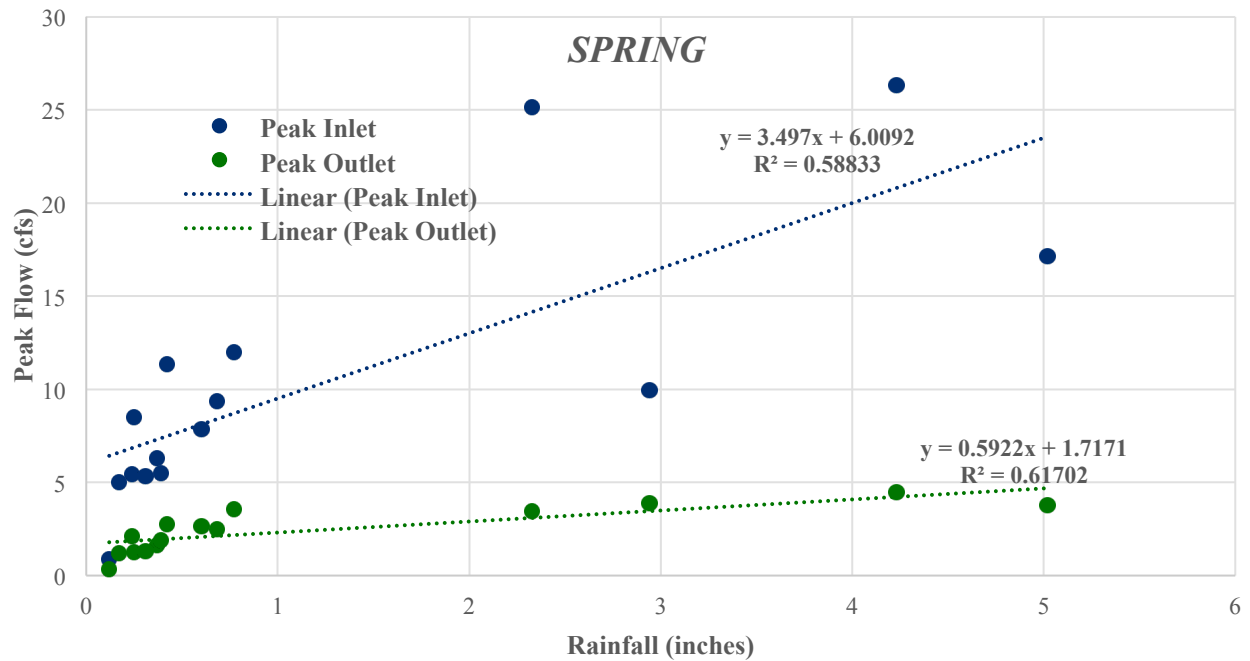

Figure C-8: Spring 2014 peak flows vs. rainfall amount.
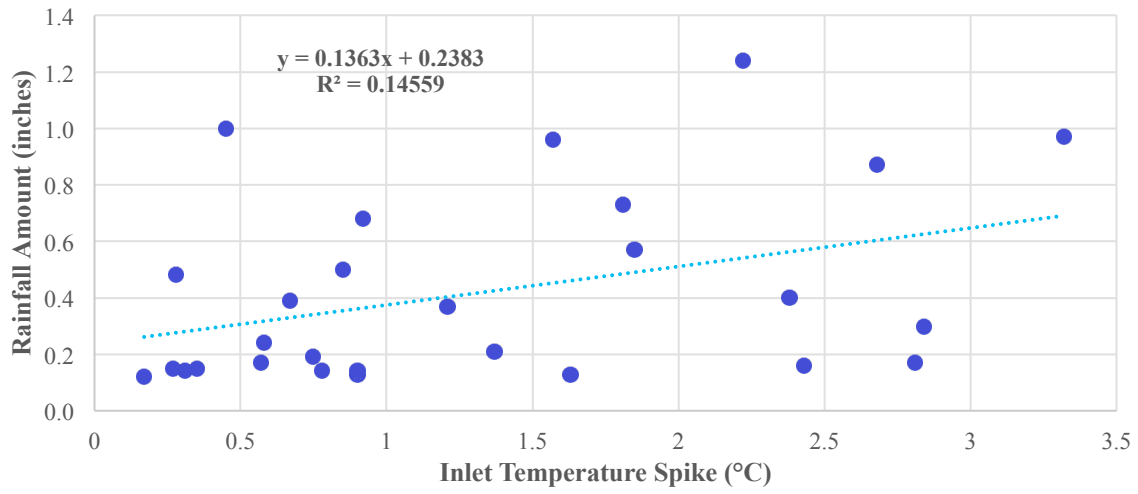
144

APPENDIX D

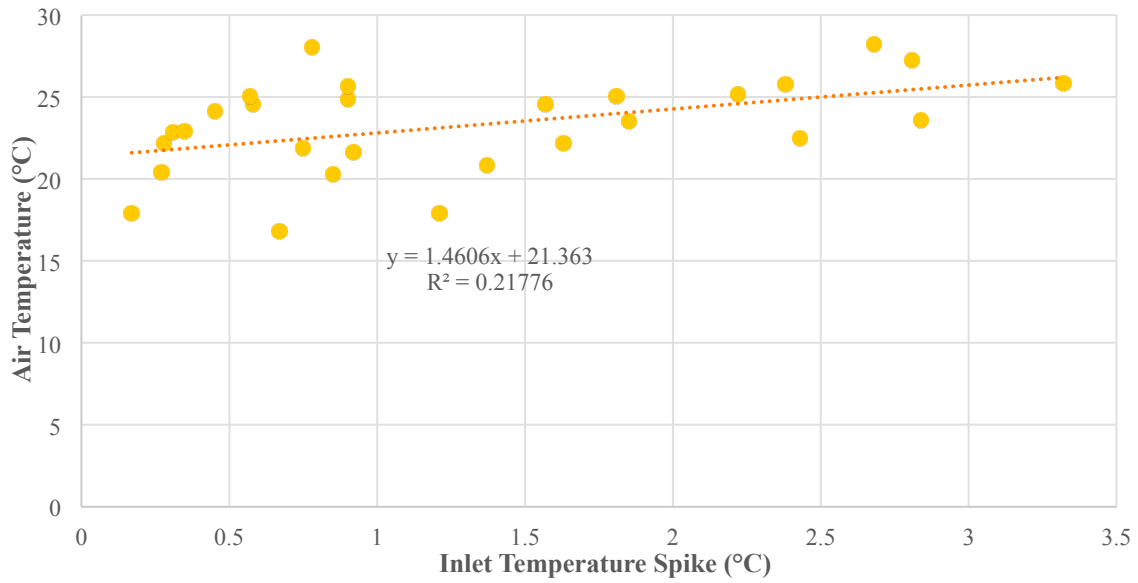*Figure D-1: Inlet temperature spike vs. rainfall amount linearity.*

Figure D-2: Inlet temperature spike vs. average air temperature linearity.

Table D-1: Average storm event air and water temperatures

Event Date	Total Rain (inches)	Intensity (in/hr)	AVERAGES (°C)				
			Air	Temp2IN	TempIMOut	Temp4Out	PT_OutTemp
4/7/2014	0.37	0.13	11.04	12.33	---	12.90	12.01
4/15/2014	2.33	0.32	6.22	12.92	---	12.80	11.34
4/25/2014	0.60	0.22	11.09	14.58	---	15.43	13.74
4/29/2014	5.02	0.28	13.01	12.83	---	14.84	13.95
5/10/2014	0.24	0.17	20.20	16.43	---	22.22	21.02
5/16/2014	4.23	0.48	13.75	16.23	---	17.63	16.19
5/22/2014	0.17	0.19	17.88	17.00	---	20.31	19.21
5/23/2014	0.31	0.31	19.61	17.09	---	20.77	19.70
5/27/2014	0.39	0.26	19.31	17.61	---	20.98	20.18
5/28/2014	0.77	0.51	15.04	16.00	---	18.11	16.67
6/3/2014	0.16	0.32	23.19	18.05	20.05	25.14	23.61
6/4/2014	0.14	0.15	19.54	17.13	18.27	22.84	20.70
6/9/2014	0.15	0.18	20.76	16.93	17.79	22.89	21.98
6/9/2014	0.68	0.48	20.14	17.24	18.18	22.72	21.96
6/11/2014	0.12	0.12	16.54	16.69	17.22	19.58	18.98
6/12/2014	0.39	0.16	21.93	18.00	18.86	21.31	20.72
6/13/2014	0.13	0.26	20.33	18.22	19.44	23.72	22.53
6/19/2014	0.14	0.17	21.88	18.83	19.45	25.16	24.37
6/19/2014	0.17	0.15	20.79	18.59	20.18	23.99	22.76
6/25/2014	0.13	0.39	26.21	21.35	23.24	27.82	27.19
6/25/2014	0.73	0.44	23.28	19.62	21.59	26.06	24.72
7/2/2014	0.87	0.58	22.38	19.78	21.69	24.85	23.76
7/13/2014	0.14	0.19	24.93	19.60	21.90	27.07	26.44
7/14/2014	0.97	0.90	24.57	20.57	22.72	26.33	25.68

7/15/2014	0.24	0.15	21.72	19.87	22.63	24.70	23.65
7/23/2014	0.40	0.28	21.49	19.62	21.46	24.62	23.04
7/26/2014	0.19	0.25	24.97	19.00	20.34	25.17	24.32
7/27/2014	1.24	0.55	20.28	19.41	21.83	22.91	21.58
8/1/2014	0.30	0.90	20.21	20.98	22.62	23.49	22.79
8/2/2014	0.48	0.14	20.46	19.67	21.50	22.56	21.67
8/2/2014	0.15	0.13	22.31	19.02	20.64	23.80	22.96
8/12/2014	1.00	0.15	21.58	19.75	20.77	22.73	21.91
8/14/2014	0.21	0.42	19.29	19.38	20.29	21.25	20.23
8/22/2014	0.57	0.49	20.08	19.63	20.59	22.40	21.41
8/23/2014	0.50	0.16	21.53	19.42	21.19	22.18	21.32
8/31/2014	0.96	0.68	26.12	20.14	21.97	25.22	24.57
9/2/2014	0.17	0.41	24.00	19.83	22.02	24.93	23.79
9/13/2014	0.37	0.26	15.85	18.32	19.48	18.91	17.59
9/24/2014	0.62	0.13	17.54	17.80	18.96	17.06	16.63
10/3/2014	0.51	0.18	13.15	16.30	16.77	13.96	13.68
10/7/2014	0.29	0.22	14.73	16.63	17.04	14.35	14.15
10/11/2014	0.40	0.13	13.29	15.58	15.87	13.84	13.26
10/15/2014	1.01	0.25	16.51	17.97	18.37	16.86	16.48
10/21/2014	0.72	0.13	12.81	14.90	15.20	12.21	12.01
11/1/2014	0.73	0.13	8.10	10.41	11.07	7.37	7.01
11/6/2014	0.45	0.12	7.16	11.06	11.38	7.63	7.48
11/13/2014	0.22	0.13	1.34	7.25	7.71	3.09	2.80
11/16/2014	0.94	0.16	0.17	6.46	7.20	5.45	2.17
11/24/2014	0.63	0.20	9.40	11.21	11.57	---	8.28
12/2/2014	0.24	0.13	2.74	8.37	8.13	---	4.91
12/3/2014	0.18	0.13	3.06	7.43	8.24	---	3.70

12/5/2014	0.16	0.13	4.33	7.41	8.13	---	4.91
12/6/2014	0.68	0.14	1.56	7.81	8.73	---	3.99
12/9/2014	0.76	0.16	1.60	7.51	7.81	---	2.58
12/16/2014	0.16	0.15	3.75	---	7.87	---	3.50
12/22/2014	0.12	0.12	7.24	---	9.16	---	5.21
12/24/2014	0.79	0.14	7.70	---	9.60	---	6.12
1/3/2015	0.98	0.15	5.48	---	7.09	---	3.36
1/4/2015	0.11	0.16	-4.04	---	7.56	---	0.17
1/12/2015	0.57	0.14	-2.67	---	6.42	---	-1.13
1/18/2015	1.49	0.21	1.36	---	6.82	---	0.40
1/23/2015	0.67	0.15	-2.73	---	6.36	---	-0.45
2/1/2015	0.81	0.13	-1.96	---	5.90	---	-0.51
2/17/2015	0.16	0.12	-9.63	---	5.63	---	-1.60
2/21/2015	0.65	0.12	-4.52	---	6.05	---	-1.55

Table D-2: Inlet temperature spikes for 2014-15 storm events.

Event Date	Avg Air Temp (°C)	Intensity (in/hr)	MAXIMUM 5 MINUTE CHANGE (°C) & TIME ELAPSED (MINS)			
			Temp2IN	Time Elapsed	TempIMOut	Time Elapsed
4/7/2014	11.04	0.13	0.13	340	---	---
4/15/2014	6.22	0.32	0.71	715	---	---
4/25/2014	11.09	0.22	0.31	575	---	---
4/29/2014	13.01	0.28	0.36	2095	---	---
5/10/2014	20.20	0.17	0.55	25	---	---
5/16/2014	13.75	0.48	0.99	110	---	---
5/22/2014	17.88	0.19	1.42	140	---	---
5/23/2014	19.61	0.31	0.92	30	---	---
5/27/2014	19.31	0.26	1.19	20	---	---
5/28/2014	15.04	0.51	0.95	10	---	---
6/3/2014	23.19	0.32	2.43	10	1.74	15
6/4/2014	19.54	0.15	0.31	500	0.71	475
6/9/2014	20.76	0.18	0.35	105	1.47	105
6/9/2014	20.14	0.48	0.92	245	1.44	245
6/11/2014	16.54	0.12	0.17	60	0.59	45
6/12/2014	21.93	0.16	0.67	1070	0.99	925
6/13/2014	20.33	0.26	1.63	20	3.07	25
6/19/2014	21.88	0.17	0.78	35	1.79	35
6/19/2014	20.79	0.15	0.57	120	0.75	110
6/25/2014	26.21	0.39	0.90	15	2.25	20
6/25/2014	23.28	0.44	1.81	15	2.81	15
7/2/2014	22.38	0.58	2.68	15	2.00	15
7/13/2014	24.93	0.19	0.90	25	1.68	20
7/14/2014	24.57	0.90	3.32	130	1.81	130

7/15/2014	21.72	0.15	0.58	55	1.01	50
7/23/2014	21.49	0.28	2.38	10	2.74	15
7/26/2014	24.97	0.25	0.75	15	2.28	15
7/27/2014	20.28	0.55	2.22	25	2.74	25
8/1/2014	20.21	0.90	2.84	10	1.37	10
8/2/2014	20.46	0.14	0.28	80	0.50	65
8/2/2014	22.31	0.13	0.27	40	0.65	40
8/12/2014	21.58	0.15	0.45	460	1.13	355
8/14/2014	19.29	0.42	1.37	10	1.34	15
8/22/2014	20.08	0.49	1.85	10	2.11	10
8/23/2014	21.53	0.16	0.85	545	0.89	545
8/31/2014	26.12	0.68	1.57	385	2.85	380
9/2/2014	24.00	0.41	2.81	10	1.20	10
9/13/2014	15.85	0.26	1.21	45	1.09	35
9/24/2014	17.54	0.13	0.09	890	0.53	210
10/3/2014	13.15	0.18	0.30	535	0.82	30
10/7/2014	14.73	0.22	0.26	140	1.18	130
10/11/2014	13.29	0.13	0.09	125	1.50	80
10/15/2014	16.51	0.25	0.50	235	0.43	235
10/21/2014	12.81	0.13	0.04	765	0.80	1875
11/1/2014	8.10	0.13	0.09	75	2.07	45
11/6/2014	7.16	0.12	0.15	215	1.00	880
11/13/2014	1.34	0.13	0.01	35	0.26	30
11/16/2014	0.17	0.16	0.33	500	2.62	880
11/24/2014	9.40	0.20	0.67	25	2.35	25
12/2/2014	2.74	0.13	0.12	425	2.17	590
12/3/2014	3.06	0.13	0.13	160	1.12	60

12/5/2014	4.33	0.13	0.24	345	2.40	115
12/6/2014	1.56	0.14	0.47	1060	1.49	50
12/9/2014	1.60	0.16	0.53	75	3.16	55
12/16/2014	3.75	0.15	---	---	1.49	20
12/22/2014	7.24	0.12	---	---	1.00	835
12/24/2014	7.70	0.14	---	---	1.04	40
1/3/2015	5.48	0.15	---	---	1.03	65
1/4/2015	-4.04	0.16	---	---	0.22	30
1/12/2015	-2.67	0.14	---	---	0.59	320
1/18/2015	1.36	0.21	---	---	1.10	30
1/23/2015	-2.73	0.15	---	---	0.51	80
2/1/2015	-1.96	0.13	---	---	0.64	190
2/17/2015	-9.63	0.12	---	---	0.28	445
2/21/2015	-4.52	0.12	---	---	0.41	750

Table D-3: P values obtained from paired t-tests

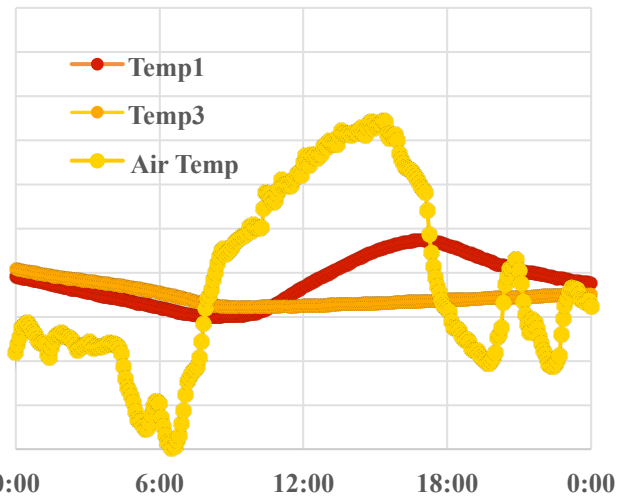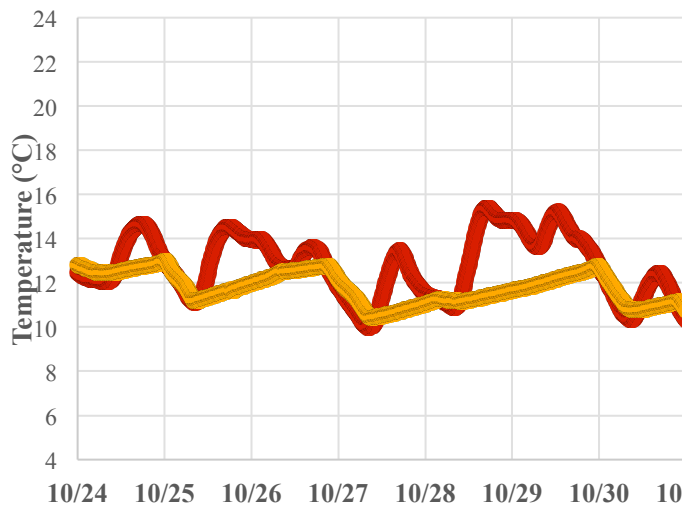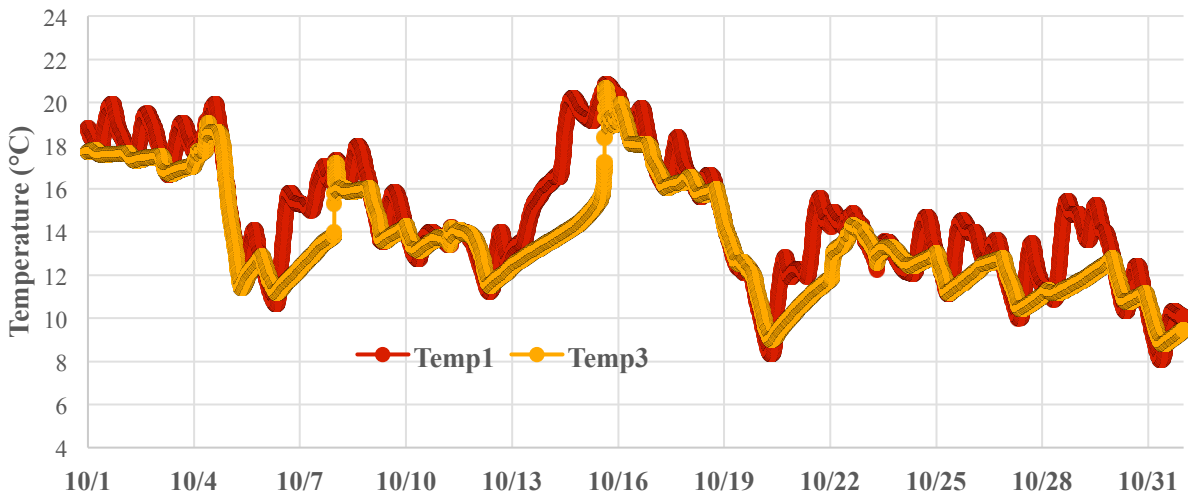|	Air Temp vs. Temp2IN	Temp2IN vs. Temp4Out	Air Temp vs. Temp4Out
April 2014	9.25E-258	5.48E-74	0.00E+00
May 2014	1.80E-90	0.00E+00	2.31E-264
June 2014	0.00E+00	0.00E+00	0.00E+00
July 2014	0.00E+00	0.00E+00	1.15E-239
August 2014	0.00E+00	0.00E+00	4.49E-75
September 2014	1.20E-51	3.66E-194	1.02E-11
October 2014	6.08E-307	0.00E+00	0.000

Figure D-3: October 2014 meander 1 temperatures for one month (top), one week (bottom left) and one day (bottom right).

APPENDIX E

Table E-1: April 30, 2014 storm volume durations for mass analysis

	Volume Duration (hours)
IN-1S	9.92
IN-2S	2.83
IN-3S	1.00
IN-4S	100.33
OUT-1S	10.83
OUT-2S	2.25
OUT-3S	1.75
OUT-4S	99.25